R & M No. 3843

R & M No. 3843

PROCUREMENT EXECUTIVE, MINISTRY OF DEFENCE

Aeronautical Research Council
Reports and Memoranda

A METHOD OF PERFORMANCE PREDICTION FOR CENTRIFUGAL COMPRESSORS

by

M.V.Herbert
National Gas Turbine Establishment
Pyestock, Farnborough, Hants

London: Her Majesty's Stationery Office
£18 NET

UDC 621.515 : 621.004.6

A METHOD OF PERFORMANCE PREDICTION FOR CENTRIFUGAL COMPRESSORS

Part I - Analysis, Part II - Comparison with experiment

By M.V.Herbert

National Gas Turbine Establishment

REPORTS AND MEMORANDA No. 3843*

February 1980

SUMMARY

The objective of this work was to develop a method capable of producing reasonably accurate stage characteristics, in terms of mass flow, pressure ratio, work input and efficiency, for any centrifugal compressor with radial outflow (i.e. with no axial component of velocity at outlet), given only overall geometric properties. Due to the scarcity of suitable experimental data, the treatment perforce is very largely analytical.

Part I gives the analytical treatment and assumptions used; Part II presents the results of applying the method to various machines and compares the predictions with test data. Prediction of choking flow is generally satisfactory, and the mass-flow/pressure-ratio characteristics produced have substantially correct form, although no general means have been found of predicting the onset of surge. For the cases examined the error in predicted efficiency level is within ±1 to 2 per cent at design speed, sometimes more at low speed.

* Replaces NGTE M78029 and NGTE M78031 dated September 1978
ARC 38 052 ARC 38 053

CONTENTS

CONTENTS - continued

PART I - ANALYSIS

1. Intention

A designer could benefit at an early stage of his work from having a means of predicting, for comparative purposes, performance maps for a variety of tentative designs of centrifugal compressor, without having their blade and passage geometry completely specified: that is to say a general method applicable with knowledge of only overall dimensions and angles. This it was the object of the present study to produce. Additional applications of such a prediction method would be to secure good matching between rotor and diffuser system, and also to assist the understanding and analysis of conventional (i.e. flow-average) test rig measurements.

But with such an objective there are severe limitations to the success which can be expected. Any serious consideration of the factors upon which centrifugal compressor performance depends immediately produces a realisation of how little is understood about the highly complex flow processes which govern that performance. Only recently have experimental measurements of conditions leaving the rotor started to become available (e.g. Reference 1), due to the sophisticated nature of the measuring techniques that are required, and at present these data serve mainly to emphasise how very far removed from simple flow concepts is the real situation. So on the one hand accurate modelling by purely theoretical means is beyond present capability, while on the other the complexities of the fluid dynamics ensure that no simple empirical correlations of overall performance quantities will be found that are satisfactory for general application.

In these circumstances, it cannot be expected that any treatment simple enough to serve the declared aims will achieve more than limited success. What we are really enquiring is how good can that simple treatment be made: what will it do and what won't it do?

2. General considerations

Certain points are clear from the outset. First and foremost is that among compressors built with the same overall geometric properties some may have better performance than others. But since a general prediction method is by definition required to ignore details of, for instance, rotor blade passage shape, it cannot discriminate between such cases. So it can never give an "absolute" answer. Some empirical datum or standard of performance must be set, and the predictions "tuned" to agree with it. Then relatively poor machines will fall below such a "standard" prediction and, it may be hoped, improved machines of the future will exceed it.

When test data come to be examined, it is quickly realised how very scarce are compressors for which adequate physical details and performance results are available. In particular, there are hardly any machines providing data both with and without a vaned diffuser system. This makes it difficult, for instance, to arrive empirically at a breakdown of measured overall loss as between rotor and diffuser. Indeed, the general paucity of test data means that our approach to the problem of prediction must throughout be primarily an analytical one, relying on experiment to contribute little more than the means for "tuning" the final answer to a selected datum.

In meeting the two requirements of a generalised analytical treatment and rapid calculation, many rather sweeping assumptions and simplifications become necessary. Arbitrary but hopefully typical features of internal flow and geometry must be introduced. The chief concern is how, in each portion of the machine, to set up a greatly simplified model of flow behaviour that is yet not so crude as to ignore the major physical effects. It is then to be discovered whether such simple modelling is "good enough".

In one portion of the machine a purely analytical approach breaks down, namely the channel of a vaned diffuser. Here boundary layer effects alone determine performance, and correct prediction of pressure recovery by analytical means would require correct modelling of the three-dimensional boundary layer problem in all its aspects —— a simple calculation is no use. Consequently it is preferable to base prediction upon experimental data for isolated channels. The chief task is then to generalise those data sufficiently to deal with the many possible geometric variants to channel shape for which specific test results are not available.

The calculations throughout are bound to be lengthy and involve a considerable amount of iteration, so a computer program is required.

3. The prediction method

This Part of the paper gives a full statement of the assumptions and modelling procedures which form the analytical treatment. This prediction method applies only to centrifugal compressors having no net axial component of velocity at rotor outlet, and with a diffuser system which is centred about a radial plane.

The Appendix entitled "Analysis of flow model" states the assumptions and working relations for each portion of the compressor stage in turn. Equations are written so as to be usable with any consistent system of units, and appropriate numerical constants and values of air properties are given in

Appendix 1 for both SI and Imperial units. Various amplifying notes and derivations to which reference is made in the analysis appear in Appendices 3 and 4.

Some compressors will have features which prevent them conforming to prediction by the standard treatment given here. Variations of entry duct shape can in certain cases be dealt with by the standard method, provided information is available to specify the required items of input data. In other cases, however, special provision must be made by adjusting some feature of the treatment: for instance, prewhirl vane blade loss could be increased to simulate empirically some entry maldistribution. Alteration to the standard treatment would also be necessary to cater for a compressor having an unconventionally large change of blade camber between inducer leading edge and throat, otherwise serious error in predicted inducer choking flow would result. When need arises the analysis can readily accommodate changes of this nature to suit particular types of compressor not conforming to what are taken as standard features. What the prediction method cannot deal with, however, are geometries of vaned diffuser channel having divergence outside a specific range —— that range being equivalent to two-dimensional channels of unity throat aspect ratio with included divergence angles between 6 and 11° (see Figure 1). Diffuser channel geometries with divergence outside that range are considered to be far from optimum designs and should not normally be encountered.

As regards surge, Appendix 5 contains some observations on the evidence relating to compressors fitted with vaned diffusers, but unfortunately no satisfactory correlation has emerged for universal application. Nor is the mechanism of surge in general as yet sufficiently understood for the problem of its prediction to be amenable to a purely theoretical approach. This performance prediction method thus does not claim to include treatment of surge.

NOTATION

A	flow area
A_g	total geometric throat area of channel diffuser
A_w	wetted surface area of semi-vaneless space
B	blockage factor (defined as 1 - blocked area/total area)
C_f	skin friction coefficient
C_L	lift coefficient
C_m	torque coefficient
C_p	specific heat at constant pressure
C_{pr}	pressure recovery coefficient
c	mean chord of prewhirl blades
D	diameter
$f( )$	a function of
F, G	wake mixing parameters (defined in text)
g	conversion factor, dependent in value upon the unit system
H	boundary layer shape factor ($= \delta^*/\theta$)
H'	boundary layer shape factor ($= \delta^{**}/\theta$)
h	height of blade or passage
I	rothalpy[/]
J	mechanical equivalent of heat[/]
i	angle of incidence
L	blade loading parameter
ℓ	equivalent flat plate length
ℓ_d	length of vaned diffuser channel
M	Mach number

[/]Not applicable to Appendix 4.

m	meridional length (measured from rotor inlet)
n_d	number of diffuser vanes
n_f	number of full rotor blades
n_i	number of rotor half-blades or intervanes
n_p	number of prewhirl blades
P	pressure
p	a function of Mach number (defined in text)
Q	mass flow
q	a function defined in the text
R	gas constant
Re	Reynolds number
r	radius
S	surface length
s	blade pitch
T	temperature
t	rotor blade thickness
U	blade velocity
V	absolute flow velocity
W	relative flow velocity
w	passage width
Y_p	profile loss coefficient } of prewhirl blades
Y_s	secondary loss coefficient } of prewhirl blades
X, Z	multiplication factors on boundary layer thickness[1]
x, y	cartesian co-ordinates, x = axial direction, y = radial direction[1]

[1] Not applicable to Appendix 4.

α	absolute flow angle	measured from meridional direction
β	relative flow angle	
β_∞	blade angle	
γ	ratio of specific heats	
δ	boundary layer thickness	
δ^*	boundary layer displacement thickness	
δ^{**}	boundary layer energy thickness	
ε, ζ	functions defined in the text	
η	isentropic efficiency	
θ	boundary layer momentum thickness	
Θ	diffuser channel divergence semi-angle	
λ	axial velocity ratio defined in text	
μ	viscosity	
ρ	density (static if without subscript)	
σ	a factor applied to inducer choking flow coefficient	
τ	compressibility ratio $\left(= \frac{P_t - P_s}{\rho v^2/2g}\right)$	
ϕ	flow angle measured from axis in meridional plane	
Ψ	a parametric group (see text for various forms)	
ψ	angular co-ordinate with respect to axis	
Ω	rotational speed (radians per sec)	
ω	angle of diffuser vane surface at leading edge, on suction side, measured from radial direction	

AR	channel diffuser geometric area ratio (outlet/throat)
AS	channel diffuser throat aspect ratio $\left(= h_{th}/w_{th}\right)$
LWR	channel diffuser length/throat width

Subscripts

eff	effective
c	compressible or quasi-compressible
f	disc friction } applied to $C_p T_t$
ℓ	leakage } applied to $C_p T_t$
ℓe	leading edge of diffuser vane
ic	incompressible
j	junction of profile arcs
m	meridional component
out	diffuser channel outlet
ps	pressure surface
ss	suction surface
sh	after normal shock
s	static condition (except Y_s)
t	stagnation or total head condition
th	diffuser channel throat
w	tangential or whirl component (of velocity)
*	inducer throat
2D	equivalent two-dimensional

Numerical subscripts refer to stations in machine as per sketch following.

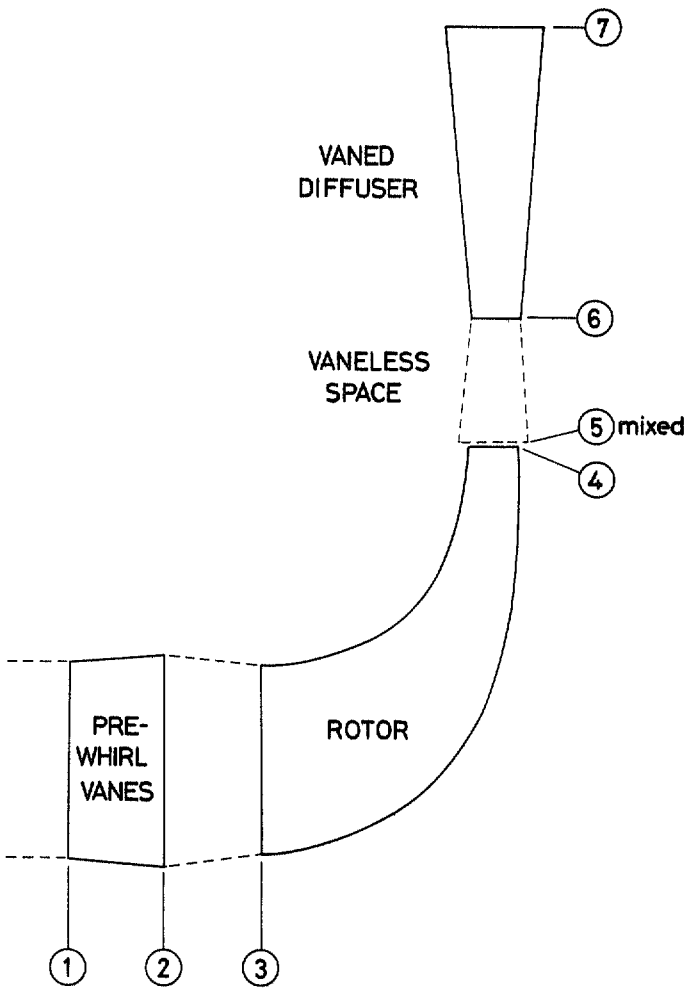

Superscripts

~	design value
-	average flow quantity (usually used to denote average of hub and tip)
^	core or mainstream quantity
'	relative condition (applied to A, M, P and T; no superscript means absolute condition)
' and "	applied to h denote reduction for boundary layer thickness (see text)

Other symbols are defined locally in text or diagrams.

APPENDIX 1

NUMERICAL CONSTANTS

Air properties

$$\mu = 1.015 \times 10^{-8} \frac{T_s^{1.5}}{T_s + 120} \qquad (T_s \text{ in } {}^{\circ}K)$$

in lb/ft sec

For SI units multiply above by 1.488 (then in kg/m s)

$$C_p = 0.27798 + 0.037079\, x - 0.021413\, x^2 - 0.007016\, x^3 + 0.012773\, x^4$$

where $x = \frac{T - 1125}{875}$ $\qquad (T \text{ in } {}^{\circ}K)$

in CHU/lb $^{\circ}K$ (from Reference 12)

For SI units multiply above by 4186.8 (then in J/kg K)

$$\gamma = \frac{14.588\, C_p}{14.588\, C_p - 1} \qquad \text{where} \quad C_p = \text{above expression in } x$$

The same value of γ applies in both Imperial and SI units.

Thus both C_p and γ require to be found at the mean of any particular range of temperature, which in practice involves iteration. However, for ease of computing it may be sufficiently accurate to take constant values of C_p and γ independent of T; if the conventional value $\gamma = 1.400$ is used, then $C_p = 0.2399$ CHU/lb $^{\circ}K$ or 1004.4 J/kg K.

Other constants

	ft-lb-sec-^{o}K	SI
R	96.02	287.05
J	1400.7	1
g	32.17	1

Use of these constants with γ = 1.400 gives the maximum value of

$$\frac{Q\sqrt{T_t}}{A\ P_t} = 0.39633 \text{ in ft-lb-sec-}^{o}\text{K units or } 0.040415 \text{ in SI units.}$$

Note relating to the conversion factor g

In Imperial units the unit of force consistent with Newton's Second Law is the pdl, but common engineering practice uses the lb_f and hence a conversion factor (g) is required, the numerical value of which is equal to the gravitational acceleration [i.e. 32.17 pdl = 1 lb_f]; g as used in this work can then be said to have units of pdl/lb_f or $lb_m.ft/(lb_f.s^2)$ and takes the value 32.17. But in SI units the unit of force consistent with Newton's Second Law, the Newton, is of course the accepted unit of force, so that no conversion factor is required and g in the equations takes the value of 1 [its units could be said to be $kg.m/(N.s^2)$].

APPENDIX 2

ANALYSIS OF FLOW MODEL

The problem is essentially as follows:-

given
- basic geometry of compressor, including rotor inlet and outlet blade angles but no other details of rotor passage shape
- mass flow and inlet conditions
- rotational speed

to determine whether the given flow is below choking, and if so to predict work input, pressure ratio, and isentropic efficiency.

The main items of compressor data required to be specified fall into three categories:-

(i) geometrical features: diameter, blade angle and blade thickness at hub and tip at rotor inlet; rotor outlet blade angle and blade thickness; diameters and axial passage widths at rotor outlet, at start and end of vaneless space, at start and end of vaned diffuser; numbers of rotor blades (and 'intervanes' or half-blades if any) and diffuser vanes; vaned diffuser passage dimensions at throat and at channel outlet, channel length, and leading edge vane angle.

(ii) estimated flow properties: gas angles at hub and tip at rotor inlet; tip/mean axial velocity ratio at rotor inlet; blockage factor at rotor inlet if different from a value determined hereafter as standard; total pressure loss after end of vaned diffuser channel.

(iii) the rotor blockage growth factor - an empirical quantity adjustable at will as discussed later.

Inlet conditions to prewhirl blades ~ station 1

Assume flow is axial at inlet, i.e. $\alpha_1 = 0$ at all diameters

Specify geometry
- $D_{1,tip}$; $D_{1,hub}$; $D_{2,tip}$; $D_{2,hub}$; no. of blades (n_p)
- chord (c) at mean diameter

and prewhirl outlet gas angles $\alpha_{2,tip}$; $\alpha_{2,hub}$

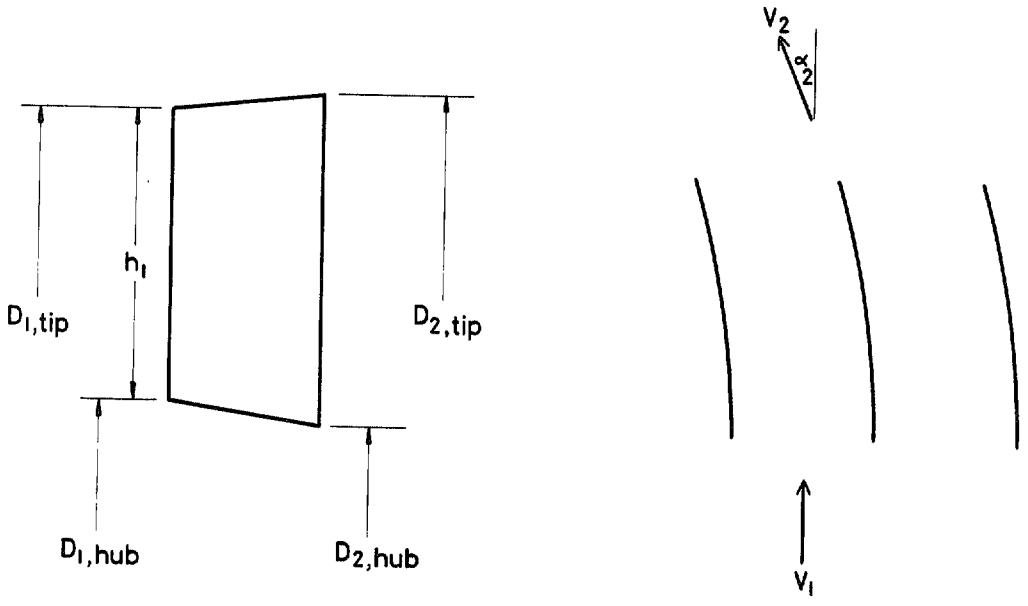

Allow for entry blockage (e.g. approach duct boundary layers) by means of blockage factor B_1 such that effective inlet flow area

$$A_1 = B_1 \cdot \frac{\pi}{4}\left(D_{1,tip}^2 - D_{1,hub}^2\right)$$

where B_1 must be specified or chosen from experience.

Then B_1 is related to mean displacement thickness $\frac{\overline{\delta_1^*}}{h_1}$ on inner and outer walls as follows

$$(1 - B_1)\,\frac{\pi}{4}\left(D_{1,tip}^2 - D_{1,hub}^2\right) = \overline{\delta_1^*}\,\pi\left(D_{1,tip} + D_{1,hub}\right)$$

$$\therefore \quad 1 - B_1 = \frac{4\,\overline{\delta_1^*}}{D_{1,tip} - D_{1,hub}}$$

But $$D_{1,tip} - D_{1,hub} = 2\,h_1$$

$$\therefore \qquad B_1 = 1 - 2\,\frac{\overline{\delta_1^*}}{h_1}$$

Hence A_1 is found.

Specify flow Q; stagnation temperature $T_{t,1}$; stagnation density $\rho_{t,1}$

Then $\qquad P_{t,1} = R\,T_{t,1}\,\rho_{t,1}$

Calculate value of

$$\text{"corrected mass flow"} = \frac{Q\sqrt{T_{t,1}}}{P_{t,1}} \cdot \frac{P_{ref}}{\sqrt{T_{ref}}}$$

where $\quad P_{ref} = 14.7$ psia $= 101.325 \times 10^3$ N/m^2; $\quad T_{ref} = 288^\circ$K

Consider mean diameter only for prewhirl blade loss assessment

$$\text{mean D} = \tfrac{1}{4}\left(D_{1,tip} + D_{1,hub} + D_{2,tip} + D_{2,hub}\right)$$

Hence mean pitch $\qquad s = \dfrac{\pi\ (\text{mean D})}{n_p}$

Mean height $\qquad h = \tfrac{1}{4}\left(D_{1,tip} - D_{1,hub} + D_{2,tip} - D_{2,hub}\right)$

Hence mean s/c and mean c/h are known

Take $\qquad \text{mean } \alpha_2 = \tfrac{1}{2}\left(\alpha_{2,tip} + \alpha_{2,hub}\right)$

Prewhirl blade loss

Profile loss from Ainley & Mathieson[2], as blades resemble turbine NGVs.

Figure 4a of that reference shows only small effect of α_2 when $|\alpha_2| < 50^\circ$ and $s/c \leq 1$, so use lowest curve in that Figure to give Y_p.

This curve approximates to

$$Y_p = 0.02 + 0.1125\left(1 - \frac{s}{c}\right)^{2.64}$$

when $s/c \leq 1$; when $s/c > 1$ put $s/c = 1$ in relation.

Reference 3 suggests factoring Ainley-Mathieson values of Y_p by 0.8, hence revised relation

$$Y_p = 0.016 + 0.09 \left(1 - \frac{s}{c}\right)^{3.64}$$

with the second term zero when $\frac{s}{c} > 1$.

Secondary loss from Ainley & Mathieson[2] modified by Dunham[4].

Assume no end clearance

$\alpha_1 = 0$

"α_m" as defined by A & M is given by $\tan \alpha_m = \frac{1}{2}\left(\tan \alpha_1 + \tan \alpha_2\right)$

Hence $\tan \alpha_m = \frac{1}{2} \tan \alpha_2$ $\quad \therefore \quad \cos \alpha_m = \left(1 + \frac{1}{4} \tan^2 \alpha_2\right)^{-\frac{1}{2}}$

Reference 4 gives

$$Y_S = \frac{c}{h} \cdot \frac{\cos \alpha_2}{\cos \alpha_1} \left(\frac{C_L}{s/c}\right)^2 \frac{\cos^2 \alpha_2}{\cos^3 \alpha_m} \left(0.0055 + 0.078 \sqrt{\frac{\delta_1^*}{c}}\right)$$

where (vide A & M)

$$\frac{C_L}{s/c} = 2 \cos \alpha_m \left(\tan \alpha_1 + \tan |\alpha_2|\right)$$

$$\text{Hence } Y_S = 4 \left(\frac{c}{h}\right) \sin^2 \alpha_2 \cos \alpha_2 \left(1 + \frac{1}{4} \tan^2 \alpha_2\right)^{\frac{1}{2}} \left(0.0055 + 0.078 \sqrt{\frac{\delta_1^*}{c}}\right)$$

$$\simeq 0.022 \left(\frac{c}{h}\right) \sin^2 \alpha_2 \cos \alpha_2 \left(1 + \frac{1}{4} \tan^2 \alpha_2\right)^{\frac{1}{2}} \left\{1 + 10 \left[(1 - B_1) \frac{h}{c}\right]^{\frac{1}{2}}\right\}$$

Total loss then given by (Dunham & Came[5])

$$\frac{P_{t,1} - \overline{P}_{t,2}}{\overline{P}_{t,2} - \overline{P}_{s,2}} = \left(Y_p + Y_s\right)\left(\frac{Re_2}{2 \times 10^5}\right)^{-0.2}$$

where $Re_2 = \dfrac{\bar{\rho}_2 \bar{V}_2 c}{\bar{\mu}_2}$

Conditions at outlet from prewhirl blades ~ station 2

Flow area at blade outlet

Assume $\overline{\delta_2^*} = \overline{\delta_1^*}$ [Note: boundary layer thickness increases in compressor blades and reduces in high deflection turbine stator blades, so constant thickness is an arbitrary but possible answer for low deflection accelerating blades.]

Hence

$$B_2 = 1 - (1 - B_1)\left[\frac{D_{1,tip} - D_{1,hub}}{D_{2,tip} - D_{2,hub}}\right]$$

Take $$A_2 = B_2 \cdot \frac{\pi}{4}\left(D_{2,tip}^2 - D_{2,hub}^2\right)\cos\left(\frac{\alpha_{2,tip} + \alpha_{2,hub}}{2}\right)$$

Mean conditions at blade outlet are found as follows

$$T_{t,2} = T_{t,1}$$

Assume a value of $\overline{P_{t,2}}$; take initially $P_{t,1} - \left(Y_p + Y_s\right)\dfrac{\bar{\rho}_1 \bar{V}_1^2}{2g}$.

Hence mean $\dfrac{Q\sqrt{T_{t,2}}}{A_2 \overline{P_{t,2}}} \longrightarrow \bar{M}_2$ (take subsonic solution)

$\bar{M}_2 \longrightarrow$ mean values of

$\dfrac{\bar{V}_2}{\sqrt{T_{t,2}}} \longrightarrow \bar{V}_2$

$\dfrac{\overline{P_{t,2}}}{\overline{P_{s,2}}} \longrightarrow \overline{P_{s,2}}$

$\dfrac{T_{t,2}}{\overline{T_{s,2}}} \longrightarrow \overline{T_{s,2}}$

$\bar{\rho}_2 = \overline{P_{s,2}}/R\overline{T_{s,2}}$

$\bar{\mu}_2 = f\left(\overline{T_{s,2}}\right)$

Substitute $\overline{P_{t,2}}$; $\overline{P_{s,2}}$; $\bar{V}_2$; $\bar{\rho}_2$ and $\bar{\mu}_2$ into equation for $Y_p + Y_s$ and iterate until this procedure gives correct value of $\overline{P_{t,2}}$.

Conditions at inlet to rotor ~ station 3

$$T_{t,3} = T_{t,2}$$

$$\overline{P_{t,3}} = \overline{P_{t,2}}$$

For the special case of no pre-whirl blades these two values become inlet conditions and $\alpha_3 = 0$ at all diameters.

Assume $\phi_3 = 0$, i.e. no radial component of velocity.

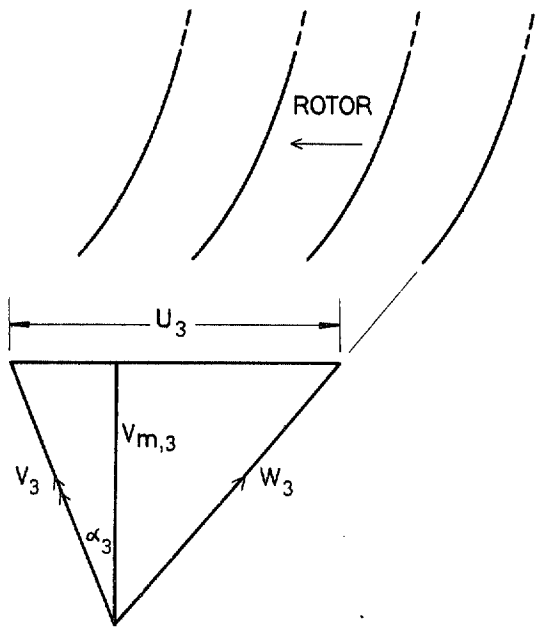

In general $$A_3 = B_3 \cdot \frac{\pi}{4}\left(D_{3,tip}^2 - D_{3,hub}^2\right) \cos(\text{mean } \alpha_3)$$

where $$B_3 = 1 - 2\frac{\overline{\delta_3^*}}{h_3}; \quad h_3 = \tfrac{1}{2}\left(D_{3,tip} - D_{3,hub}\right)$$

Values for B_3 $\left(\text{or } \frac{\overline{\delta_3^*}}{h_3}\right)$ and α_3 will depend upon passage shape and length between stations 2 and 3 unless these be taken as coincident.

Specify geometry

- $D_{3,tip}$; $D_{3,hub}$; D_4; h_4 (including running clearance)
- no. of full blades (n_f)
- no. of intervanes or half-blades (n_i)
- proportion of meridional length where intervanes start (treat as 0.5 if unknown)
- blade angles: $\beta_{\infty 3,tip}$; $\beta_{\infty 3,hub}$; $\beta_{\infty 4}$
- blade thickness: $t_{3,tip}$; $t_{3,hub}$; mean t_4

Also specify

gas angles $\alpha_{3,tip}$ and $\alpha_{3,hub}$ (α values 0 for no prewhirl)

Note: if better knowledge is lacking take

$\alpha_{3,tip} = \alpha_{2,tip}$

$\alpha_{3,hub} = \alpha_{2,hub}$

B_3 must be specified or chosen from experience (see Appendix 3-8 for typical value).

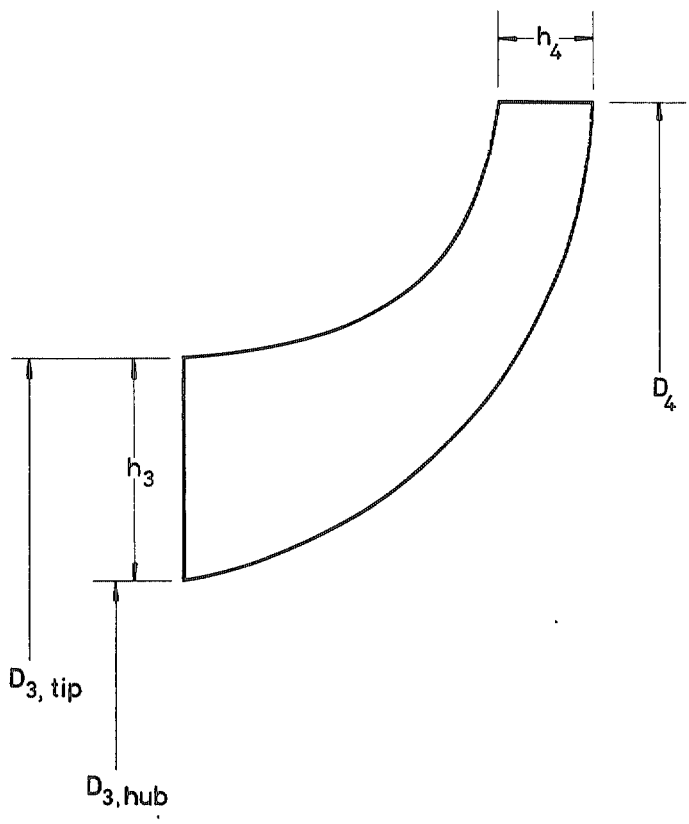

Allow for non-uniform axial velocity profile at station 3:

assume axial velocity at any diameter D_3

$$= \overline{V_{m,3}} \left[1 + (\lambda - 1) \frac{D_3 - D_{3,ref}}{D_{3,tip} - D_{3,ref}} \right]$$

where $\overline{V_{m,3}}$ = mean axial velocity

i.e. $\lambda = \frac{\text{tip axial velocity}}{\text{mean axial velocity}}$ (could be > or <1)

Specify λ

Then from continuity (see Appendix 3-1)

$$D_{3,ref} = \frac{2}{3} \frac{D_{3,tip}^2 + D_{3,tip} D_{3,hub} + D_{3,hub}^2}{D_{3,tip} + D_{3,hub}}$$

Hence $D_{3,ref}$

Take "mean α_3" as value of α_3 at $D_{3,ref}$ if α profile were linear

i.e. $$\bar{\alpha}_3 = \alpha_{3,tip} - \left(\alpha_{3,tip} - \alpha_{3,hub} \right) \left(\frac{D_{3,tip} - D_{3,ref}}{D_{3,tip} - D_{3,hub}} \right)$$

Hence A_3

Mean flow quantities at station 3

Know Q; A_3; $\overline{P_{t,3}}$; $T_{t,3}$

Hence $\frac{Q \sqrt{T_{t,3}}}{A_3 \overline{P_{t,3}}} \longrightarrow \bar{M}_3$ (take subsonic solution), whence $\bar{V}_3$

$\overline{V_{m,3}} = \bar{V}_3 \cos \bar{\alpha}_3$

Hence $\overline{V_{m,3}}$

Hence
$$\begin{cases} \text{tip axial velocity} = V_{m,3,tip} = \overline{V}_{m,3} \cdot \lambda \\ \text{hub axial velocity} = V_{m,3,hub} \\ \qquad = \overline{V}_{m,3} \left[1 - (\lambda - 1) \dfrac{D_{3,ref} - D_{3,hub}}{D_{3,tip} - D_{3,ref}} \right] \end{cases}$$

[Note: since same value $\bar{\alpha}_3$ is used both for A_3 and in getting $\overline{V}_{m,3}$ from $\bar{V}_3$, the values of axial velocity everywhere will not be sensitive to the assumed α_3 profile, so linear assumption is acceptable.]

Relative conditions at rotor inlet

Specify { rotational speed (Ω) at operating condition; design rotational speed $\left(\tilde{\Omega}\right)$

Conditions are wanted at hub and tip

Know { absolute values $T_{t,3}$; $\overline{P}_{t,3}$ (assume $\overline{P}_{t,3}$ applies to hub and tip); α_3; $V_{m,3}$; U_3 ($= \frac{1}{2} D_3 \Omega$) at hub and tip

The following treatment of the rotor applies at either hub or tip and distinguishing suffices are in general omitted.

Velocity triangle is defined, and

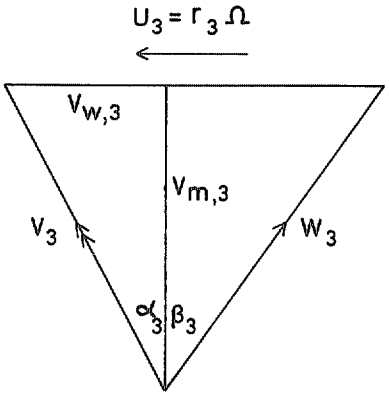

$$V_{w,3} = V_{m,3} \tan \alpha_3$$

hence $V_{w,3}$

$$\text{Rothalpy } I_3 = C_p T_{t,3} - \frac{U_3 V_{w,3}}{gJ} = C_p T_{t,3}' - \frac{U_3^2}{2gJ}$$

hence $\begin{cases} I_3 \text{ from left-hand expression} \\ \text{relative } T_t \text{ from} \end{cases}$

$$C_p T_{t,3}' = C_p T_{t,3} + \frac{U_3 \left(U_3 - 2 V_{w,3} \right)}{2gJ}$$

Relative P_t from

$$P_{t,3}' = \overline{P}_{t,3} \left(\frac{T_{t,3}'}{T_{t,3}} \right)^{\frac{\gamma}{\gamma-1}}$$

I_3; $T_{t,3}'$; $P_{t,3}'$ are thus all different at hub and tip, unless there is no prewhirl or prewhirl is of free vortex type in which cases I_3 is same at hub and tip.

Incidence at rotor inlet

Define the zero incidence condition as $\tilde{\beta}_3 = \beta_{\infty 3}$

[Note: hub and tip values of $\tilde{\beta}_3$; $\tilde{V}_{m,3}$ etc. will not necessarily occur at the same value of Q; i.e. the $\tilde{V}_{m,3}$ values will not fit the relation involving λ. Thus superscript ~ relates not to any unique running point, but to the condition giving zero incidence at either hub or tip as the case may be.]

Then at hub or tip α_3; $\beta_{\infty 3}$; r_3 $(= \frac{1}{2} D_3)$ are known.

From the velocity triangle (see Appendix 3-2)

$$\tan \beta_3 = \frac{r_3 \Omega}{V_{m,3}} - \tan \alpha_3$$

Hence β_3

$$i = \beta_3 - \beta_{\infty 3}$$

Hence i

$W_s = V_{m,s} \sec \beta_s$

Hence W_s

Know $T_{t,s}'$; $P_{t,s}'$

Then

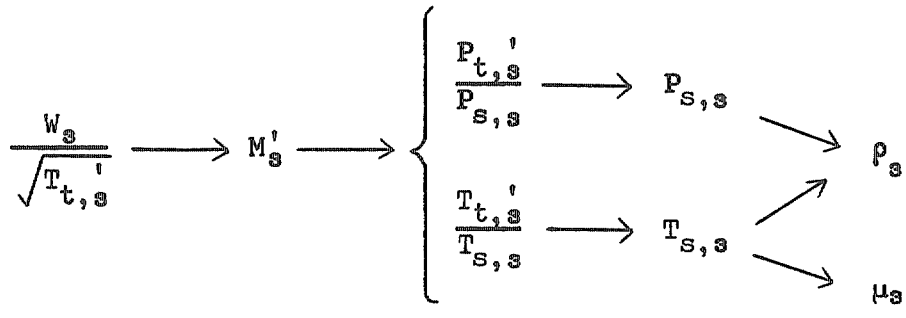

(all quantities being different at hub and tip)

Note: it is possible to have $M_s' > 1$ at either hub or tip (but not both).

Prescribed functions and geometry of rotor

[Note: The prescribed forms for W, β and β_∞ which follow are arbitrary, and later experience may suggest improvements more typical of successful design.]

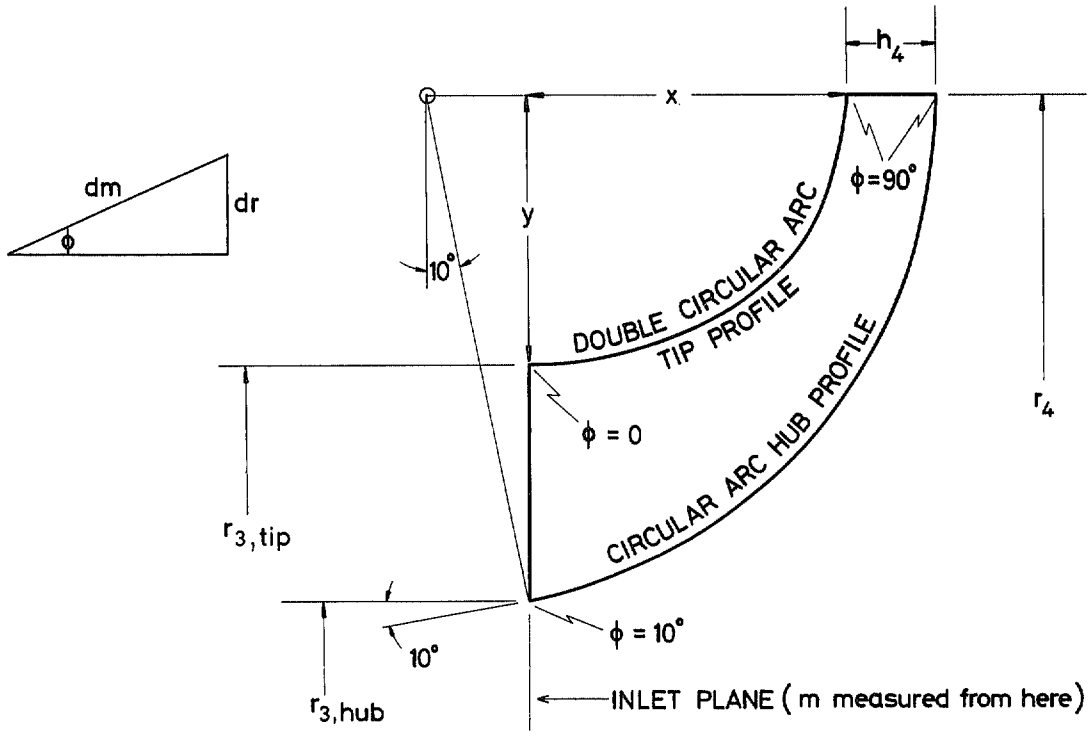

For tip profile

$$\begin{cases} x = \left(r_4 - r_{3,hub}\right)\left(\sec\frac{\pi}{18} - \tan\frac{\pi}{18}\right) - h_4 \\ y = r_4 - r_{3,tip} \end{cases}$$

where $r_4 = \frac{1}{2} D_4$

Assume profile formed of 2 circular arcs with their common normal at 45° to axis

Let m_j denote value of m at the junction of arcs

Then $$\frac{m_j}{m_{4,tip}} = \frac{x + \left(1 - \sqrt{2}\right) y}{\left(2 - \sqrt{2}\right)\left(x + y\right)}$$ (see Appendix 3-3)

	TIP	HUB
$m_{\clubsuit}$	$\frac{\pi}{4}(x + y)$	$\frac{4\pi}{9} \sec \frac{\pi}{18}\left(r_{\clubsuit} - r_{s,hub}\right)$
ϕ	when $\frac{m}{m_{\clubsuit}} < \frac{m_j}{m_{\clubsuit}}$ $\frac{\pi}{4} \frac{m/m_{\clubsuit}}{m_j/m_{\clubsuit}}$	$\frac{\pi}{18} + \frac{4\pi}{9} \frac{m}{m_{\clubsuit}}$
	when $\frac{m}{m_{\clubsuit}} > \frac{m_j}{m_{\clubsuit}}$ $\frac{\pi}{4}\left[1 + \frac{\left(m/m_{\clubsuit}\right) - \left(m_j/m_{\clubsuit}\right)}{1 - \left(m_j/m_{\clubsuit}\right)}\right]$	
r	when $\frac{m}{m_{\clubsuit}} < \frac{m_j}{m_{\clubsuit}}$ $r_{s,tip} + (1 - \cos\phi)\left[\frac{x + \left(1 - \sqrt{2}\right)y}{2 - \sqrt{2}}\right]$	$r_{s,hub} + \left(r_{\clubsuit} - r_{s,hub}\right)\left(1 - \frac{\cos\phi}{\cos\frac{\pi}{18}}\right)$
	when $\frac{m}{m_{\clubsuit}} > \frac{m_j}{m_{\clubsuit}}$ $r_{s,tip} + \left(1 - \cos\frac{\pi}{4}\right)\left[\frac{x + \left(1 - \sqrt{2}\right)y}{2 - \sqrt{2}}\right] +$ $+ \left(\cos\frac{\pi}{4} - \cos\phi\right)\left[\frac{\left(1 - \sqrt{2}\right)x + y}{2 - \sqrt{2}}\right]$	

W
(mean
relative
velocity)

TIP

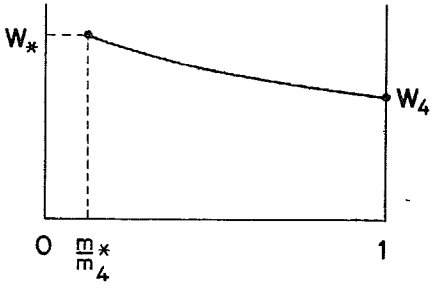

$$W_4 + (W_* - W_4)\left(\frac{1 - m/m_4}{1 - m_*/m_4}\right)^2$$

HUB

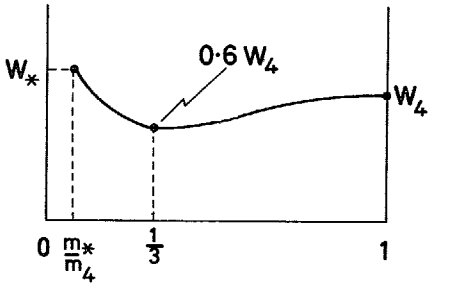

when $\frac{m_*}{m_4} < \frac{m}{m_4} < \frac{1}{3}$

$$0.6\ W_4 + (W_* - 0.6\ W_4)\left(\frac{\frac{1}{3} - m/m_4}{\frac{1}{3} - m_*/m_4}\right)^2$$

when $\frac{1}{3} < \frac{m}{m_4} < 1$

$$W_4\left[1 - 2.7\ \frac{m}{m_4}\left(1 - \frac{m}{m_4}\right)^2\right]$$

Hub and tip have different values of W_* and of $\frac{m_*}{m_4}$ but same W_4.

TIP

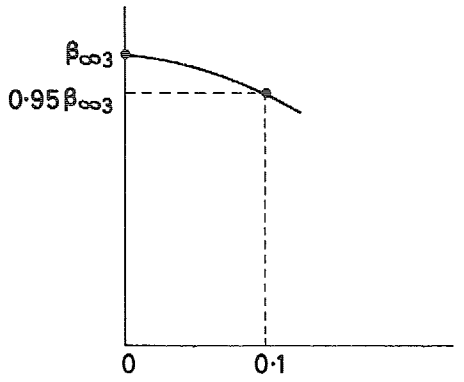

β_∞ (blade angle)

near leading edge

$$\beta_{\infty 3}\left[1 - 5\left(\frac{m}{m_4}\right)^2\right]$$

HUB

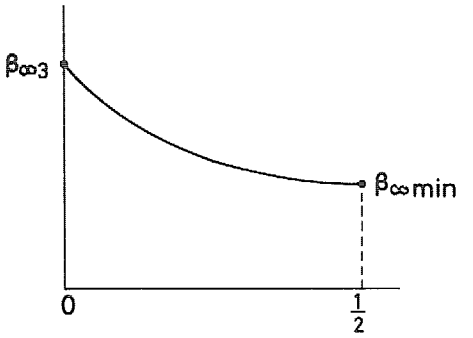

near leading edge

$$\beta_{\infty 3} - 4\left(\beta_{\infty 3} - \beta_{\infty min}\right)\frac{m}{m_4}\left(1 - \frac{m}{m_4}\right)$$

where $$\beta_{\infty min} = \tfrac{1}{6}\beta_{\infty 4}\left(1 + \tfrac{1}{15}\beta_{\infty 3}\right)$$

noting that $\beta_{\infty 3}$ is in degrees.

The prescribed variation of β_∞ is only used to find the throat position $\frac{m_*}{m_4}$, whence $\beta_{\infty *}$ and $\left[\frac{d\beta_\infty}{d(m/m_4)}\right]_*$; hub and tip have different values of $\beta_{\infty 3}$, $\beta_{\infty *}$ etc:

$$\left[\frac{d\beta_\infty}{d(m/m_4)}\right]_* = -10\,\beta_{\infty 3}\frac{m_*}{m_4}$$

$$\left[\frac{d\beta_\infty}{d(m/m_4)}\right]_* = -4\left(\beta_{\infty 3} - \beta_{\infty min}\right)\left(1 - 2\frac{m_*}{m_4}\right)$$

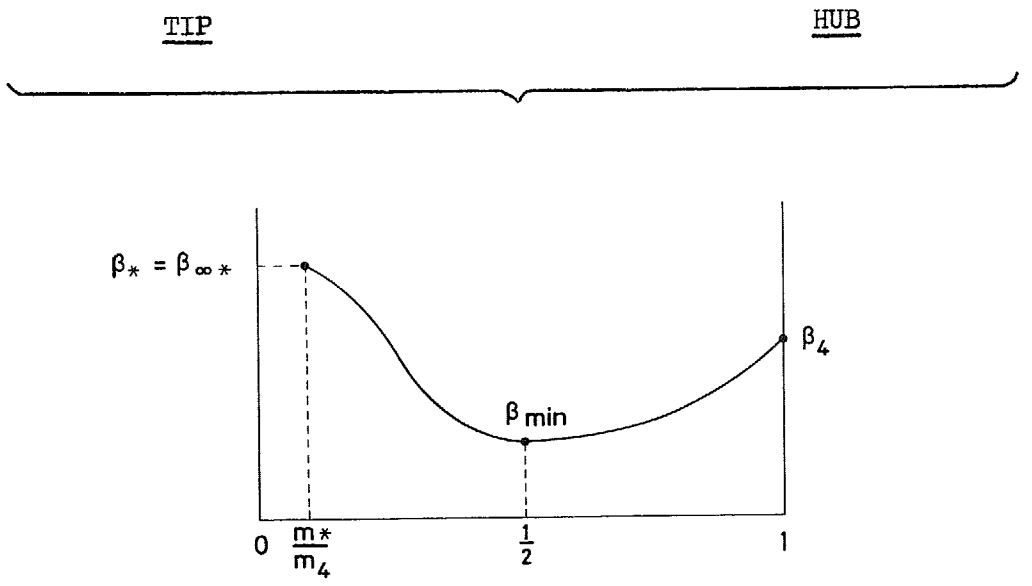

β
(flow
angle)

when $\frac{m_*}{m_4} < \frac{m}{m_4} < \frac{1}{2}$

$$\left[E_1\left(\frac{m}{m_4}\right)^3 + E_2\left(\frac{m}{m_4}\right)^2 + E_3\left(\frac{m}{m_4}\right) + E_4\right]\left(\frac{1}{2} - \frac{m_*}{m_4}\right)^{-3}$$

β (cont'd)

where

$$\begin{cases} E_1 = \left(\frac{1}{2} - \frac{m_*}{m_4}\right)\left[\frac{d\beta_\infty}{d(m/m_4)}\right]_* + 2\left(\beta_* - \beta_{min}\right) \\ E_2 = -\left(\frac{1}{2} - \frac{m_*}{m_4}\right)\left(1 + \frac{m_*}{m_4}\right)\left[\frac{d\beta_\infty}{d(m/m_4)}\right]_* - 3\left(\frac{1}{2} + \frac{m_*}{m_4}\right)\left(\beta_* - \beta_{min}\right) \\ E_3 = \left(\frac{1}{2} - \frac{m_*}{m_4}\right)\left(\frac{1}{4} + \frac{m_*}{m_4}\right)\left[\frac{d\beta_\infty}{d(m/m_4)}\right]_* + 3\frac{m_*}{m_4}\left(\beta_* - \beta_{min}\right) \\ E_4 = -\frac{1}{4}\left(\frac{1}{2} - \frac{m_*}{m_4}\right)\left(\frac{m_*}{m_4}\right)\left[\frac{d\beta_\infty}{d(m/m_4)}\right]_* + \frac{1}{4}\left(\frac{1}{2} - 3\frac{m_*}{m_4}\right)\beta_* + \left(\frac{3}{2} - \frac{m_*}{m_4}\right)\left(\frac{m_*}{m_4}\right)^2\beta_{min} \end{cases}$$

when $\frac{1}{2} < \frac{m}{m_4} < 1$

$$\beta_4 - 4\left(\beta_4 - \beta_{min}\right)\frac{m}{m_4}\left(1 - \frac{m}{m_4}\right)$$

where $\beta_{min} = \frac{1}{6}\beta_4\left(1 + \frac{1}{15}\beta_*\right)$ noting that β_* is in degrees.

Hub and tip have different values of β_* and of $\frac{m_*}{m_4}$ but same β_4.

Notes: 1. W_* and β_* can be found ab initio (see later) but not W_4 and β_4; initial values of W_4 and β_4 must be assumed as part of an iterative procedure.

2. W as prescribed is regarded as being the velocity in an assumed local isentropic core, i.e. on the edge of the surface boundary layer; the flow angle β is assumed to be the same through the boundary layer as in the local isentropic core.

Flow adjustment at rotor inlet

Consider mid-stream path only. At any incidence assume that the flow angle equals the blade angle at the throat, slip being there ignored since ϕ is small: i.e. $\beta_* = \tilde{\beta}_* = \beta_{\infty *}$. At zero incidence the flow and blade angles are equal all the way from inlet to throat.

Define the throat as follows (see Appendix 3-4), ignoring any change of ϕ between inlet and throat $\left(\text{as } \frac{m_*}{m_4} \text{ is typically } <5 \text{ per cent}\right)$:-

$$m_* = \frac{\frac{1}{2} s_3}{\cot \beta_{\infty a} + \tan \beta_{\infty b}} + \frac{1}{2} t_3$$

where $\begin{cases} \beta_{\infty a} \text{ is value of } \beta_\infty \text{ at } m = 2m_* - t_3 \\ \beta_{\infty b} = \frac{1}{2}\left(\beta_{\infty 3} + \beta_{\infty a}\right) \end{cases}$

$$s_3 = \frac{2\pi r_3}{n_f}$$

$$\therefore \quad \frac{m_*}{m_4} = \frac{\pi r_3}{n_f m_4}\left(\frac{1}{\cot \beta_{\infty a} + \tan \beta_{\infty b}}\right) + \frac{t_3}{2m_4}$$

where all quantities (including t_3) differ between hub and tip.

Since variation of β_∞ with $\frac{m}{m_4}$ is known, $\frac{m_*}{m_4}$ can be found by iteration (assume m_*; find $\beta_{\infty a}$; check relation for m_*; repeat to agree).

Note: the above expression is not very sensitive to t_3, and if this is not known a value of 0.05 × mean inlet radius may reasonably be used.

Hence β_*

To find W_*

Because the throat is close to the leading edge, $r_3 \approx r_*$, and little error should result from assuming at either hub or tip

$$s_* = s_3 \qquad \text{and} \qquad T_{t,*}' = T_{t,3}'$$

Hence $P_{t,*}' = P_{t,3}'$ (except as below in case of shock)

But strictly

$$s_* = \frac{2\pi r_*}{n_f} \qquad \text{where } r_* \text{ is known from } m_*$$

$T_{t,*}'$ is found from

$$C_p T_{t,*}' = I_3 + \frac{(r_* \Omega)^2}{2gJ}$$

Hence

$$P_{t,*}' = P_{t,3}' \left(\frac{T_{t,*}'}{T_{t,3}'} \right)^{\frac{\gamma}{\gamma-1}}$$

If $M_3' > 1$ there will be a shock system around the leading edge (at hub or tip as appropriate), and then

$$P_{t,*}' = P_{t,3}' \left\{ \left[\frac{(\gamma - 1)\left(M_3'\right)^2 + 2}{(\gamma + 1)\left(M_3'\right)^2} \right]^{\gamma} \left[\frac{2\gamma\left(M_3'\right)^2 - (\gamma - 1)}{\gamma + 1} \right] \right\}^{-\frac{1}{\gamma-1}} \left(\frac{T_{t,*}'}{T_{t,3}'} \right)^{\frac{\gamma}{\gamma-1}}$$

[Note: the loss of P_t is small, only 1 per cent at $M_3' = 1.2$]

Now also assume at hub or tip

$$t_* = t_3 \quad \text{(as in Appendix 3-4)}$$

$$V_{m,*} = V_{m,3} \cdot \frac{\rho_3}{\rho_*} \cdot \frac{s_3}{s_* - t_* \sec \beta_{\infty *}} \cdot \frac{1}{\sigma}$$

where σ is a contraction coefficient treated as equal at hub and tip.

[Note: this implies that change of streamtube thickness in the spanwise direction between inlet and throat is the same for hub and tip.]

From velocity triangle at hub or tip

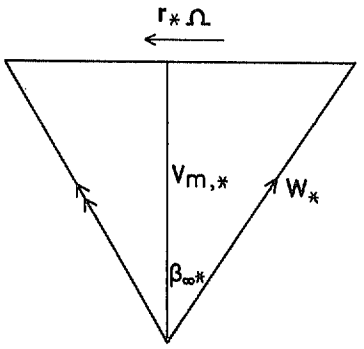

$$W_* = V_{m,*} \sec \beta_{\infty *}$$

Hence $$W_* \cos \beta_{\infty *} = W_3 \cos \beta_3 \left(\frac{\rho_3}{\rho_*}\right) \frac{s_3}{s_* - t_* \sec \beta_{\infty *}} \cdot \frac{1}{\sigma}$$

or $$\frac{W_* \rho_*}{W_3 \rho_3} = \frac{s_3 \cos \beta_3}{s_* \cos \beta_{\infty *} - t_*} \cdot \frac{1}{\sigma}$$

Thus $$\left[\frac{Q\sqrt{T_t}}{A P_t}\right]'_* = \left[\frac{Q\sqrt{T_t}}{A P_t}\right]'_3 \frac{s_3 \cos \beta_3}{s_* \cos \beta_{\infty *} - t_*} \cdot \frac{1}{\sigma} \cdot \frac{P'_{t,3}}{P'_{t,*}} \sqrt{\frac{T'_{t,*}}{T'_{t,3}}}$$

Given σ (see presently) then knowing M'_3

$$M'_3 \longrightarrow \left[\frac{Q\sqrt{T_t}}{A P_t}\right]'_3 \longrightarrow \left[\frac{Q\sqrt{T_t}}{A P_t}\right]'_* \longrightarrow M'_* \longrightarrow \frac{W_*}{\sqrt{T_{t,*}}} \longrightarrow W_*$$

taking subsonic solution for M'_*.

[Note: The above treatment ignores slip, but since ϕ is small at the throat this is reasonable.]

If at either hub or tip

$$\left[\frac{Q\sqrt{T_t}}{A\,P_t}\right]' \geq 0.39633 \text{ in ft-lb-sec-}^{\circ}\text{K units (or } 0.040415 \text{ in SI units)}$$

see later.

Rotor inlet choking limit

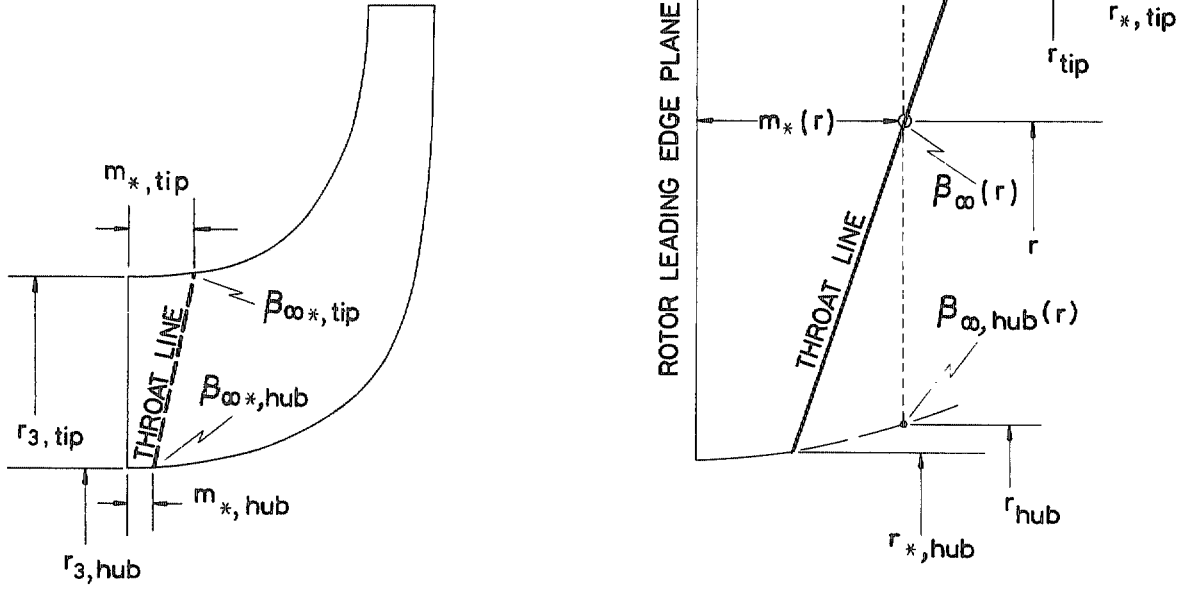

Knowing m_*, find r_* and $\beta_{\infty*}$ (all different at hub and tip).

Assume throat line from hub to tip follows the relation

$$m_*(r) = m_{*,hub} + \left(m_{*,tip} - m_{*,hub}\right)\frac{r - r_{*,hub}}{r_{*,tip} - r_{*,hub}}$$

hence m_* at any value of r $\left[= m_*(r)\right]$ is known.

At $m_*(r)$, values of $\left\{\begin{matrix}\beta_\infty \\ r\end{matrix}\right\}$ at hub and tip are known $\left[\begin{matrix}\beta_{\infty hub}(r); & \beta_{\infty tip}(r) \\ r_{hub} & ; \quad r_{tip}\end{matrix}\right]$

Assume that, at any value of $m_*(r)$, $\tan \beta_\infty$ varies linearly with radius

$$\tan\left[\beta_\infty(r)\right] = \tan\left[\beta_{\infty tip}(r)\right] - \left\{\tan\left[\beta_{\infty tip}(r)\right] - \tan\left[\beta_{\infty hub}(r)\right]\right\} \frac{r_{tip} - r}{r_{tip} - r_{hub}}$$

hence $\beta_\infty(r)$ is known at all points along the throat line.
Throat area is

$$A'_* = B_* \int_{r_{*,hub}}^{r_{*,tip}} \left\{2\pi r \cos\left[\beta_\infty(r)\right] - n_f\, t_*(r)\right\} dr$$

Assume linear variation of t with r

$$t_*(r) = t_{s,hub} + \left(t_{s,tip} - t_{s,hub}\right) \frac{r - r_{*,hub}}{r_{*,tip} - r_{*,hub}}$$

Assume $B_* = B_s \cdot \sigma$

σ is chosen empirically in the light of experiment[*] and should lie in the range $0.9 < \sigma < 1$. It may depend upon the highest M'_s between hub and tip (max M'_s), and a tentative relation is

$$\sigma = \frac{1}{B_s}\left[0.94 - 0.13\ (\max M'_s - 1)\right]$$

when max $M'_s > 1$

or $\frac{0.94}{B_s}$ when max $M'_s \leq 1$

---

[*] See reference to B_s and B_* in Appendix 3-8.

Thus all quantities determining A_*' are known. Integrate by evaluating the $\{\ \}$ term at, say, 10 equal intervals of r and using Simpson's rule.

Hence A_*'.

Take $$\begin{cases} \overline{T_{t,*}}' \simeq \frac{1}{2}\left(T_{t,*,tip}' + T_{t,*,hub}'\right) \\ \overline{P_{t,*}}' \simeq \frac{1}{2}\left(P_{t,*,tip}' + P_{t,*,hub}'\right) \end{cases}$$

Knowing Q ; $\overline{T_{t,*}}'$; $\overline{P_{t,*}}'$; A_*' evaluate $\dfrac{Q\sqrt{\overline{T_{t,*}}'}}{A_*'\,\overline{P_{t,*}}'}$

and if $\geqslant 0.39633$ in ft-lb-sec-$^{\circ}$K units (or 0.040415 in SI units) the inducer is choked, and the calculation ends.

If the flow as a whole is not choked, i.e. if $\dfrac{Q\sqrt{\overline{T_{t,*}}'}}{A_*'\,\overline{P_{t,*}}'} < 0.39633$, but at either hub or tip $\left[\dfrac{Q\sqrt{T_t}}{A\,P_t}\right]_*' \geqslant 0.39633$ as previously evaluated, then

proceed as follows.

Assume streamtube thickness adjusts so that $M_*' = 1$ at whichever of hub or tip has $\left[\dfrac{Q\sqrt{T_t}}{A\,P_t}\right]_*' \geqslant 0.39633$

Also assume $M_{*,hub}' + M_{*,tip}' = 2\,\bar{M}_*'$

where $\bar{M}_*'$ corresponds to $\dfrac{Q\sqrt{\overline{T_{t,*}}'}}{A_*'\,\overline{P_{t,*}}'}$ as evaluated for whole flow, taking subsonic solution for $\bar{M}_*'$.

Thus M_*' is known at both hub and tip; hence values of $\dfrac{W_*}{\sqrt{T_{t,*}'}}$ and $W_{\perp *}$.

Initial choice of W_4 and β_4

Both W_4 and β_4 are the same for hub and tip.

Since it is easier to make a reasonable first guess at β_4 than at W_4, this condition is used, and thereafter the main iterative loop will operate via change of β_4. Experience suggests that the first guess for β_4 be taken as about 12° more than $\beta_{\infty 4}$, the value increasing with reduction of Q below choking and decreasing with reduction of Q below $\tilde{Q}$.

It is then necessary to select an initial value of W_4 for the preliminary iterative loop. For this purpose assume a value of B_4 (typically say 0.8); then the continuity relation gives W_4, as follows.

I_3 is known at hub and tip and I is constant along any streamline (secondary flows being ignored),

thus
$$\begin{cases} I_{3,tip} = I_{4,tip} \\ I_{3,hub} = I_{4,hub} \end{cases}$$

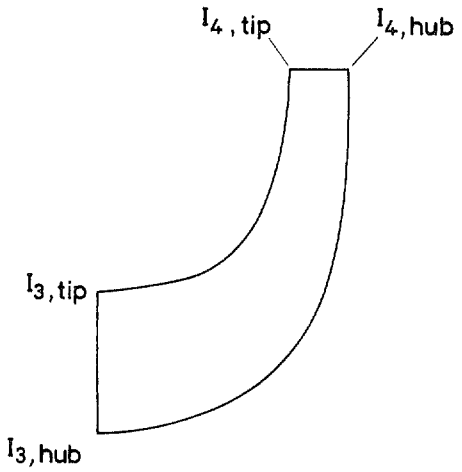

Thus at outlet

$$C_p T_{t,4}' = I_3 + \frac{(r_4 \Omega)^2}{2gJ}$$

Hence $T_{t,4}'$ (different at hub and tip)

Assuming flow outside boundary layers to be locally isentropic

$$P_{t,4}' = P_{t,3}' \left(\frac{T_{t,4}'}{T_{t,3}'} \right)^{\frac{\gamma}{\gamma-1}} \qquad \text{(different at hub and tip)}$$

Hence average values
$$\begin{cases} \overline{T_{t,4}'} = \frac{1}{2} \left(T_{t,4,hub}' + T_{t,4,tip}' \right) \\ \overline{P_{t,4}'} = \frac{1}{2} \left(P_{t,4,hub}' + P_{t,4,tip}' \right) \end{cases}$$

Q is known

$A_4' = B_4 \cdot 2\pi r_4 h_4 \cos \beta_4$, B_4 and β_4 being assumed as above.

Hence $$\frac{Q\sqrt{T_{t,4}'}}{A_4' P_{t,4}'} \longrightarrow M_4' \longrightarrow \frac{W_4}{\sqrt{T_{t,4}'}} \longrightarrow W_4$$

taking subsonic solution for M_4'.

The iterative procedure is then as depicted.

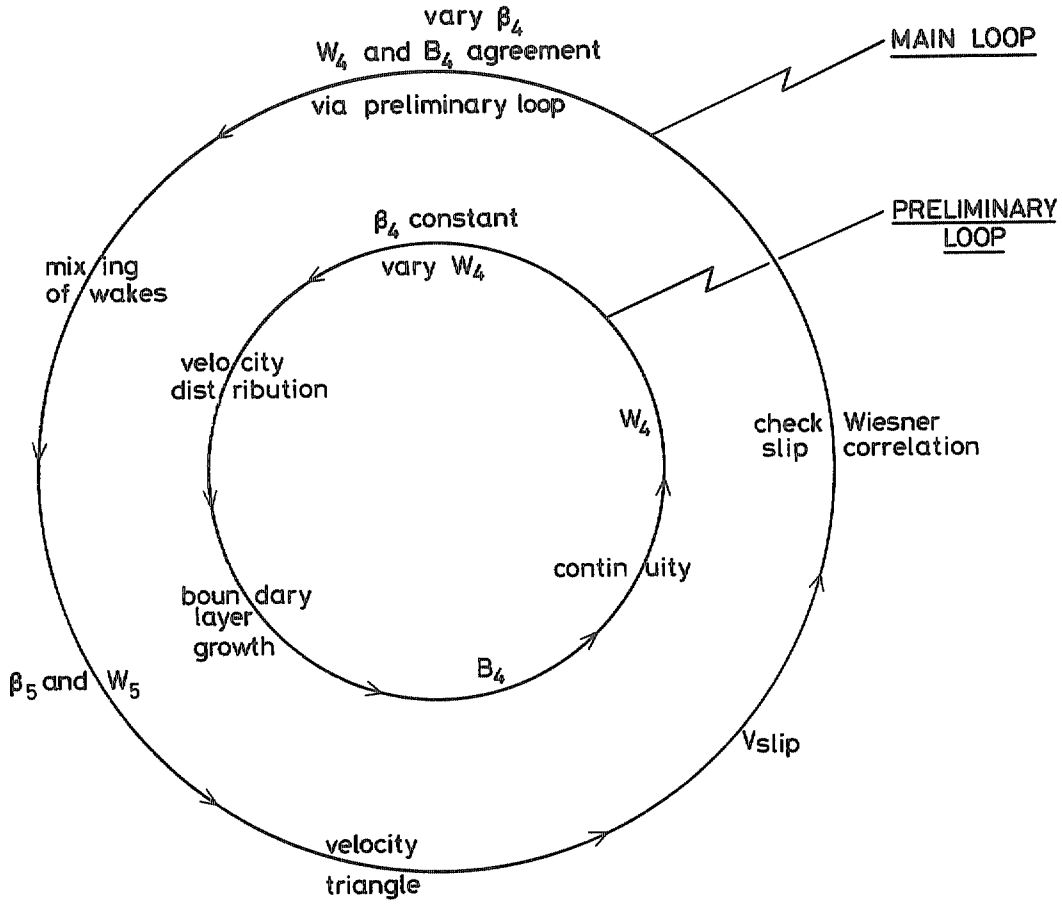

Each choice of β_4 in the main loop requires a solution for W_4 and B_4 via the preliminary loop.

It is necessary to check continuously throughout the iterative procedures that values of B_4 and β_4 at any stage do not give $\left[\frac{Q\sqrt{T_t}}{A\ P_t}\right]_4$ above the limiting value. In cases when the boundary layer growth assumed is extremely high, it is possible for choking to occur at rotor outlet, in which event no solution can be achieved.

Calculation of mean velocity through rotor

This is expressed as $\frac{W}{W_3}$ (always +ve, and = 1 at inlet).

W_3 is known and W_* is known (both different at hub and tip).

Assume a linear variation of $\frac{W}{W_3}$ between inlet and throat

$$\text{i.e.} \qquad \frac{W}{W_3} = 1 + \frac{(m/m_4)}{(m_*/m_4)}\left(\frac{W_*}{W_3} - 1\right)$$

Between throat and outlet, the form is as prescribed for either hub or tip. Hence W everywhere is known.

Calculation of whirl velocity

The quantity wanted is $\frac{r\ V_w}{m_4\ W_3} = L$ (different at hub and tip)

At inlet $V_{w,3}$ and W_3 are known

$$\text{hence} \qquad L_3 = \frac{r_3\ V_{w,3}}{m_4\ W_3}$$

At the throat and thereafter the complete velocity triangle is defined (see Appendix 3-5), and V_w is known from

$$V_w = r\Omega - W \sin \beta$$

hence L is known from throat to outlet.

The variation of L between inlet and throat is as given presently, knowing

$\frac{L_* - L_3}{(m_*/m_4)}$, chosen in order that the inlet loading is zero.

Calculation of blade loading

This is expressed as $\frac{\Delta W}{W_3}$ (required to be zero at inlet; elsewhere may be +ve or -ve)

In general $\frac{\Delta W}{W_3} = \frac{2\pi}{n} \cos \beta_\infty \frac{d(L)}{d(m/m_4)}$ (see Appendix 3-7)

At the throat and any station thereafter $\frac{d(L)}{d(m/m_4)} \left[= \dot{L}\right]$ must be obtained

from the calculated values of L. This may conveniently be done by fitting a cubic (or perhaps quadratic) to the neighbouring values of L at each calculation point and differentiating.

Hence $\dot{L}$.

Between inlet and throat prescribe a maximum value of $\dot{L}$ as

$$\dot{L}_{max} = k \frac{L_* - L_3}{(m_*/m_4)}$$

where a reasonable value of k may be 1.2.

Then L_3, L_*, $\dot{L}_*$, $\dot{L}_{max}$ are known, and $\dot{L}_3$ is taken as zero in order to give zero inlet loading in all cases.

This region (between inlet and throat) is divided into three parts

(i) for $0 < \frac{m}{m_4} < \frac{\dot{L}_{max}}{q}$

take $\begin{cases} L = \frac{q}{2}\left(\frac{m}{m_4}\right)^2 + L_3 \\ \dot{L} = q\left(\frac{m}{m_4}\right) \end{cases}$

(ii) for $\frac{\dot{L}_{max}}{q} < \frac{m}{m_4} < \left(\frac{m_*}{m_4} - \frac{\dot{L}_{max} - \dot{L}_*}{q}\right)$

take
$$\begin{cases} L = \dot{L}_{max}\left(\frac{m}{m_4}\right) + \left[L_3 - \frac{\left(\dot{L}_{max}\right)^2}{2q}\right] \\ \dot{L} = \dot{L}_{max} \end{cases}$$

(iii) for $\left(\frac{m_*}{m_4} - \frac{\dot{L}_{max} - \dot{L}_*}{q}\right) < \frac{m}{m_4} < \frac{m_*}{m_4}$

take
$$\begin{cases} L = -\frac{q}{2}\left(\frac{m}{m_4}\right)^2 + \left[\dot{L}_* + q\left(\frac{m_*}{m_4}\right)\right]\left(\frac{m}{m_4}\right) + \\ \qquad + \left[L_* - \dot{L}_*\left(\frac{m_*}{m_4}\right) - \frac{q}{2}\left(\frac{m_*}{m_4}\right)^2\right] \\ \dot{L} = -q\left(\frac{m}{m_4}\right) + \left[\dot{L}_* + q\left(\frac{m_*}{m_4}\right)\right] \end{cases}$$

where
$$q = \frac{\left(\dot{L}_{max} - \dot{L}_*\right)^2 + \left(\dot{L}_{max}\right)^2}{2\left[\dot{L}_{max}\left(\frac{m_*}{m_4}\right) - \left(L_* - L_3\right)\right]}$$

These relations ensure no sudden change of $\dot{L}$ and hence of loading at the throat

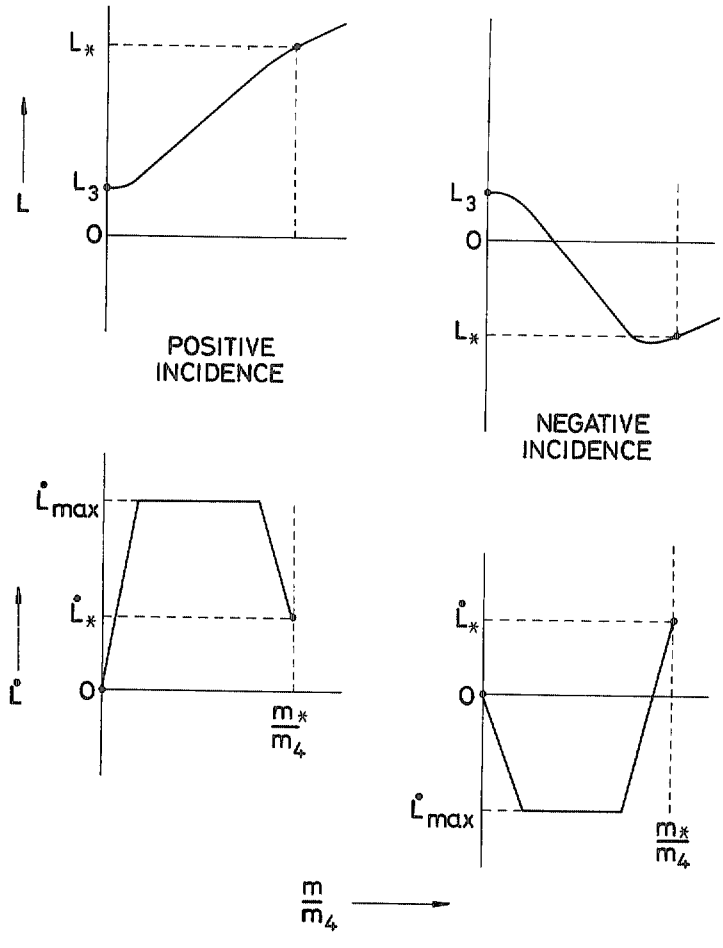

$\dot{L}$ is now known everywhere.

β_∞ is not known between throat and outlet. The difference between β_∞ and β increases from throat to outlet, and for the present purpose it should be adequate to assume that this difference varies linearly with m from zero at the throat to the known outlet value, i.e.

$$\beta_\infty = \beta - \left(\frac{m/m_4 - m_*/m_4}{1 - m_*/m_4}\right)\left(\beta_4 - \beta_{\infty 4}\right)$$

Hence $\frac{\Delta W}{W_3}$ everywhere.

Treatment of intervanes

Where intervanes start, the full-blade value of $\frac{\Delta W}{W_3}$ will change from $\left[\frac{2\pi}{n_f}\left(\cos \beta_\infty\right)\dot{L}\right]$ to $\left[\frac{2\pi}{n_f + n_i}\left(\cos \beta_\infty\right)\dot{L}\right]$, normally being halved, and thereafter both full and half blades have same $\frac{\Delta W}{W_3}$.

An instantaneous change of $\frac{\Delta W}{W_3}$ is not acceptable for either full or half blades, and in addition the half-blade loading should be zero at its leading edge; hence proceed as follows.

Treat the half blades as starting at the calculating station immediately after the specified leading edge position. At that station the full-blade value of $\frac{\Delta W}{W_3}$ is $\left[\frac{2\pi}{n_f}\left(\cos \beta_\infty\right)\dot{L}\right]$ as evaluated by the foregoing method, and the half-blade value of $\frac{\Delta W}{W_3}$ is zero.

Assume linear variation of $\frac{\Delta W}{W_3}$ between the above values and that calculated at the immediately following station according to $\left[\frac{2\pi}{n_f + n_i}\left(\cos \beta_\infty\right)\dot{L}\right]$.

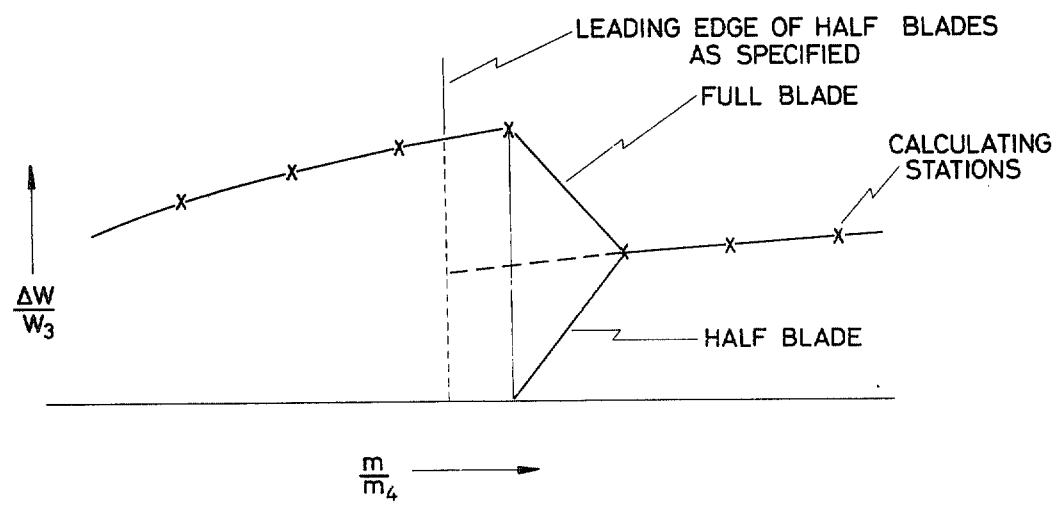

Calculation of surface velocities

Suction surface : $\frac{W_{ss}}{W_3} = \frac{W}{W_3} + \frac{1}{2}\frac{\Delta W}{W_3}$

Pressure surface : $\frac{W_{ps}}{W_3} = \frac{W}{W_3} - \frac{1}{2}\frac{\Delta W}{W_3}$

In general this procedure yields four different full-blade surface velocity distributions:-

tip suction surface	$\left(W_{ss}/W_3\right)_{tip}$
tip pressure surface	$\left(W_{ps}/W_3\right)_{tip}$
hub suction surface	$\left(W_{ss}/W_3\right)_{hub}$
hub pressure surface	$\left(W_{ps}/W_3\right)_{hub}$

With intervanes there are a total of eight different pressure and suction surface velocity distributions, those on full and half blades being equal beyond the second calculating station following the specified half-blade leading edge, since the same value of W is applied to both full and half blades.

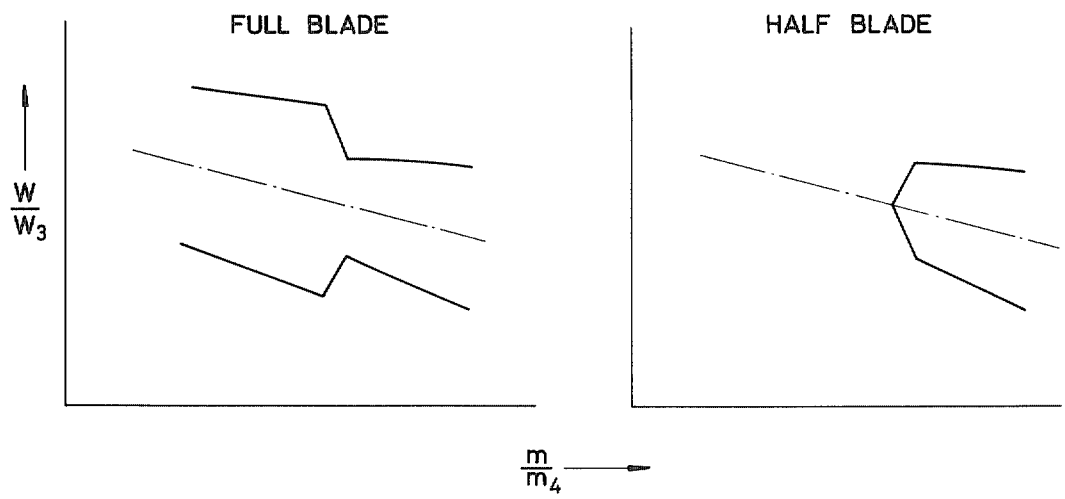

If this treatment gives any negative values of $\frac{W}{W_3}$ (e.g. on pressure surface at high positive incidence), these are replaced by zero.

Also there are two mean velocity distributions

$$\text{tip mean} \qquad \left(W/W_3\right)_{tip}$$

$$\text{hub mean} \qquad \left(W/W_3\right)_{hub}$$

which are considered as applying to shroud and hub (i.e. non-blade) surfaces respectively.

[Note: Although hub mean and tip mean values of W_4 are the same, the pressure and suction surface values at outlet $\left(W_{ss,4} \text{ and } W_{ps,4}\right)$ are not equal to that mean W_4. In reality blades cannot support any loading at their trailing edge, and some adjustment must take place; this probably leads to a rapid off-loading very close to the trailing edge which cannot be predicted in this treatment. But see presently for method of allowing for this off-loading in calculation of boundary layer thickness at trailing edge.]

Calculation of boundary layer thickness at rotor outlet

The values of W just obtained are regarded as being the distribution of velocity at the edge of the boundary layer that has grown on each surface.

Assume that in association with each individual surface a local isentropic "core" or mainstream exists, having properties P_t' and T_t' (see Appendix 3-8). Values of P_t' and T_t' at any station are different for hub and tip, but for either hub or tip the values of P_t' and T_t' are the same for suction, pressure, and mean (non-blade) surfaces. Thus it follows that all surfaces are treated as having different static pressure at any station.

For each velocity distribution values of δ^* and θ are calculated (see Appendix 3-8 for general comments on the procedure adopted).

Rothalpy is constant at either hub or tip, and inlet value I_3 is known at hub and tip. Hence at any point

$$C_p T_t' - \frac{U^2}{2gJ} = I_3$$

$$\therefore \qquad T_t' = \frac{I_3 + (r\Omega)^2/2gJ}{C_p} \qquad \text{which is then known}$$

Taking a particular surface velocity distribution $\left(\frac{W}{W_3} \text{ vs: } \frac{m}{m_4}\right)$, the value of $\frac{W}{\sqrt{T_t'}}$ is determined at any station on the surface.

Hence the relative Mach number M' at that station; this is the local core or mainstream value on the edge of the boundary layer growing on the particular surface.

Evaluate $$p = \left[\frac{M'}{1 + 0.2\,(M')^2}\right]^4$$ (see Stratford & Beavers[6] for turbulent boundary layer)

If S is surface length, $dS = \sec \beta_\infty \, dm$

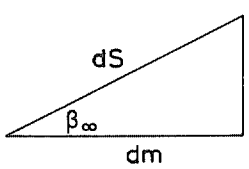

Then "equivalent flat plate length" (ℓ) is given by

$$\ell = \frac{1}{p}\int_0^S p \, dS \qquad \therefore \qquad \frac{\ell}{m_4} = \frac{1}{p}\int_0^{m/m_4} p \sec \beta_\infty \, d(m/m_4)$$

where p outside the integral is the local value corresponding to M' at the station in question.

The integral is evaluated assuming linear variation of p sec β_∞ over each calculation interval, using some means like Simpson's rule.

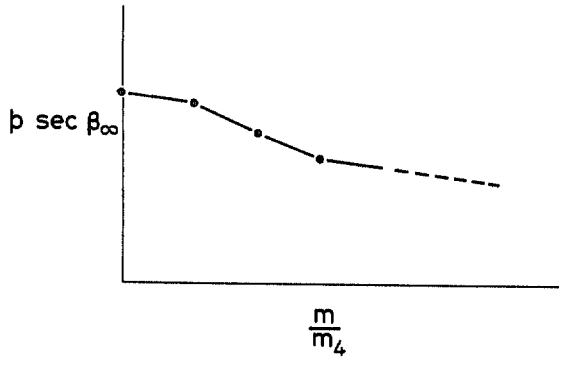

Hence is derived, for each surface considered, the quantity

$$\text{int} = \int_0^1 p \sec \beta_\infty \, d(m/m_4)$$ at rotor outlet, the integral being evaluated on the basis that the value of p at rotor outlet corresponds to the outlet velocity for that surface as given by the foregoing treatment (i.e. with finite blade loading at the trailing edge). This is done for convenience in order to permit fairly large calculation intervals near outlet (e.g. 0.1 in m/m_4), as

$\int p \sec \beta_\infty \, d(m/m_4)$ changes only slightly towards rotor outlet.

Allowance for closure of the velocity distribution at the trailing edge is then made by putting

$$\frac{\ell_4}{m_4} = \frac{1}{p_4} (\text{int})$$

in which M_4' and p_4 for all surfaces are taken as corresponding to the unique <u>mean</u> condition W_4.

In the case of the hub and shroud surfaces (treated as having the mean velocity distributions) boundary layer growth effectively starts not from zero thickness at rotor inlet but from a condition corresponding to the inlet blockage. Hence for these surfaces

$$\frac{\ell_4}{m_4} = \frac{1}{p_4}\left[(\text{int}) + \frac{\ell_3\, p_3}{m_4}\right]$$

where
$$\ell_3 = \left\{ \frac{\overline{\delta_3^*}}{0.046\left[1 + 0.8\left(M_3'\right)^m\right]^{0.44}\left(\frac{\rho_3 V_3}{\mu_3}\right)^{-0.2}} \right\}^{1.25}$$

and $\overline{\delta_3^*} = \frac{1}{2} h_3 (1 - B_3)$ as before

(ℓ_3 is different for hub and tip)

[Note: if inlet boundary layer proportions are known, different values can be used for $\delta^*_{3,tip}$ and $\delta^*_{3,hub}$, rather than taking $\overline{\delta_3^*}$ for each wall. For axial compressor situations it is often found that the outer wall boundary layer thickness is approximately twice the inner. In the general case

$$\delta^*_{3,tip} = k \cdot \delta^*_{3,hub} = \frac{k}{2}\left(\frac{D_{3,tip} + D_{3,hub}}{k \cdot D_{3,tip} + D_{3,hub}}\right) h_3 (1 - B_3)$$]

Everywhere on all blade surfaces use β_∞ as written above, and between throat and outlet take β_∞ according to the linear relation adopted in the Section "Calculation of blade loading". But on shroud and hub surfaces (corresponding to mean W distributions) replace β_∞ by the following:

from throat to outlet, use β as prescribed
from inlet to throat, use β evaluated from

$$\sin\beta = \frac{r\Omega - m_4 W_3 L/r}{W}$$

where distributions of W and L are known.

Then, for a one-seventh-power velocity profile and probable range of Re, thicknesses at outlet are (from Stratford & Beavers[6])

$$\frac{\delta^*}{m_4} = 0.046\left[1 + 0.8\left(M_4'\right)^2\right]^{0.44}\frac{\ell_4}{m_4}\left(Re_{\ell,4}\right)^{-0.2}$$

$$\frac{\theta}{m_4} = 0.036\left[1 + 0.1\left(M_4'\right)^2\right]^{-0.7}\frac{\ell_4}{m_4}\left(Re_{\ell,4}\right)^{-0.2}$$

where $$Re_{\ell,4} = \left(\frac{\ell_4}{m_4}\right)\frac{\rho_4\, W_4\, m_4}{\mu_4}$$

In these expressions M_4', ρ_4 and μ_4 again correspond to the unique mean condition W_4 (i.e. they differ between hub and tip but not between pressure and suction surfaces).

ρ_4 and μ_4 are still to be fixed. Since $T_{t,4}'$ is known (from rothalpy), the assumption of local isentropic cores gives $P_{t,4}'$ from

$$P_{t,4}' = P_{t,3}'\left(\frac{T_{t,4}'}{T_{t,3}'}\right)^{\frac{\gamma}{\gamma-1}}$$

Both $T_{t,4}'$ and $P_{t,4}'$ are different for hub and tip.

Then for either hub or tip

$$M_4' \longrightarrow \begin{cases} \dfrac{P_{t,4}'}{P_{s,4}} \longrightarrow P_{s,4} \\ \dfrac{T_{t,4}'}{T_{s,4}} \longrightarrow T_{s,4} \end{cases} \qquad \rho_4 = \frac{P_{s,4}}{RT_{s,4}} \qquad \mu_4 = f(T_{s,4})$$

Hence $\frac{\delta^*}{m_4}$ and $\frac{\theta}{m_4}$ for each surface.

Average boundary layer thickness and blockage

Consider two adjacent blade passages at outlet (with intervanes)

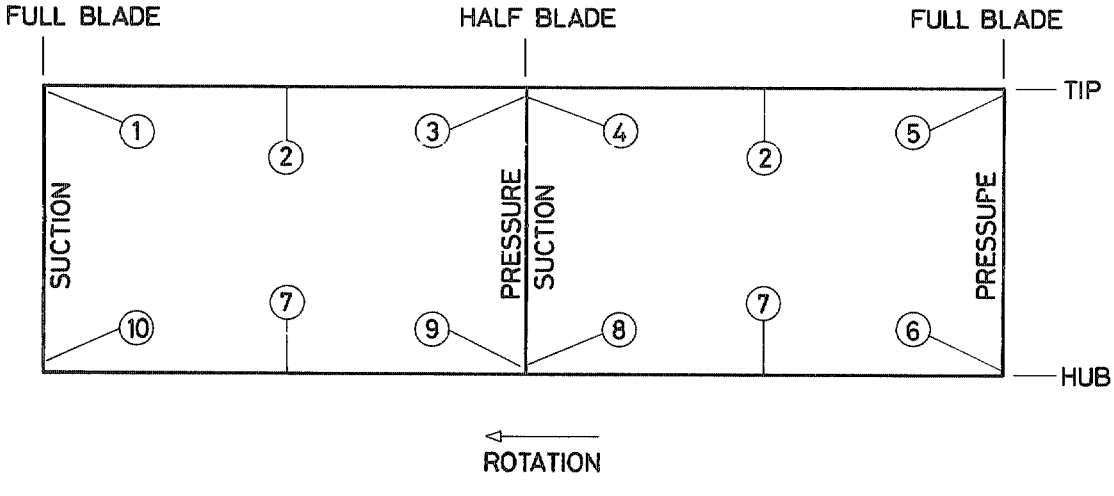

Boundary layer thickness is evaluated at points (1) to (10).

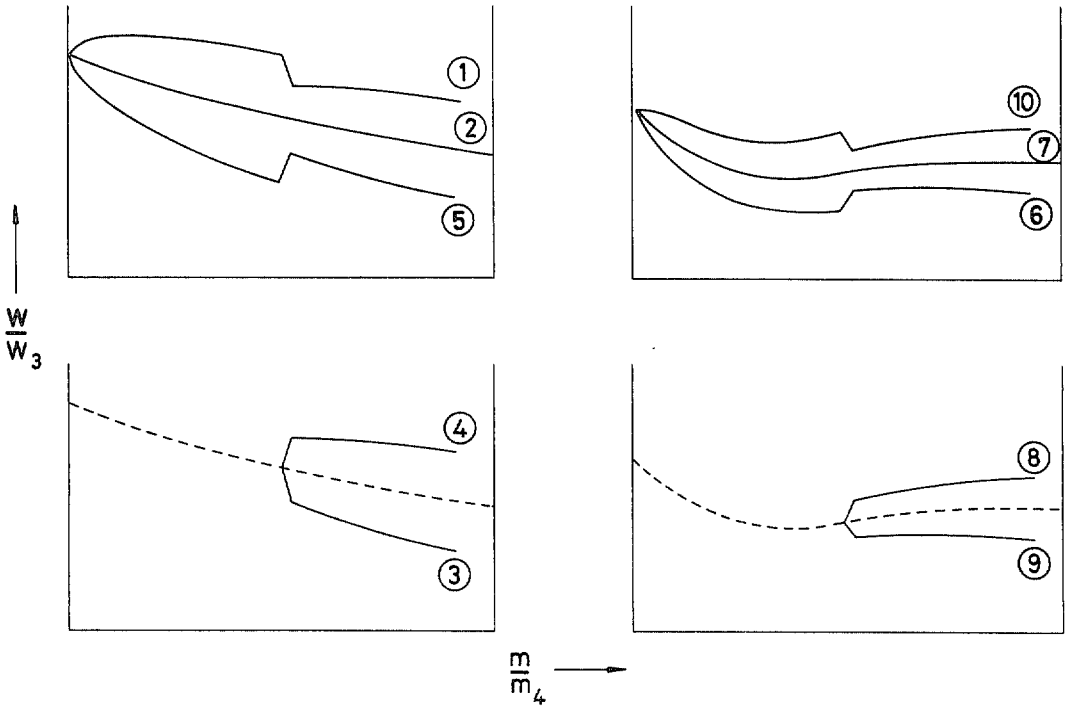

If no intervanes then (3) → (5), (4) → (1), (8) → (10), (9) → (6).
Average thicknesses are required for (i) all axial surfaces, (ii) all tangential surfaces, to apply thus:-

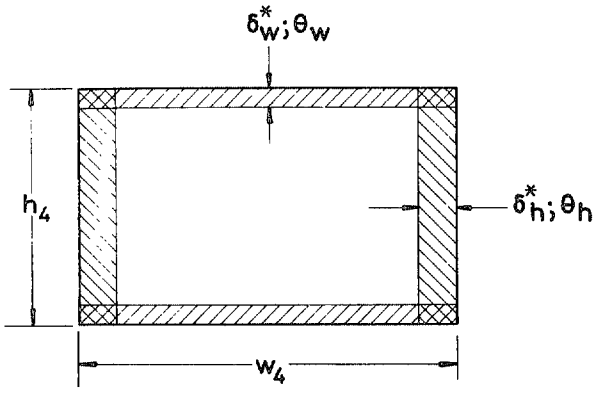

where w_4 is the passage width normal to the flow at rotor outlet, determined as follows:

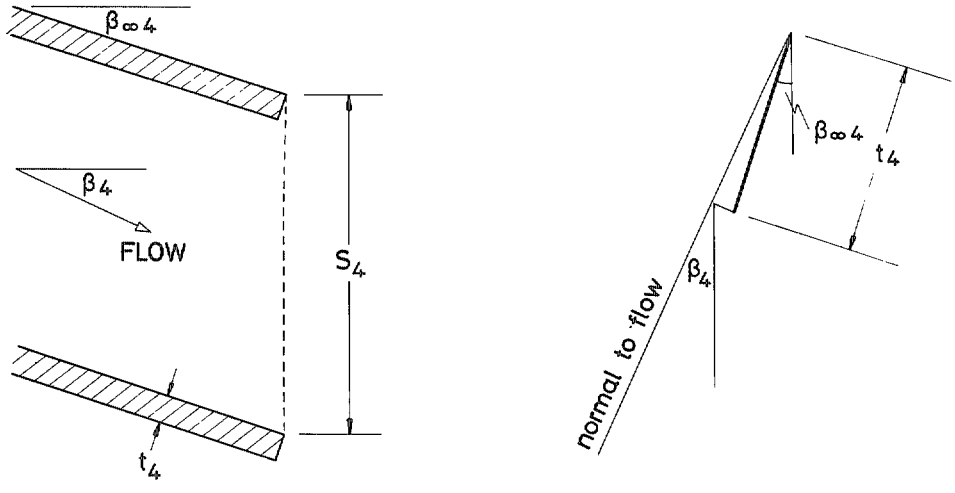

$$s_4 = \frac{2\pi r_4}{n_f + n_i}$$

Blade thickness normal to direction of mainstream flow =

$$t_4 \cos\left(\beta_4 - \beta_{\infty 4}\right)$$

Thus $$w_4 = s_4 \cos \beta_4 - t_4 \cos\left(\beta_4 - \beta_{\infty 4}\right)$$

Increase thicknesses on all suction surfaces [(1), (4), (8), (10)] by factor Z (see Appendix 3-8), where Z is to be specified.

Take average thickness on axial surfaces (suffix h) as mean of (1), (3), (4), (5), (6), (8), (9), (10)

and average thickness on tangential surfaces (suffix w) as mean of (2), (7)

Total passage area = $w_4 h_4 (n_f + n_i)$

Boundary layer blockage per passage is

$$w_4 h_4 - \left(w_4 - 2\delta_h^*\right)\left(h_4 - 2\delta_w^*\right)$$

Hence $$A_4' = B_4 w_4 h_4 (n_f + n_i)$$

where $$B_4 = \frac{\left(w_4 - 2\delta_h^*\right)\left(h_4 - 2\delta_w^*\right)}{w_4 h_4}$$

The foregoing treatment does not cater for rake of blades at trailing edge

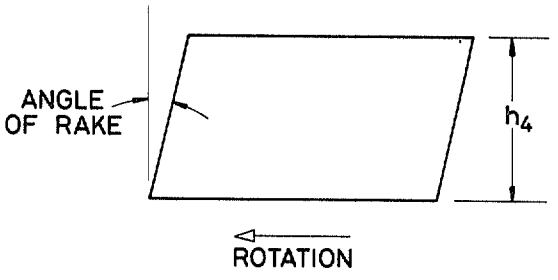

Provided that $\beta_{\infty 4}$ remains the same at hub as at tip, then

$$w_4 = s_4 \cos\beta_4 - t_4 \cos\left(\beta_4 - \beta_{\infty 4}\right) \sec(\text{rake})$$

$$A_4' = B_4\, w_4\, h_4 \left(n_f + n_i\right) \qquad \text{as before}$$

where now $$B_4 = \frac{\left[w_4 - 2\,\delta_h^*\sec(\text{rake})\right]\left(h_4 - 2\,\delta_w^*\right)}{w_4\, h_4}$$

Relative conditions at rotor outlet

We require the average core or mainstream flow conditions relating to the area (A_4') that allows for blockage.

Know $\begin{cases} Q;\ A_4' \\ T_{t,4}';\ P_{t,4}' \quad \text{different at hub and tip} \end{cases}$

take $\begin{cases} \overline{T_{t,4}'} = \frac{1}{2}\left(T_{t,4',\text{hub}} + T_{t,4',\text{tip}}\right) \\ \overline{P_{t,4}'} = \frac{1}{2}\left(P_{t,4',\text{hub}} + P_{t,4',\text{tip}}\right) \end{cases}$

[Note: in most normal cases $T_{t,4',\text{hub}}$ and $T_{t,4',\text{tip}}$ differ by only some 10°K, so that this simple averaging of $T_{t,4}'$ and $P_{t,4}'$ is reasonable. Where the hub and tip values differ much more widely, as in the case of a large difference in $\alpha_{3,\text{hub}}$ and $\alpha_{3,\text{tip}}$, then it may be that some

mass-weighted averaging of $T_{t,4}'$ and $P_{t,4}'$ should be used - in other words that the conservation of rothalpy applied to streamlines at hub and tip should be associated with proportions of flow representative of those streamlines, more flow at the tip than at the hub. But such flow weighting can only be arbitrary, and in view of the uncertainties involved is omitted.]

Then $$\frac{Q\sqrt{\overline{T_{t,4}'}}}{A_4'\,\overline{P_{t,4}'}} \longrightarrow M_4' \longrightarrow \frac{W_4}{\sqrt{\overline{T_{t,4}'}}} \longrightarrow W_4$$

taking subsonic solution for M_4'.

This defines the situation before mixing-out of "wakes" to a one-dimensional flow (station 5).

[Note: uniform static pressure $\left(\overline{P_{s,4}}\right.$: corresponding to $\overline{P_{t,4}'}$ and $\left.M_4'\right)$ is assumed throughout the whole flow passage for the mixing calculation.]

Check on value of W_4

Each circuit of the main iterative loop corresponds to a particular value of β_4. For that β_4, an initial choice of W_4 is obtained as given previously, leading via surface velocity distributions and boundary layer growth to a value of B_4 and hence, as just set out, to a further value of W_4. The latter must match the input W_4. Thus it is necessary to do a subsidiary iteration at this stage, keeping constant β_4 and varying W_4 until match of W_4 is obtained.

Mixing of "wakes"

The equations are written to include a change of dimension ($h_5 \neq h_4$). Many arrangements of geometry are possible at rotor outlet; A, B, C are three examples. In cases A and B, $h_5 = h$, but in case C the effective axial dimension for the flow is open to doubt. Variation of h_5 leads to variation of work input, and some limited experience from

test data suggests that in case C the value used should be

$$h_5 \simeq \frac{h + h_4}{2}$$

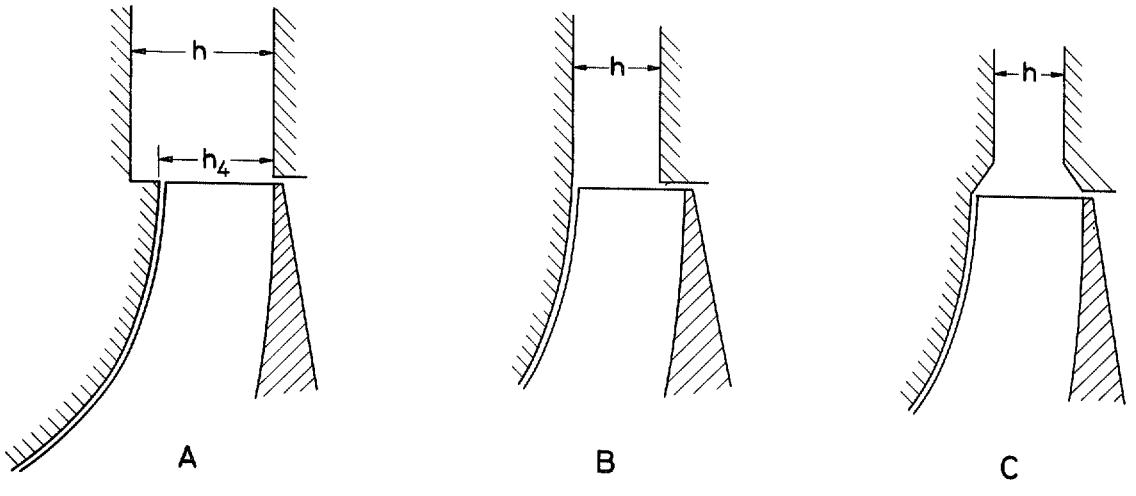

[Note: mixing is assumed to be instantaneous so that no change of radius is involved (c.f. the small radius ratio noted in experiments by Dean & Senoo[7]). This means that relative momenta are conserved (see Appendix 3-9) and T_t' is constant (from rothalpy). The problem in the relative frame is then essentially the same as that analysed in Reference 8.]

$$r_4 = r_5; \quad T_{t,5}' = \overline{T}_{t,4}'$$

For consistency with Reference 8 the terms (1 - F) and (1 - G) are retained, where now

$$1 - F = \frac{h_4}{h_5} B_4 \left[1 - \frac{t_4 \cos\left(\beta_4 - \beta_{co4}\right) \sec(\text{rake})}{s_4 \cos \beta_4}\right]$$

$$= \frac{h_4}{h_5}\left[\frac{h_4 - 2\,\delta_w^*}{s_4\, h_4 \cos \beta_4}\right] \times$$

$$\times \left\{s_4 \cos \beta_4 - \left[2\,\delta_h^* + t_4 \cos\left(\beta_4 - \beta_{co4}\right)\right] \sec(\text{rake})\right\}$$

$$1 - G = \frac{h_4}{h_5}\left[\frac{h_4 - 2\left(\delta_w^* + \theta_w\right)}{s_4\, h_4 \cos\beta_4}\right] \times$$

$$\times \left\{s_4 \cos\beta_4 - \left[2\left(\delta_h^* + \theta_h\right) + t_4 \cos\left(\beta_4 - \beta_{co_4}\right)\right] \sec(\text{rake})\right\}$$

Then equation (23) of Reference 8 gives

$$\Psi_d\left(\Psi_c - \Psi_a\right) - \Psi_b\left(\Psi_c - \Psi_a\right)^{\frac{1}{2}} + \Psi_a = 0$$

where

$$\Psi_a = \left[(\sin\beta_4)\,\frac{1 - G}{1 - F}\right]^2$$

$$\Psi_b = \frac{\gamma\left(M_5' \cos\beta_4\right)^2 (1 - G) + \left(M_5'/M_4'\right)^2}{(\cos\beta_4)\,(1 - F)}$$

$$\Psi_c = \left(\frac{M_5'}{M_4'}\right)^2 \left[\frac{1 + \frac{1}{2}(\gamma - 1)\left(M_4'\right)^2}{1 + \frac{1}{2}(\gamma - 1)\left(M_5'\right)^2}\right]$$

$$\Psi_d = 1 + \gamma\left(M_5'\right)^2$$

The only unknown is M_5' so that the equation may be solved (by trial and error). Hence M_5' and Ψ_a etc.

From equations (12), (13) and (22) of Reference 8

$$\tan\beta_5 = \frac{(\sin\beta_4)\,(1 - G)}{\left(\Psi_c - \Psi_a\right)^{\frac{1}{2}}\,(1 - F)} \qquad \text{and} \qquad W_5 = W_4\left(\Psi_c\right)^{\frac{1}{2}}$$

Hence β_5 and W_5

$A_5' = 2\pi r_5\, h_5 \cos\beta_5$; hence A_5'

Thus Q; $T_{t,5}'$; A_5'; W_5; M_5' are known

Then $M_5' \longrightarrow \dfrac{Q\sqrt{T_{t,5}'}}{A_5' P_{t,5}'}$; hence $P_{t,5}'$.

This defines the situation after mixing.

After the final values at station 5 have been obtained, evaluate also $P_{s,5}$ and $T_{s,5}$

$$M_5' \longrightarrow \begin{cases} \dfrac{P_{t,5}'}{P_{s,5}} \longrightarrow P_{s,5} \\ \dfrac{T_{t,5}'}{T_{s,5}} \longrightarrow T_{s,5} \end{cases} \longrightarrow \rho_5 \text{ and } \mu_5$$

Check on value of β_4

Throughout the calculation of rotor velocity distribution, boundary layer growth, preliminary iteration on W_4, and mixing, an assumed value of β_4 has been used. This must now be corrected by making the mixed-out flow situation compatible with Wiesner's slip correlation[9].

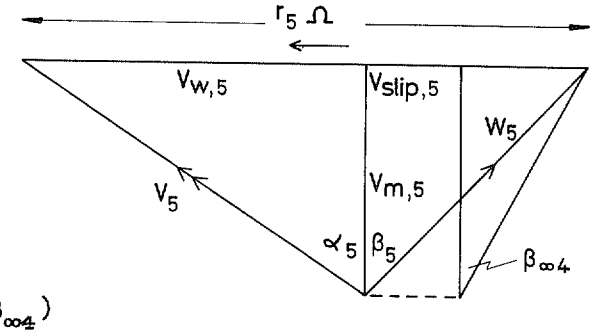

From velocity triangle

$$V_{m,5} = W_5 \cos \beta_5$$

$$V_{slip,5} = V_{m,5} (\tan \beta_5 - \tan \beta_{\infty 4})$$

$$= W_5 \cos \beta_5 (\tan \beta_5 - \tan \beta_{\infty 4})$$

Compare that value of $V_{slip,5}$ with $\dfrac{r_5 \Omega \sqrt{\cos \beta_{\infty 4}}}{\left(n_f + n_i\right)^{0.7}}$

β_4 must be changed until these agree. That is then the correct value of β_4.

For a realistic solution $\beta_4 > \beta_{\infty 4}$.

For each value of β_4 used in the second and subsequent circuits of the main iterative loop, the preliminary iteration on W_4 should start with an initial value of W_4 equal to the converged value of W_4 obtained on the preceding circuit of the main iterative loop.

Hence final values of M_5'; A_5'; $P_{t,5}'$; W_5; ρ_5; μ_5 etc.

Absolute conditions after mixing

From velocity triangle

$$V_{w,5} = r_5 \Omega - W_5 \sin \beta_5$$

Hence $V_{w,5}$

Rothalpy $$I_5 = C_p T_{t,5} - \frac{r_5 \Omega V_{w,5}}{gJ} = C_p T_{t,5}' - \frac{(r_5 \Omega)^2}{2gJ}$$

$$\therefore \quad C_p T_{t,5} = C_p T_{t,5}' + \frac{r_5 \Omega (2 V_{w,5} - r_5 \Omega)}{2gJ}$$

Hence $T_{t,5}$

Absolute P_t from

$$P_{t,5} = P_{t,5}' \left(\frac{T_{t,5}}{T_{t,5}'} \right)^{\frac{\gamma}{\gamma - 1}}$$

$P_{s,5}$; ρ_5 etc. already known, hence $\frac{P_{t,5}}{P_{s,5}} \longrightarrow M_5$

From velocity triangle

$$\tan \alpha_5 = \frac{r_5 \Omega - W_5 \sin \beta_5}{W_5 \cos \beta_5} ; \quad \text{hence } \alpha_5$$

V_5 can be obtained either from

$$V_5 = \frac{V_{w,5}}{\sin \alpha_5}$$

or from

$$M_5 \longrightarrow \frac{V_5}{\sqrt{T_{t,5}}} \longrightarrow V_5$$

Work input to rotor

Useful work supplied to fluid = $Q\left(C_p T_{t,5} - C_p T_{t,3}\right)$

There are various parasitic losses which require additional (wasted) work input.

Friction between rotor and casing ("disc friction" - see Appendices 3-11, 3-13)

$$Q\,\Delta\left(C_p T_t\right)_f = 0.08 \frac{\bar{\rho}\,\Omega^3\, r_5^5}{2gJ} \left(\frac{\bar{\rho}\,\Omega\, r_5^2}{\bar{\mu}}\right)^{-0.2}$$

where $\bar{\rho}$ and $\bar{\mu}$ are some mean values between stations 3 and 5.

Take these as $\begin{cases} \bar{\rho} = \frac{1}{4}\left(\rho_{3,hub} + \rho_{3,tip} + 2\rho_5\right) \\ \bar{\mu} = \frac{1}{4}\left(\mu_{3,hub} + \mu_{3,tip} + 2\mu_5\right) \end{cases}$

Leakage (see Appendices 3-12, 3-13)

Specify "gap" = axial clearance between rotor tip and casing at rotor outlet, at design speed.

In the normal range of $\frac{gap}{h_4}$ (≥ 0.02), Appendix 3-12 suggests

$$Q\,\Delta\left(C_p T_t\right)_\ell = \left[0.475\left(\frac{gap}{h_4}\right) + 0.02\right] \frac{D_{3,tip}}{D_4} \quad \text{(useful work)}$$

Total work input =

$$Q\left[\left(C_p\,T_{t,5} - C_p\,T_{t,3}\right) + \Delta\left(C_p\,T_t\right)_f + \Delta\left(C_p\,T_t\right)_\ell\right]$$

Rotor efficiency and pressure ratio (total-to-total)

Rotor isentropic work input corresponds to increase of P_t from $P_{t,1}$ to $P_{t,5}$

Now $$\frac{T_{t,5,is}}{T_{t,1}} = \left(\frac{P_{t,5}}{P_{t,1}}\right)^{\frac{\gamma-1}{\gamma}}$$

Hence $T_{t,5,is}$

Rotor isentropic work input = $Q\left(C_p\,T_{t,5,is} - C_p\,T_{t,1}\right)$

Rotor efficiency = $\dfrac{\text{rotor isentropic work input}}{\text{total work input}}$

Rotor pressure ratio = $\dfrac{P_{t,5}}{P_{t,1}}$

Vaneless space

Specify D_6; h_6

Assume wall profile is linear between stations 5 and 6,

i.e. $$h = h_5 + \frac{r - r_5}{r_6 - r_5}\left(h_6 - h_5\right)$$

[Note: starting from a fully-mixed state at station 5, the boundary layer is treated as growing from zero on each of the two side walls, subject to a condition regarding transition which is introduced presently to ensure that calculations are performed as for a turbulent boundary layer throughout.]

Equations must be solved for successive incremental steps of radius between r_5 and r_6; convenient steps may be 0.01 in r/r_5. The main equations are (see Appendix 3-14):

$$\frac{1}{\hat{M}}\frac{d\hat{M}}{dr}\left\{\frac{h\,(1-\hat{M}^2+\varepsilon\tan^2\alpha)+2H\,(1+H)\,\theta}{1+\frac{\gamma-1}{2}\hat{M}^2}-2H\theta\left[\frac{0.704\,\hat{M}^2}{1+0.8\,\hat{M}^2}+\frac{0.14\,\hat{M}^2}{1+0.1\,\hat{M}^2}\right]\right\}$$

$$= H\,C_f\,\zeta\,\sec\alpha-\frac{h\sec^2\alpha}{r}-\frac{dh}{dr} \qquad \ldots.(\underline{A})$$

$$\frac{1}{\tan\alpha}\frac{d\alpha}{dr} = -\frac{\varepsilon}{\hat{M}}\frac{d\hat{M}}{dr}\left(\frac{1}{1+\frac{\gamma-1}{2}\hat{M}^2}\right)-\frac{1}{r} \qquad \ldots.(\underline{B})$$

$$\frac{d\theta}{dr} = \frac{C_f\,\zeta\sec\alpha}{2}-\frac{\theta\sec^2\alpha}{r}-\frac{\theta}{\hat{M}}\frac{d\hat{M}}{dr}\left(\frac{2+H-\hat{M}^2+\varepsilon\tan^2\alpha}{1+\frac{\gamma-1}{2}\hat{M}^2}\right) \qquad \ldots.(\underline{C})$$

where

$$\varepsilon = \left[1-\frac{2\theta}{h}\,(1+H)\right]^{-1}$$

$$\zeta = \left[1+\tfrac{1}{4}\left(\frac{dh}{dr}\right)^2\right]^{\frac{1}{2}}$$

These equations assume that T_t, P_s and flow direction α are everywhere the same in both boundary layer and mainstream; all other flow properties relate only to the mainstream or core flow, namely: $\hat{M}$; $\hat{V}$; $\hat{\rho}$; $\hat{T}_s$; $\hat{P}_t$.

Step-by-step solution

Conditions at the beginning of a step are known, as follows:-

geometric quantities : r; h

mainstream flow quantities: $\hat{M}$; a

boundary layer quantities: θ; also H from

$$H = 1.286\left(1 + 0.8\,\hat{M}^2\right)^{0.44}\left(1 + 0.1\,\hat{M}^2\right)^{0.7}$$ (see Stratford & Beavers[6])

knowing $\hat{M}$; $\hat{P}_t$ (constant = $P_{t,s}$); T_t (constant = $T_{t,s}$)

$$\hat{M} \longrightarrow \begin{cases} \dfrac{\hat{V}}{\sqrt{T_t}} \longrightarrow \hat{V} \\ \dfrac{\hat{P}_t}{P_s} \longrightarrow P_s \longrightarrow \hat{\rho} \\ \dfrac{T_t}{\hat{T}_s} \longrightarrow \hat{T}_s \longrightarrow \hat{\rho},\ \hat{\mu} \end{cases}$$

hence $\hat{\rho}$; $\hat{V}$; $\hat{\mu}$; $Re_\theta = \dfrac{\hat{\rho}\,\hat{V}\,\theta}{\hat{\mu}}$

then C_f from Green et al[10], viz:

$$C_f = C_{f_o}\left\{\frac{0.9}{\left(\frac{H+1}{1+0.2\,\hat{M}^2} - 1\right)\left[1 - 6.55\sqrt{\tfrac{1}{2}\,C_{f_o}}\left(1 + 0.04\,\hat{M}^2\right)\right] - 0.4} - 0.5\right\}$$

where

$$C_{f_o} = \frac{1}{\sqrt{1 + 0.2\,\hat{M}^2}}\left\{\frac{0.01013}{\log_{10}\left[Re_\theta\left(1 + 0.056\,\hat{M}^2\right)\right] - 1.02} - 0.00075\right\}$$

For a chosen step length Δr, the values of Δh and hence ζ are known. Then values of $\hat{M}$, a, θ and all dependent quantities at the end of each step are obtained from simultaneous solution of equations A, B and C. $\frac{d\hat{M}}{dr}$ is negative, $\frac{d\theta}{dr}$ is positive, and the sign of $\frac{da}{dr}$ depends upon the relation between h_5 and h_e.

First step

In order that the boundary layer may be treated as turbulent at the end of the first step, it is assumed that Re_θ has by then reached the value 320. This decides the values of θ and C_f at the end of the first step. Little error will be introduced by writing for convenience

$$Re_\theta = \frac{\rho_5 V_5 \theta}{\mu_5} \quad (= 320)$$

in order to save extra iteration; this is justified by the arbitrary nature of the assumption regarding Re_θ.

Thus the calculation starts as follows:-

station 5

$\hat{M} = M_5$ $\qquad$ $Re_\theta = 320$

$\theta = 0$ $\qquad$ $\theta = 320\ \mu_5/\rho_5 V_5$

$\qquad$ $H = f\left[\hat{M}\right]$

C_f is indeterminate $\qquad$ $C_f = f\left[\hat{M};\ H;\ Re_\theta\right]$

For the first step, therefore, $\Delta\theta$ is known, and C_f can be eliminated between equations A and C, to leave one equation in $\frac{d\hat{M}}{dr}$ which is solved simultaneously with B.

$$\frac{1}{\hat{M}}\frac{d\hat{M}}{dr}\left\{\frac{\left(h - 2H\theta\right)\left(1 - \hat{M}^2 + \varepsilon \tan^2\alpha\right)}{1 + \frac{\gamma - 1}{2}\hat{M}^2} - 2H\theta\left[\frac{0.704\,\hat{M}^2}{1 + 0.8\,\hat{M}^2} + \frac{0.14\,\hat{M}^2}{1 + 0.1\,\hat{M}^2}\right]\right\}$$

$$= 2H\frac{d\theta}{dr} - \frac{dh}{dr} - \left(h - 2H\theta\right)\frac{\sec^2\alpha}{r}$$

Check on boundary layers

For the foregoing treatment to be valid, the boundary layers on the two walls must not join, and it is thus necessary to check after each step (excluding the first and perhaps early ones) that $2\delta < h$, i.e. that

$$\theta < \frac{h}{20.6\left(1 + 0.1\,\hat{M}^2\right)^{0.7}}$$

When this limit is reached, $\hat{P}_t$ becomes the centreline value and ceases to be constant (likewise $\hat{M}$ etc. are now centreline values).

Thereafter equations A, B and C are replaced with the following (see Appendix 3-15):

$$\frac{1}{\hat{M}}\frac{d\hat{M}}{dr}\left[\frac{\hat{M}^2 - \sec^2\alpha - \gamma\hat{M}^2\left(\Gamma_a + \Gamma_b\right)}{1 + \frac{\gamma-1}{2}\hat{M}^2} + \frac{\Gamma_c}{1-\Gamma_a} + \left(\frac{\tan^2\alpha}{\Gamma_e} - \gamma\hat{M}^2\right)\left(\frac{\Gamma_b\,\Gamma_c}{1-\Gamma_a} - \Gamma_d\right)\right]$$

$$= \frac{1}{h}\frac{dh}{dr} + \frac{\sec^2\alpha}{r} + \left(\frac{\tan^2\alpha}{\Gamma_e} - \gamma\hat{M}^2\right)\frac{C_f\,\zeta}{h\cos\alpha} \qquad \ldots.(\underline{D})$$

$$\frac{1}{\tan\alpha}\frac{d\alpha}{dr}\left(\tan^2\alpha - \gamma\hat{M}^2\,\Gamma_e\right) = \frac{1}{\hat{M}}\frac{d\hat{M}}{dr}\left[\frac{1+(\gamma-1)\hat{M}^2}{1+\frac{\gamma-1}{2}\hat{M}^2} - \frac{\Gamma_c}{1-\Gamma_a}\right] +$$

$$+ \frac{1}{h}\frac{dh}{dr} + \frac{1+\gamma\hat{M}^2\,\Gamma_e}{r} \qquad \ldots.(\underline{E})$$

$$\frac{1}{\hat{P}_t}\frac{d\hat{P}_t}{dr}\left(\frac{\tan^2\alpha}{\gamma\hat{M}^2\,\Gamma_e} - 1\right) = \frac{1}{\hat{M}}\frac{d\hat{M}}{dr}\left[\frac{1-\hat{M}^2+\frac{\tan^2\alpha}{\Gamma_e}}{1+\frac{\gamma-1}{2}\hat{M}^2} - \frac{\Gamma_c}{1-\Gamma_a}\right] +$$

$$+ \frac{1}{h}\frac{dh}{dr} + \frac{\sec^2\alpha}{r} \qquad \ldots.(\underline{F})$$

where

$$\begin{cases} \Gamma_a = 0.125\left(1 + 0.8\,\hat{M}^2\right)^{0.44} \\ \Gamma_b = 0.097\left(1 + 0.1\,\hat{M}^2\right)^{-0.7} \\ \Gamma_c = 0.088\,\hat{M}^2\left(1 + 0.8\,\hat{M}^2\right)^{-0.56} \\ \Gamma_d = 0.0136\,\hat{M}^2\left(1 + 0.1\,\hat{M}^2\right)^{-1.7} \\ \Gamma_e = 1 - \Gamma_a - \Gamma_b \end{cases}$$

Solution of equations D, E and F requires knowledge of H and Re_θ to obtain C_f, as before. H is the same function of $\hat{M}$, and $\frac{\theta}{h}$ is now also a function of $\hat{M}$ only.

$$\theta = \frac{h}{2}\, 0.097 \left(1 + 0.1\, \hat{M}^2\right)^{-0.7}$$

As before evaluate $\hat{\rho}$; $\hat{V}$; $\hat{\mu}$ and use

$$Re_\theta = \frac{\hat{\rho}\, \hat{V}\, \theta}{\hat{\mu}}$$

Hence C_f.

Conditions at end of vaneless space

$$T_{t,e} = T_{t,s}$$

If boundary layers have not joined then $\hat{P}_{t,e} = P_{t,s}$; otherwise $\hat{P}_{t,e}$ is the value of $\hat{P}_t$ after the last step.

$\hat{M}_e$; α_e; θ_e; H_e are obtained from the step-by-step procedure.

$$\delta_e^* = H_e\, \theta_e$$

$$B_e = 1 - \frac{2\delta_e^*}{h_e}$$

$$A_e = B_e \cdot 2\pi r_e\, h_e \cos \alpha_e$$

Knowing $\hat{M}_e$; $\hat{P}_{t,e}$; $T_{t,e}$

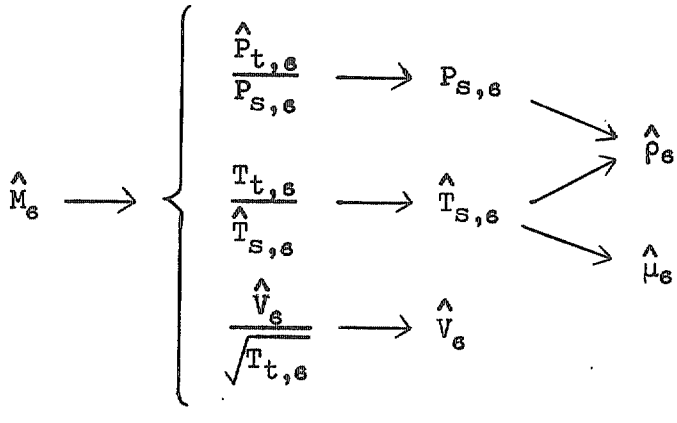

Mean total pressure $\left(\overline{P_{t,6}}\right)$ is only required when no vaned diffuser follows the vaneless space, and in that case $\hat{M}_6$ is likely to be fairly low ($\simeq 0.5$) and the boundary layers well developed. In those circumstances it is reasonable to assume (see Appendix 3-16)

$$\overline{P_{t,6}} = P_{s,6} + \left(\hat{P}_{t,6} - P_{s,6}\right)\left(1 - 4.572\,\frac{\theta_6}{h_6}\right)$$

Vaned diffuser

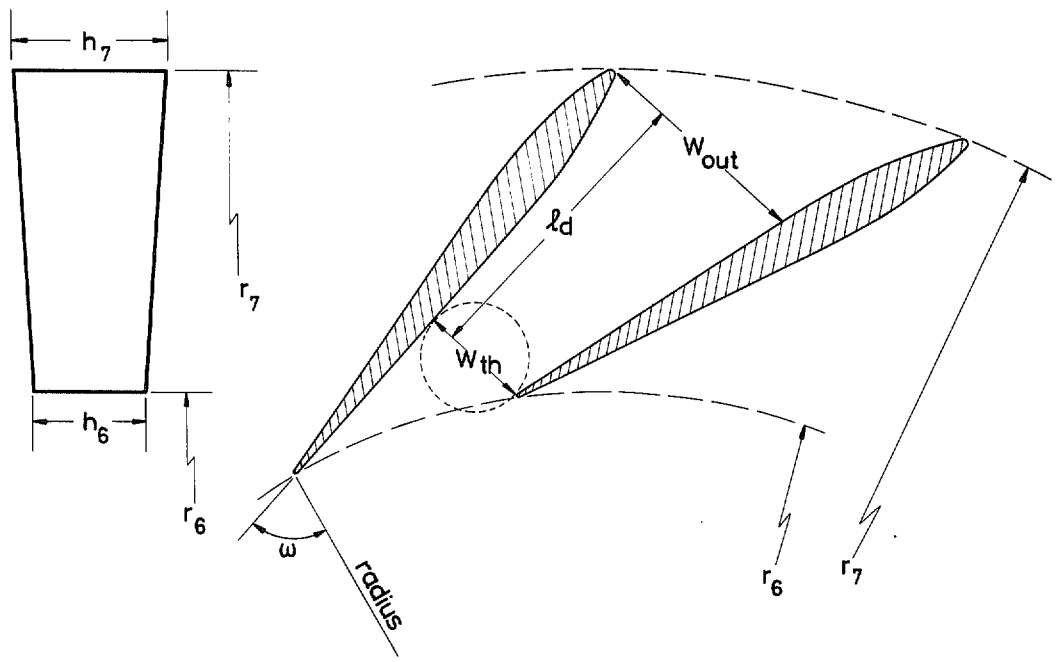

Specify
- D_7; h_7; number of vanes n_d
- total geometric throat area A_g
- channel geometric area ratio (outlet/throat) AR
- channel centreline length ℓ_d
- channel throat width in radial plane w_{th}
- angle of lower vane surface at leading edge ω

Axial dimension at throat $\quad h_{th} = \dfrac{A_g}{w_{th}\, n_d}$

Throat aspect ratio $AS = \frac{h_{th}}{w_{th}}$

If $h_6 = h_7$ $LWR = \frac{\ell_d}{w_{th}}$

If $h_6 \neq h_7$, also specify w_{out}

then $h_{out} = \frac{AR \cdot A_g}{w_{out}\, n_d}$

Assume conditions in the channel throat are those at the end of the vaneless space (station 6) modified for area change, including blockage, and loss of total pressure. As $\hat{M}_6$ is normally <1.2, shocks if present at all should be weak, so ignore any loss of $\hat{P}_t$ at shocks. But introduce an arbitrary schedule of $\hat{P}_t$ loss with increase of diffusion as described hereafter. (For general discussion, see Appendix 3-17.)

Throat conditions:

$\hat{M}_{th}$ and $\hat{P}_{t,th}$ are bulk mean values

T_t is constant, hence $T_{t,th} = T_{t,6}$

$\hat{P}_{t,th} \leq \hat{P}_{t,6}$ according to assumed schedule

take $A_{th} = B_{th} \cdot A_g$, where B_{th} is to be calculated

[Note: when the vaneless space is followed by a channel diffuser $\hat{M}_6$ is likely to be >0.8 and the sidewall boundary layers at station 6 are usually nowhere near meeting in the middle.]

For boundary layer growth between station 6 and throat, consider

(i) vane surface, taking length of surface = $2\pi r_6/n_d$ (as an approximation); thickness (δ_h^*) grows from 0 at leading edge

(ii) sidewalls, taking mean length of path = $\pi r_6/n_d$; thickness (δ_w^*) grows from δ_6^* at station 6.

For simplicity linear distribution of $\hat{M}$ is assumed along both vane surface and sidewall mean path, the initial values depending on

(i) Mach no. level, $\hat{M}_6$ either ≤ 1 or >1, and

(ii) incidence to vane surface at leading edge ($= \alpha_6 - \omega$)

in the following arbitrary manner:-

$\hat{M}_s$	incidence	vane surface	sidewall mean
≤ 1	0	$\hat{M}_s$	$\hat{M}_s$
≤ 1	$\alpha_s > \omega$	$\hat{M}_s \sec(\alpha_s - \omega)$	$\hat{M}_s$
≤ 1	$\alpha_s < \omega$	$\hat{M}_s \cos(\omega - \alpha_s)$	$\hat{M}_s$
>1	0	$\hat{M}_s$	$\hat{M}_s$
>1	$\alpha_s > \omega$	$\hat{M}_{\ell e}$ ($\hat{M}_{\ell e}$ after expansion from $\hat{M}_s$ through angle $\alpha_s - \omega$)	$\frac{\hat{M}_{\ell e} + \hat{M}_s}{2}$
>1	$\alpha_s < \omega$	$\hat{M}_{\ell e}$ ($\hat{M}_{\ell e}$ after reverse expansion from $\hat{M}_s$ through $\omega - \alpha_s$) if solution $\hat{M}_{\ell e} \geq 1$ exists, otherwise $\hat{M}_{sh} \cos(\omega - \alpha_s)$	$\frac{\hat{M}_{\ell e} + \hat{M}_s}{2}$ $\frac{\hat{M}_{sh} \cos(\omega - \alpha_s) + \hat{M}_s}{2}$

where $\hat{M}_{sh}$ is given by the normal shock relation $\left(\hat{M}_6 > 1\right)$:

$$\hat{M}_{sh} = \sqrt{\frac{(\gamma - 1)\left(\hat{M}_6\right)^2 + 2}{2\gamma\left(\hat{M}_6\right)^2 - (\gamma - 1)}}$$

Expansion relation $\left(\hat{M}_6 > 1\right)$: $\hat{M}_{\ell e}\left(> \hat{M}_6\right)$ is given by

$$\chi \tan^{-1}\left[\frac{\sqrt{\left(\hat{M}_{\ell e}\right)^2 - 1}}{\chi}\right] - \tan^{-1}\sqrt{\left(\hat{M}_{\ell e}\right)^2 - 1} =$$

$$\alpha_6 - \omega + \chi \tan^{-1}\left[\frac{\sqrt{\left(\hat{M}_6\right)^2 - 1}}{\chi}\right] - \tan^{-1}\sqrt{\left(\hat{M}_6\right)^2 - 1}$$

where $\chi = \sqrt{\frac{\gamma + 1}{\gamma - 1}}$

Reverse expansion $\left(\hat{M}_6 > 1\right)$: $\hat{M}_{\ell e}\left(< \hat{M}_6\right)$ is given by same relation, provided solution $\hat{M}_{\ell e} \geqslant 1$ exists (i.e. r.h.s. of equation $\geqslant 0$).

Thus assumed distributions of $\hat{M}$ between station 6 and throat are:

for vane surface

$$\hat{M} = \hat{M}_{initial} - \left(\hat{M}_{initial} - \hat{M}_{final}\right)\frac{S_h}{2\pi r_6/n_d}$$

for sidewall mean

$$\hat{M} = \hat{M}_{initial} - \left(\hat{M}_{initial} - \hat{M}_{final}\right)\frac{S_w}{\pi r_6/n_d}$$

where $\hat{M}_{final}$ is taken as $\hat{M}_{th}$ in both cases

Values of δ^* at the throat are then

for vane surface

$$\delta^*_{th,h} = 0.046\left[1 + 0.8\left(\hat{M}_{th}\right)^2\right]^{0.44}\left(\ell_{th,h}\right)^{0.8}\left(\frac{\hat{\rho}_{th}\,\hat{V}_{th}}{\hat{\mu}_{th}}\right)^{-0.2}$$

$$\text{where}\quad \ell_{th,h} = \frac{1}{p_{th}}\int_0^{2\pi r_s/n_d} p\, dS_h \qquad \text{and} \qquad p = \left(\frac{\hat{M}}{1 + 0.2\,\hat{M}^2}\right)^4$$

for sidewall mean

$$\delta^*_{th,w} = 0.046\left[1 + 0.8\left(\hat{M}_{th}\right)^2\right]^{0.44}\left(\ell_{th,w}\right)^{0.8}\left(\frac{\hat{\rho}_{th}\,\hat{V}_{th}}{\hat{\mu}_{th}}\right)^{-0.2}$$

where

$$\ell_{th,w} = \frac{1}{p_{th}}\left\{p_s\left[\frac{\delta^*_s\left(\hat{\rho}_s\,\hat{V}_s/\hat{\mu}_s\right)^{0.2}}{0.046\left[1 + 0.8\left(\hat{M}_s\right)^2\right]^{0.44}}\right]^{1.25} + \int_0^{\pi r_s/n_d} p\, dS_w\right\}$$

Note: $\hat{M}_{th}$; p_{th}; $\hat{V}_{th}$; $\hat{\rho}_{th}$; $\hat{\mu}_{th}$ are the same for vane surface and sidewall mean; all are unknown at this stage.

This situation must be resolved by iteration. The iteration procedure is followed twice, the first time taking $\hat{P}_{t,th} = \hat{P}_{t,s}$. Start the iteration by assuming a value for $\hat{M}_{th}$ (say 0.9 initially, or $\hat{M}_s$ if that is <0.9).

Now

$$\left[\frac{Q\sqrt{T_t}}{A\,\hat{P}_t}\right]_{th} = \left[\frac{Q\sqrt{T_t}}{A\,\hat{P}_t}\right]_{e} \cdot \frac{B_e}{B_{th}} \cdot \frac{2\pi r_e\, h_s \cos \alpha_s}{A_g} \cdot \frac{\hat{P}_{t,s}}{\hat{P}_{t,th}}$$

In this relation B_{th} is the only unknown; hence a first value for B_{th}.

But also

$\hat{M}_{th}$ → { $\frac{\hat{P}_{t,th}}{P_{s,th}}$ → $P_{s,th}$ → $\hat{\rho}_{th}$; $\frac{T_{t,th}}{\hat{T}_{s,th}}$ → $\hat{T}_{s,th}$ → $\hat{\rho}_{th}$, $\hat{\mu}_{th}$; $\frac{\hat{V}_{th}}{\sqrt{T_{t,th}}}$ → $\hat{V}_{th}$ }

Whence $\delta^*_{th,h}$ and $\delta^*_{th,w}$ can be calculated from relations given.

Then throat blockage is given by

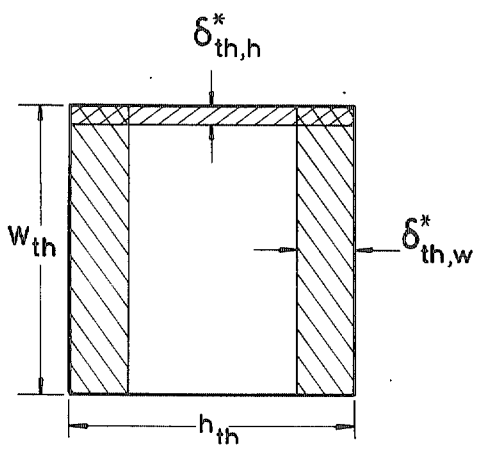

$$B_{th} = \frac{\left(h_{th} - 2\,\delta^*_{th,w}\right)\left(w_{th} - \delta^*_{th,h}\right)}{h_{th}\, w_{th}}$$

Compare the latter value of B_{th} with the first value obtained and iterate on $\hat{M}_{th}$ until the values of B_{th} agree. Hence solution values of $\hat{M}_{th}$; B_{th} etc.

After the iterative procedure has been concluded the first time (corresponding to $\hat{P}_{t,th} = \hat{P}_{t,e}$), replace $\hat{P}_{t,th}$ with a value given by the arbitrary relation

$$\hat{P}_{t,e}\left(0.36 + 1.28\ B_{th} - 0.64\ B_{th}^{2}\right)$$

using for B_{th} the first solution value, and follow the iterative procedure through a second time. Take the results as correct values of $\hat{M}_{th}$; B_{th} etc.

If the diffuser throat is choking the foregoing iterative procedure will not find a solution. Whether or not the diffuser throat is choking can be ascertained by putting $\hat{M}_{th} = 1$ and for that condition evaluating

$\left\{\begin{array}{l} B_{th} \text{ from continuity relation} \\ B_{th} \text{ from boundary layer growth} \end{array}\right.$

as previously set out; then taking these values of B_{th} the throat is choking if (see Appendix 3-18)

$$B_{th}\ (\text{continuity}) - B_{th}\ (\text{boundary layer}) \geq 0$$

In that case the calculation ends.

Otherwise, having obtained $\hat{M}_{th}$ by iteration, $\hat{P}_{t,th}$ and $P_{s,th}$ are then known; the channel pressure recovery coefficient is defined as

$$C_{pr} = \frac{P_{s,out} - P_{s,th}}{\hat{P}_{t,th} - P_{s,th}}$$

Appendix 4 shows how to evaluate C_{pr} from a table of data appropriate to single channels with parallel sidewalls, straight centrelines, and throat aspect ratio (AS) = 1, given values of the following quantities:

B_{th}; LWR; AR

The data of Appendix 4 are taken from work by Runstadler[11], with uncertain extrapolation to lower LWR by means described in Appendix 3-19.

Of the geometric restrictions mentioned, an approximate method is suggested for dealing with the usual case of AS ≠ 1 (see Appendix 3-19):
When AS > 1 (not likely to exceed say 2), ignore the effect
When AS < 1, calculate

$$\text{actual } 2\Theta = 2 \tan^{-1}\left(\frac{AR - 1}{2 \times LWR}\right)$$

$$\Delta(2\Theta) = \left(\frac{1}{6\ AS} + 1\right)\left(\frac{1}{AS} - 1\right)$$

then

$$\text{effective } 2\Theta = \text{actual } 2\Theta - \Delta(2\Theta)$$

and use Appendix 4 with quantities

$$B_{th};\ LWR;\ AR_{eff} = 1 + 2 \cdot LWR \cdot \tan\left[\tfrac{1}{2}\ (\text{effective } 2\Theta)\right]$$

If channel sidewalls diverge, a suggested treatment is to define the properties of an "equivalent two-dimensional channel" (see Appendix 3-19) as

$$B_{th};\quad LWR_{2D} = \frac{\ell}{w_{th,2D}};\quad AR;\quad AS_{2D} = \frac{h_{out}}{w_{th,2D}}$$

$$\text{where } w_{th,2D} = w_{th} \cdot \frac{h_{th}}{h_{out}}$$

for which C_{pr} is evaluated in the manner previously described.

Channel centreline curvature may reasonably be neglected if only slight; if appreciable then the value of C_{pr} as given by Appendix 4 for the same input quantities will be too high.

As alternative to the data of Appendix 4, it may be convenient to use a specified value of the ratio $C_{pr}/C_{pr,ideal}$ where $C_{pr,ideal}$ is taken to

be a function of $\hat{M}_{th}$ and AR. In certain cases $C_{pr}/C_{pr,ideal}$ can be correlated in simple manner with B_{th}, so that then

$C_{pr} = f\left(AR;\ \hat{M}_{th};\ B_{th}\right)$.

Using $C_{pr}/C_{pr,ideal}$ the calculation proceeds thus

(i) $\hat{M}_{th} \longrightarrow \left[\begin{matrix}\text{choking}\\ \text{area ratio}\end{matrix}\right]$ at $M = \hat{M}_{th}$

(ii) $\left[\begin{matrix}\text{choking}\\ \text{area ratio}\end{matrix}\right]$ at $M = \hat{M}_{out,ideal}$ is equal to

$$AR \times \left[\begin{matrix}\text{choking}\\ \text{area ratio}\end{matrix}\right] \text{ at } M = \hat{M}_{th}$$

(iii) $\left[\begin{matrix}\text{choking}\\ \text{area ratio}\end{matrix}\right]$ at $M = \hat{M}_{out,ideal} \longrightarrow \hat{M}_{out,ideal} \longrightarrow$

$$\frac{\hat{P}_{t,th}}{P_{s,out,ideal}} \longrightarrow P_{s,out,ideal}$$

(iv) $$C_{pr,ideal} = \frac{P_{s,out,ideal} - P_{s,th}}{\hat{P}_{t,th} - P_{s,th}}$$

Hence C_{pr}.

In either case, having found C_{pr}, hence $P_{s,out}$.

Conditions at end of diffuser channel

$T_{t,out} = T_{t,th} \left(= T_{t,s}\right)$

Geometric area $= AR \cdot A_g$

A one-dimensional mean total pressure $\left(\overline{P_t}_{,out}\right)$ can be obtained approximately from

$$\frac{Q\sqrt{T_{t,out}}}{(AR \cdot A_g)\ P_{s,out}} \longrightarrow \bar{M}_{out} \longrightarrow \frac{\overline{P_{t,out}}}{P_{s,out}} \longrightarrow \overline{P_t}_{,out}$$

Compressor outlet (station 7)

Some loss of P_t is likely to occur between channel outlet and the final measuring station. Introduce a loss factor defined as

$$\frac{\overline{P_{t,out}} - P_{t,final}}{\overline{P_{t,out}} - P_{s,out}}$$

$\overline{P_{t,out}}$ is a continuity-mean total pressure at channel outlet, so that boundary layers in that plane have already been allowed for, but there will be a "dump" loss due to vane boat-tails and/or trailing edges. The total pressure loss factor for this "dump" is approximately equal to

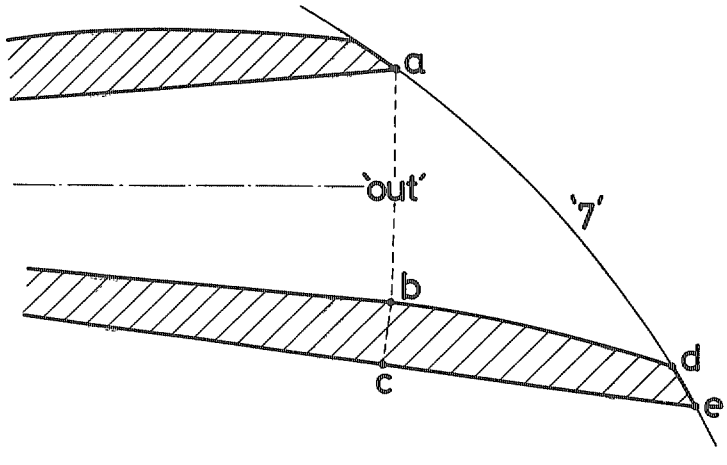

$$\frac{t}{s}\left(\frac{t}{s} - C_{p,te}\right)$$

where
- t = distance 'bc' (in sketch)
- s = distance 'ab' + 'bc'
- $C_{p,te}$ = mean pressure coefficient on surface 'bde' $\left(= \dfrac{P_{s,mean} - P_{s,out}}{\overline{P_{t,out}} - P_{s,out}}\right)$ for which a value around -0.15 may reasonably be taken.

Hence $P_{t,7}$.

In addition to the trailing edge "dump" will be losses associated with any ductwork, bends, deswirl vanes etc. located between station 7 (the trailing edge pitch circle) and the final measuring station.

In the case of a vaneless space but no vaned diffuser

$$P_{t,7} = \overline{P_{t,6}} \quad \text{and} \quad P_{s,7} = P_{s,6}$$

Overall efficiency and pressure ratio

Overall isentropic work input = $Q\left(C_p T_{7,is} - C_p T_{t,1}\right)$

Overall efficiency = $\dfrac{\text{overall isentropic work input}}{\text{total work input}}$

Now $T_{7,is}$ can be evaluated as

either (i) $\dfrac{T_{7,is}}{T_{t,1}} = \left(\dfrac{P_{t,7}}{P_{t,1}}\right)^{\frac{\gamma-1}{\gamma}}$

or (ii) $\dfrac{T_{7,is}}{T_{t,1}} = \left(\dfrac{P_{s,7}}{P_{t,1}}\right)^{\frac{\gamma-1}{\gamma}}$

leading respectively to

(i) overall efficiency (total-to-total)

(ii) overall efficiency (total-to-static)

Corresponding values are

(i) overall pressure ratio (total-to-total) = $\dfrac{P_{t,7}}{P_{t,1}}$

(ii) overall pressure ratio (total-to-static) = $\dfrac{P_{s,7}}{P_{t,1}}$

APPENDIX 3

NOTES AND DERIVATIONS

1. Axial velocity profile at rotor inlet

Let

$$\begin{bmatrix}\text{axial velocity}\\ \text{at diameter D}\end{bmatrix} = \left[\text{mean axial velocity}\right]\left\{1 + (\lambda - 1)\,\frac{D - D_{ref}}{D_{tip} - D_{ref}}\right\}$$

Now from continuity

$$Q = \bar{\rho}\left[B\,\frac{\pi}{4}\left(D_{tip}^2 - D_{hub}^2\right)\right]\left[\text{mean axial velocity}\right] =$$

$$\bar{\rho} \cdot B \int \left[\text{axial velocity}\right] d\left[\text{axial area}\right]$$

$$\therefore \quad \frac{\pi}{4}\left(D_{tip}^2 - D_{hub}^2\right) = \int_{D_{hub}}^{D_{tip}} \left\{1 + (\lambda - 1)\,\frac{D - D_{ref}}{D_{tip} - D_{ref}}\right\}\frac{\pi D}{2}\,dD$$

$$\therefore \quad \frac{1}{2}\left(D_{tip}^2 - D_{hub}^2\right) = \int_{D_{hub}}^{D_{tip}} D \cdot dD + \frac{\lambda - 1}{D_{tip} - D_{ref}} \int_{D_{hub}}^{D_{tip}} \left(D^2 - D_{ref} \cdot D\right) dD$$

$$= \frac{1}{2}\left(D_{tip}^2 - D_{hub}^2\right) +$$

$$+ \frac{(\lambda - 1)\left[\frac{1}{3}\left(D_{tip}^3 - D_{hub}^3\right) - \frac{1}{2} D_{ref}\left(D_{tip}^2 - D_{hub}^2\right)\right]}{D_{tip} - D_{ref}}$$

$$\therefore \quad (\lambda - 1)\,\frac{D_{tip} - D_{hub}}{D_{tip} - D_{ref}}\left[\frac{D_{tip}^2 + D_{tip}\,D_{hub} + D_{hub}^2}{3} - \frac{D_{ref}\left(D_{tip} + D_{hub}\right)}{2}\right] = 0$$

$$\therefore \quad D_{ref} = \frac{2}{3} \cdot \frac{D_{tip}^2 + D_{tip}\,D_{hub} + D_{hub}^2}{D_{tip} + D_{hub}}$$

2. Rotor inlet velocity triangles

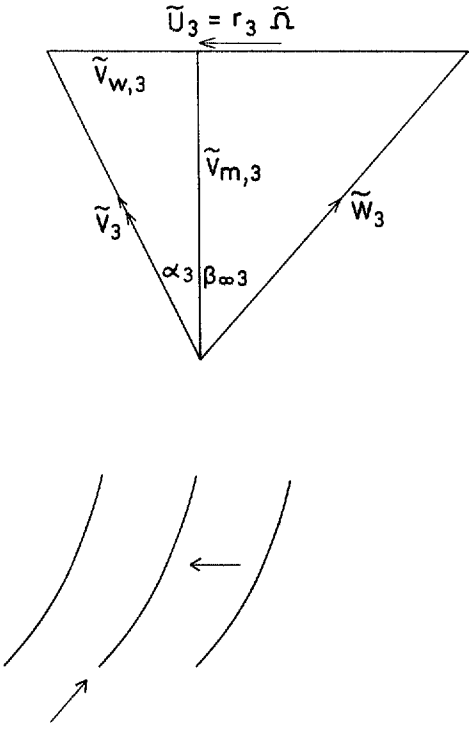

Zero incidence

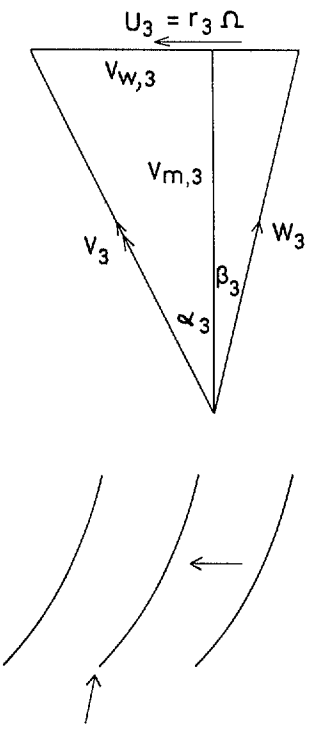

General
(-ve incidence as drawn)

3. Rotor blade tip profile

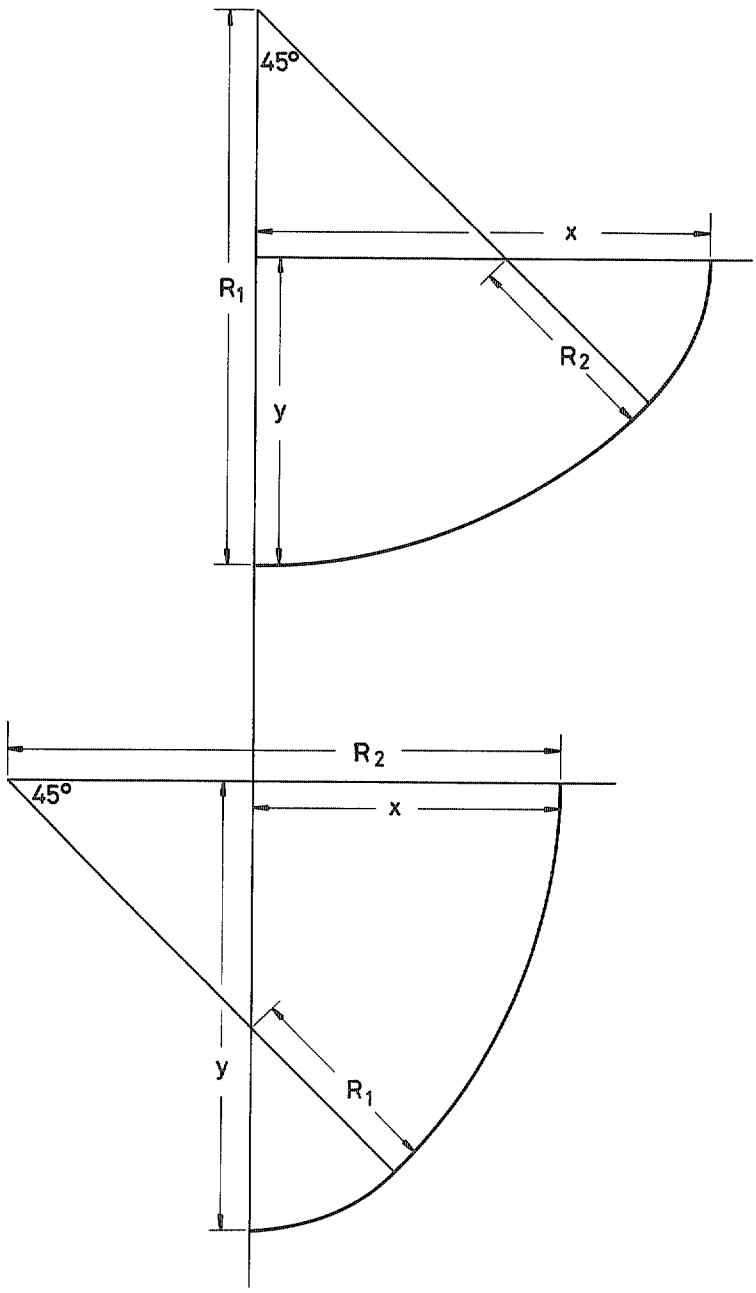

Two circular arcs with common normal at 45°

In general

$$x - R_2 = R_1 - y$$

$$\therefore \quad R_1 + R_2 = x + y$$

$$R_1 - R_2 = \sqrt{2}\,(R_1 - y)$$

$$\text{Hence } R_1 = \frac{x + \left(1 - \sqrt{2}\right)y}{2 - \sqrt{2}}$$

$$\text{and } R_2 = \frac{\left(1 - \sqrt{2}\right)x + y}{2 - \sqrt{2}}$$

Total arc length $\left(m_{4,\text{tip}}\right)$ =

$$\frac{\pi}{4}\,(R_1 + R_2)$$

$$= \frac{\pi}{4}\,(x + y)$$

Arc length at junction $(m_j) = \frac{\pi}{4} R_1$

$$\therefore \quad \frac{m_j}{m_{4,\text{tip}}} = \frac{R_1}{R_1 + R_2} = \frac{x + \left(1 - \sqrt{2}\right)y}{\left(2 - \sqrt{2}\right)\left(x + y\right)}$$

4. Rotor passage throat geometry

Assume blades have constant thickness (t_3) and circular arc leading edges.

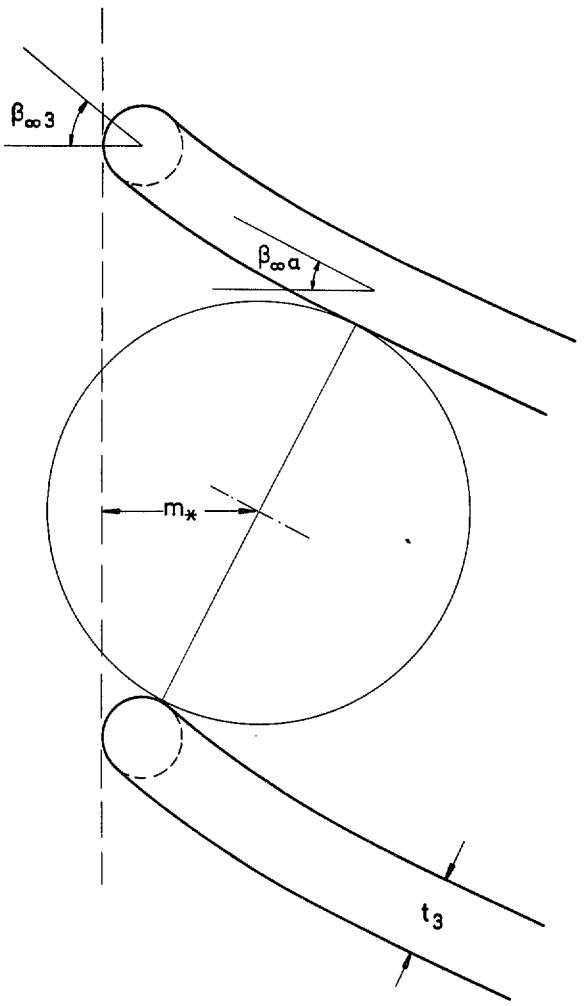

$\beta_{\infty a}$ is value of β_∞ at $m = 2m_* - t_3$

take $\beta_{\infty b} \simeq \frac{1}{2}\left(\beta_{\infty 3} + \beta_{\infty a}\right)$

Approximate the geometry thus:-

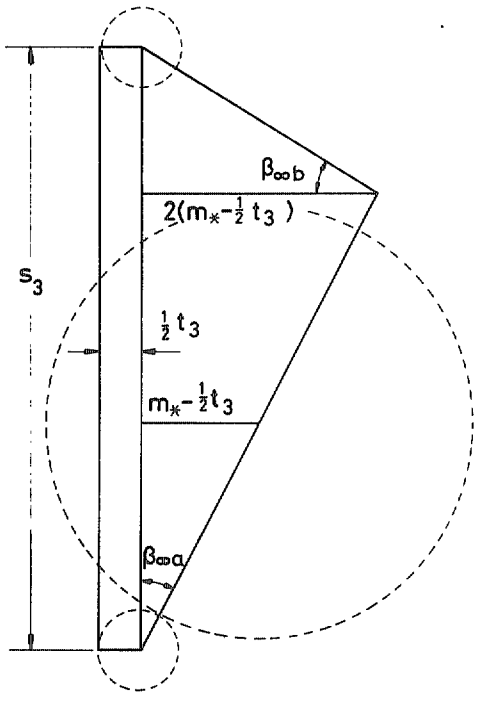

$$s_3 = \left(2m_* - t_3\right)\left(\cot \beta_{\infty a} + \tan \beta_{\infty b}\right)$$

$$\therefore \quad m_* = \frac{\frac{1}{2} s_3}{\cot \beta_{\infty a} + \tan \beta_{\infty b}} + \frac{1}{2} t_3$$

5. Rotor velocity triangle from throat to outlet

At rotor outlet there are two situations of importance

(i) that before mixing-out of wakes, i.e. with blockage present and velocities relating to the average isentropic "core" or mainstream flow

(ii) that after mixing-out of wakes, when the flow is assumed to be one-dimensional with zero blockage.

Correlations of slip (see Appendix 3-6) relate to the velocity triangle for the second situation. Distributions of surface velocity, as used throughout the rotor for assessment of boundary layer growth and hence outlet blockage, are obviously concerned with conditions of the assumed local isentropic core, and thus the outlet quantities β_4 and W_4 (which are used to derive those velocity distributions) relate to the first situation.

In analogous manner two different velocity triangles can be imagined for any station within the rotor. The local surface properties β, W, ΔW (and hence V_w) are those appropriate to the existence of a local boundary layer and hence some local blockage, for which a velocity triangle may be drawn thus:-

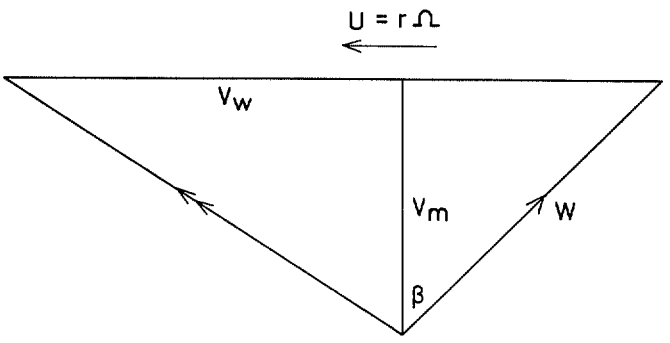

Then $V_w = r\Omega - W \sin \beta$

(Note that β is assumed to be the same through the boundary layer as in the local isentropic core.)

Some slip exists within the rotor (see Appendix 3-6), and this must again be regarded as applying to a one-dimensional (zero blockage) situation, depicted thus:-

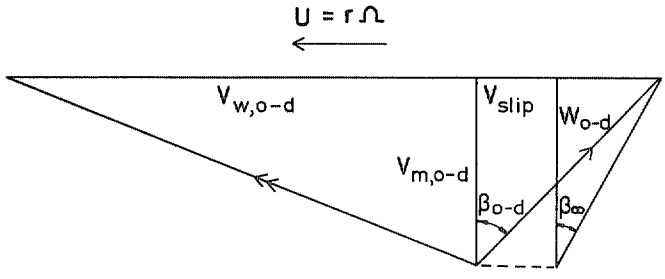

However, it is difficult at any station other than outlet to reconcile quantitatively a value of V_{slip} in the second triangle with the viscous flow properties of the first triangle; note that $V_w \neq V_{w,o-d}$ (see Appendix 3-10).

At rotor outlet this difficulty is removed, since the same values of β_4 and W_4 apply to both hub and tip, and an overall blockage factor B_4 is known. Thus an overall mixing treatment can be used to relate the two triangles.

6. Slip

The phenomenon of slip, manifest as a flow angle leaving the rotor which is greater than the blade outlet angle, is primarily due to what is often termed the relative eddy effect, and exists in inviscid flow. This effect can be deduced from a potential flow analysis; Stanitz & Ellis[13] give results of such for a wholly-radial-bladed compressor. Comparison of the slip factors so obtained with the empirical real-machine correlation of Wiesner[9] is as follows $\left(\text{slip factor} = 1 - V_{slip}/U\right)$

	30 blades	20 blades
Potential flow	0.9354	0.8955
Experiment	0.9074	0.8773
Difference	0.0280	0.0182

indicating that this effect accounts for perhaps 70 to 85 per cent of the slip, this proportion being greatest with few blades. The latter trend is reasonable, since slip increases as blade number is reduced. The residue not due to potential flow would then correspond to a slip factor of 0.97 to 0.98. This relatively small residue is presumably due to viscous effects; whether it should depend upon blade outlet angle is not known. When experimental correlations of slip are sought (e.g. Wiesner[9]), the procedure will generally be to derive the absolute whirl velocity at rotor outlet from measurement of work input, and the meridional velocity from mass flow (assuming zero blockage), so allowing construction of the velocity triangle from which V_{slip} is obtained. That procedure cannot recognise boundary layers or wakes; thus the velocity triangle which includes V_{slip} relates to flow that is one-dimensional and axisymmetric.

Slip likewise occurs within the rotor passage, where the relative eddy exists. For a passage with radial walls, Stanitz's work indicates that the circumferential mean value of slip velocity within the passage decreases quite rapidly as radius diminishes and eventually becomes negative at passage inlet. This, however, will not apply to a real rotor having a nearly-axial inducer section at inlet. Elsewhere Stanitz (discussion of Wiesner's paper[9]) proposes that departure from flow in a radial plane at

outlet can be allowed for by introducing the term sin ϕ, thus giving at outlet

$$V_{slip} = \frac{r\Omega \sin \phi \sqrt{\cos \beta_\infty}}{n^{0.7}}$$

Within a passage where ϕ changes from 0 at inlet to $\frac{\pi}{2}$ at outlet one can therefore surmise that slip velocity is zero at inlet and increases in some manner to the Wiesner value of V_{slip} at outlet. The manner of the variation is uncertain.

Nor is it clear exactly how intervanes affect the situation; if the eddy is mainly contained within the portion of passage which includes the intervanes, then Wiesner's formula for V_{slip} at outlet should apply unchanged with $n = n_f + n_i$. But within the passage, the sudden change in blade number must influence the radial development of slip velocity both up and downstream of the intervane leading edges.

There are two further effects likely to influence V_{slip} which Wiesner's relation does not take into account. First, it is fairly certain that V_{slip} must depend in some manner upon h_5/h_4; if this ratio is far from unity (in either direction) the Wiesner relation is likely to be in error. Second, there may be significant variation of V_{slip} with flow at a given rotational speed. In neither case are adequate test data available to introduce the effects.

7. Rotor blade loading

Stanitz & Prian[14] give an analysis which depends upon the condition that there is zero absolute circulation around an element of flow in a blade passage. Applied to blades with pressure and suction surfaces having the same angle at a particular radius, and with backwards sweep (rather than forwards as in Reference 14), the argument can be adapted as below.

Although the mean angle of flow in a blade-to-blade direction (e.g. β_{tip} or β_{hub}) is generally not equal to the local blade angle, either due to slip or - ahead of the throat - due to incidence, nevertheless at the blade surfaces the flow is taken to be at the blade angle.

Then at the blade surfaces the component of absolute velocity in the direction of the local surface is, from the velocity triangle

$$\pm (W - r\Omega \sin \beta_\infty)$$

and the circulation around the circuit ABCD is

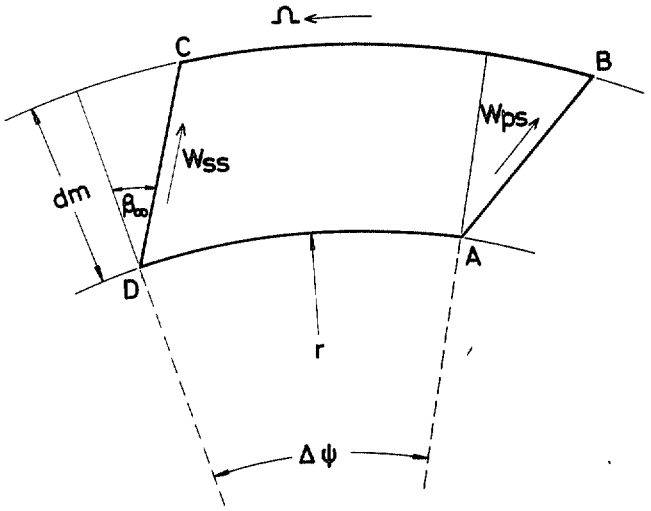

$$\frac{dm}{\cos \beta_\infty}\left[\left(W_{ps} - r\Omega \sin \beta_\infty\right) - \left(W_{ss} - r\Omega \sin \beta_\infty\right)\right] + d\left[\left(V_w\right)_{mean} \cdot r\,\Delta\psi\right] = 0$$

Ignoring blade thickness, $\Delta\psi = 2\pi/n$

$$\therefore \quad W_{ss} - W_{ps} = \frac{2\pi}{n} \cos \beta_\infty \frac{d\left[r \cdot \left(V_w\right)_{mean}\right]}{dm}$$

$$\text{or} \quad \frac{\Delta W}{W_3} = \frac{2\pi}{n} \cos \beta_\infty \frac{d\left[r \cdot \left(V_w\right)_{mean} / m_4\, W_3\right]}{d\left(m/m_4\right)}$$

Davis & Dussourd[15] give a similar relation. Their equation (1) is

$$\Delta W = \Delta\psi \frac{d\left(r\, V_w\right)}{dS}$$ where S is measured along the blade surface

thus $dS = \sec \beta_\infty\, dm$

and $$\Delta W = \frac{2\pi}{n} \cos \beta_\infty \frac{d\left(r\, V_w\right)}{dm}$$ as above.

8. Boundary layers at rotor outlet

No simple treatment of boundary layer growth in the rotor is really defensible, and the assumptions used here are open to serious criticism. In the real flow situation at rotor outlet there are no discrete boundary layers as such, and no uniform core. As a result partly of separation the effective blockage of the flow passage is high, and representation of this by summation of displacement thickness (δ^*) on the various walls obviously implies geometric thickness (δ) greater than is physically possible with a conventional power-law velocity profile. A measure of this blockage is, however, necessary for calculation of loss due to the mixing known to take place immediately after rotor outlet. And factors such as the incidence at which flow meets the rotor blades at inlet, that varies with operating condition, contribute to the loss and so require to be taken somehow into account: this is most satisfactorily done by an attempt to estimate blockage from a boundary layer approach. Consequently it must be reckoned that "the end justifies the means", and illogical features of the treatment are accepted.

As discussed further in Appendix 3-13, the rotor is treated for the purposes of boundary layer growth and other losses as if it has an integral rotating shroud. Thus all four walls of the rectangular flow passages are regarded as growing boundary layers appropriate to the local relative flow conditions.

In reality the total pressure, static pressure, velocity, and flow angle all vary everywhere round the passage perimeter, and steep gradients in all these quantities exist across the passage (see Eckart[1]). The present treatment establishes velocity and flow angle distributions (W and β) in the meridional plane at six positions around the passage perimeter, and boundary layer growth is evaluated for each of these six distributions as if two-dimensional flow existed locally, with uniform static pressure and uniform flow angle (β) through the boundary layer, and with the given velocity (W) occurring at the edge of the boundary layer. Thus the values of δ^* and θ so derived for each position relate the flow and momentum in the boundary

layer to conditions at its edge where "mainstream" gradients of velocity, static pressure, flow angle, etc. are deemed to begin. The resulting values of δ^* at rotor outlet are then averaged to form a blockage factor.

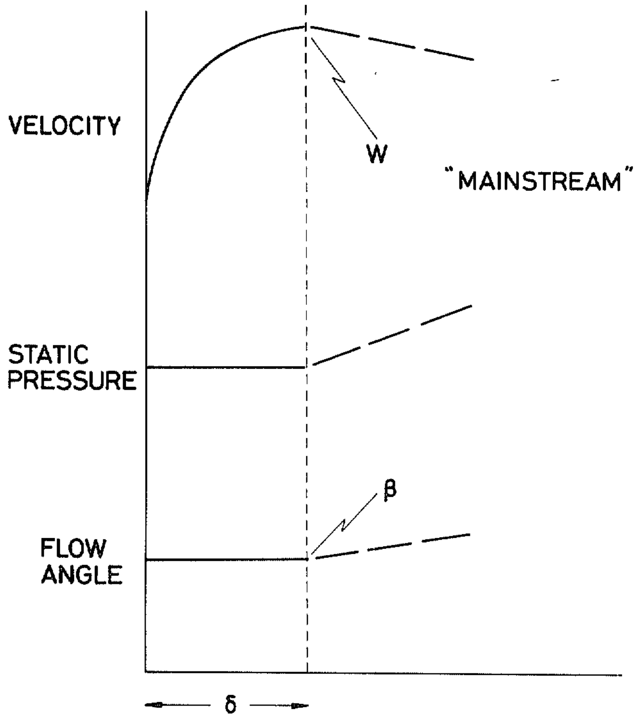

Major defects obviously exist in this procedure. In the first place it takes no account of the important secondary flows arising from the effects of rotation and wall curvature. Secondly, if relations are used that correspond to turbulent attached flow throughout, the effective mean value of shape factor H at outlet is around 1•4. This value of H is certainly unrealistic for surfaces where separated "wakes" develop. In general H rises at separation, to some local value around 3, and if the flow manages to negotiate a separation "bubble" and subsequently re-attach to the surface then H must fall again during the re-attachment process. On the other hand, for a boundary layer which becomes a wake downstream of a terminated surface, H decays from the terminal boundary layer value towards unity. Thus it is uncertain what behaviour of H should be assumed for a surface where permanent separation is maintained. When there is virtually zero net flow through the separated region, informed opinion* suggests that

---

*Private communication by staff of R.A.E.

H may be around 2. In Moore's incompressible experiment[16], resembling the rotating channel of a centrifugal compressor, values of H were deduced to be between 3 and 4 following separation on the suction surface. Moore's selected wake profile relation implies H = 3.89. That experiment indicated absence of any reverse flow in the wake, which carried a significant and increasing portion of the through-flow (being fed by secondary flow in the channel), and Moore points out that this situation is considerably different from the case of normal two-dimensional boundary layer separation. Apparently, then, quite a high value of H should be attributed to the wakes which in a real machine represent the major source of channel blockage at rotor outlet.

It is found, however, that the calculated mixed-out conditions at rotor outlet are rather insensitive to the assumptions made regarding H. Since the complexities of the real flow situation cannot be properly modelled by any boundary layer treatment simple enough to be used in a "quick" prediction method of this type, and because of other imperfections such as the arbitrary nature of the velocity and camber angle distributions assumed[*], it is necessary to introduce an empirical factor somewhere into the relations for rotor outlet blockage to bring predicted performance into line with experiment. Such a factor may be applied either to all passage surfaces or, more realistically, to blade suction surfaces only.

Two alternative procedures have been examined:-

A. Attributing to all surfaces a value of H derived for one-seventh-power velocity profiles (H = 1.4), and increasing both δ^* and θ by a factor Z applied to suction surfaces only.

B. Surfaces other than suction treated as having one-seventh-power velocity profiles (H = 1.4) with no factor applied; suction surfaces treated as having a specified higher value of H (e.g. $H_{SS} = 3$), θ being evaluated as for an attached boundary layer with one-seventh-power velocity profile, and δ^* from θ and H_{SS}, with a factor X applied to both δ^* and θ.

---

[*] If a certain pressure distribution exists on a surface with attached flow, that distribution will be changed in an unknown manner by separation taking place. The wall pressure distributions corresponding to the surface velocities arbitrarily assumed in this treatment are not intended to be an accurate model of those existing in a real compressor with separated wakes. But in general form they are thought to be sufficiently typical of current design practice to form a basis for calculation of blockage via boundary layer growth.

Clearly neither model is fundamentally satisfactory, and the pretence of calculating discrete boundary layer thicknesses is only a convenient way of introducing the effect of variations in surface velocity distribution (e.g. due to incidence), and of enabling the mixing process at rotor outlet to be handled in a reasonable manner. But comparison of these two systems is informative, and demonstrates some important features of the iterative procedure within which the boundary layer calculations are contained.

Figures 2 and 3 show results obtained from the complete prediction method using two alternative sets of boundary layer assumptions, viz:-

1. $H_{ss} = 1.5$
2. $H_{ss} = 3$

} X varying in each case

Case 1 corresponds closely with system A above. The following points deserve note:-

(i) The values of B_4 and β_4 (before mixing) are significantly affected by choice of H_{ss}. [When $H_{ss} = 3$, β_4 can be as low as the blade angle, but the value of X is then unrealistically high.]

(ii) But the value of $B_4 \cos \beta_4$, which is a function primarily of $\hat{M}'_4$, is not much changed, and the conditions after mixing - see β_5 and M'_5 - are nearly the same. Consequently rotor efficiency is insensitive to H_{ss} at realistic X (experience suggests Z or X as circa 3 to 5 for match to experiment).

(iii) β_4 is considerably smaller than β_5 when $H_{ss} = 3$, but more nearly equal to β_5 when $H_{ss} = 1.5$. As noted in Appendix 3-10, the condition $\beta_4 < \beta_5$ tends towards the case of purely mechanical blockage (when "mixing" is simply a sudden enlargement of flow area), which would correspond to $\theta = 0$ or $H = \infty$.

(iv) It can be concluded that within the possible range of H_{ss} (say 1.4 to 4) its effect on rotor efficiency is slight and outweighed by whatever factor (e.g. Z or X) is used to tune the level of predicted performance.

(v) For a given rotor efficiency, X is slightly less at higher H_{ss}.

(vi) In this analysis the rotor outlet chokes (i.e. $\hat{M}'_4 = 1$) when blockage is increased sufficiently by means of high Z or X. For the examples shown, this occurs at $X \simeq 13.5$ with $H_{ss} = 3$, or $X \simeq 18.5$ with $H_{ss} = 1.5$.

(vii) It should be noted that for converged solutions the total boundary layer blockage would not change pro rata with the multiplication factor even if that factor were applied to all surfaces. This is because the underlying surface velocity distributions change with the factor: a large factor means high $\hat{M}_4'$, less rotor diffusion, and hence reduced boundary layer thickness before multiplication by the factor.

The comparison embodied in Figures 2 and 3 thus indicates that choice of H_{SS} is not important. In view of this, alternative A, using the factor Z rather than X, is adopted.

A quantity comparable in significance to the multiplication factor (Z or X) is the value of $\overline{\delta_3^*}$ assumed to exist at rotor inlet. In the examples just cited a value of $\overline{\delta_3^*}/h_3 = 0.01$ is assumed for both hub and shroud walls, corresponding to $B_3 = 0.98$. This value of B_3 is arbitrarily chosen, and the equal division between the two walls is arbitrary; particular configurations of entry ducting may in practice produce different overall values of B_3 and different division between walls. The effect of B_3 is illustrated by the following example, also relating to equal division between walls:-

B_3	rotor efficiency
1.0	0.930
0.98	0.895
0.96	0.860

giving $1\frac{3}{4}$ per cent efficiency drop per one per cent of inlet blockage. This, therefore, is an effect of much greater magnitude than H, and represents a major uncertainty in the whole method of treatment.

So far as their influence on the calculation is concerned, the two quantities B_3 and Z are complementary and to some extent interchangeable in function, and it is clearly undesirable to leave more than one such major quantity adjustable to suit individual experimental results. Hence there is a strong need to select an average value of B_3 for general prediction purposes. Some guidance in this choice may be obtained from the combination of

(a) knowledge of the inducer throat blockage factor (B_*) required to match empirically the measured choking flow

(b) calculation of the inducer throat blockage due to boundary layer growth, over a range of different values of B_3.

The latter calculation is of dubious accuracy due to the many assumptions upon which it depends (given in the main text) in relation to flow angle and surface velocity distributions and the treatment of incidence, and it ignores possible effects of separation near the leading edge (due to shocks or otherwise) and of flow curvature in the throat (this effect is likely to be small, <1 per cent blockage). But an approximate estimate may be made as follows:-

Knowing distributions of W and T_t', and hence M'

$$\frac{\ell_*}{m_4} = \frac{1}{p_*}\left[\int_0^{m_*/m_4} p \sec\beta \, d(m/m_4) + \frac{\ell_3 \, p_3}{m_4}\right]$$

where

$$p_* = \left[\frac{M_*'}{1 + 0.2\left(M_*'\right)^2}\right]^4$$

ℓ_3 = 0 for blade surfaces, and for hub and shroud surfaces depends upon δ_3^* and hence on B_3 as given in the main text

Then for each surface at the throat

$$\delta^* = 0.046\left[1 + 0.8\left(M_*'\right)^2\right]^{0.44} \ell_* \left[\frac{\mu_*}{\rho_* \, W_* \, \ell_*}\right]^{0.2}$$

where μ_* and ρ_* are obtained from knowledge of M_*' (different for each surface) and of $P_{t,*}'$ and $T_{t,*}'$ (different for hub and tip only).

Writing

$d_{(2)}$ = δ^* on shroud surface

$d_{(1)}$ blade suction surface, tip

$d_{(5)}$ blade pressure surface, tip

$d_{(7)}$ hub surface

$d_{(10)}$ blade suction surface, hub

$d_{(6)}$ blade pressure surface, hub

the boundary layer blockage at the throat[*] is approximately

$$d_{(2)} \left(2\pi r_{*,tip} \cos \beta_{\infty *,tip} - n_f \, t_{*,tip}\right) +$$

$$+ d_{(7)} \left(2\pi r_{*,hub} \cos \beta_{\infty *,hub} - n_f \, t_{*,hub}\right) +$$

$$+ \tfrac{1}{2} n_f \left[d_{(1)} + d_{(5)} + d_{(6)} + d_{(10)}\right] \left[\left(r_{*,tip} - r_{*,hub}\right) - d_{(2)} - d_{(7)}\right]$$

and

$$B_{*(BL)} = 1 - \frac{\text{boundary layer blockage}}{\text{geometric throat area}}$$

This quantity, $B_{*(BL)}$, may be compared with B_* ($= \sigma B_s$) as determined to fit measured choking flow, for several compressors.

---

[*] i.e. in this treatment at a distance of m_* from the leading edge on all surfaces

		B_3 assumed in calc.*	$B_{*(BL)}$	B_* from test	calculated $M'_{3,tip}$
CASE 1	choking flow	0.98 1.0	0.955 0.991	0.94	1.011 1.002
CASE 2	choking flow	0.98 1.0	0.944 0.984	0.94	0.999 0.994
	lower flow	0.98	0.921	-	-
CASE 3	choking flow	0.98 1.0	0.951 0.990	0.91	1.237 1.229
	lower flow	0.98	0.939	-	-

*Equal division between hub and shroud

From this table the following points may be noted:-

(i) As flow decreases the calculated boundary layer throat blockage rises, for constant B_3; this is due to incidence becoming more positive with consequently more diffusion (or less acceleration) between inlet and throat.

(ii) At choking B_* determined from tests, Cases 1 and 2, agrees roughly with the calculated $B_{*(BL)}$ corresponding to $B_3 = 0.98$ and not at all with that corresponding to $B_3 = 1$.

(iii) The lower B_* for Case 3 is associated with $M'_{3,tip} > 1$, involving some thickening of the inlet boundary layer due to shock interaction which is not allowed for in calculating $B_{*(BL)}$ in the foregoing manner.

Thus it may be generally reasonable to take $B_3 = 0.98$, leaving Z as the remaining factor for adjustment to suit individual test results.

With such considerable uncertainties present as have been noted, there is little point in attempting refinement of other boundary layer assumptions, save for seeking to give the analysis an appearance that is more or less philosophically reasonable. Much more sophisticated and laborious treatment of boundary layer growth (including secondary flows)

could be introduced to try and simulate the real situation, without material benefit in these circumstances.

Typical boundary layer proportions on the different surfaces at rotor outlet as computed using $H_{SS} = 1.5$, $X = 3$, $B_3 = 0.98$ are as follows:-

	Full blade suction	Intervane suction	Non-blade ("mean")	Intervane pressure	Full blade pressure
Hub	157	82	47	7	19
Tip	201	97	98	10	20

In this example the aspect ratio of the passage at rotor outlet, measured normal to the flow between a full blade and an adjacent intervane, is approximately 3. Thus the non-blade (hub and shroud) surfaces account for three-quarters of the perimeter, which is why a factor such as Z or X applied to suction surfaces only has to be fairly large in order to have much overall effect.

It has been suggested earlier in this section that $Z \approx 4$ gives optimum match to experiment, and this value is adopted as "standard". The experience on which that choice is based relates to good current designs of rotor all with substantially similar amounts of diffusion. Poor machines would obviously require a higher value of Z. And in cases where the rotor relative velocity ratio is much greater or much less than conventional, then it is likely that Z should be taken as also greater or less than the "standard" value.

A question remains as to whether Z should be scheduled with, for example, design pressure ratio. The quantity Z in effect chiefly represents blockage growth due to separation and wake formation. Now increase of pressure ratio essentially means higher rotational speed and hence raising of the Mach number level generally throughout the rotor; this perhaps advances the onset of separation and/or increases the growth of wakes into which low energy fluid is swept by the action of secondary flows. It might therefore be reasonable to relate Z to rotor pressure ratio.

9. Absolute and relative momenta

Consider any flow situation

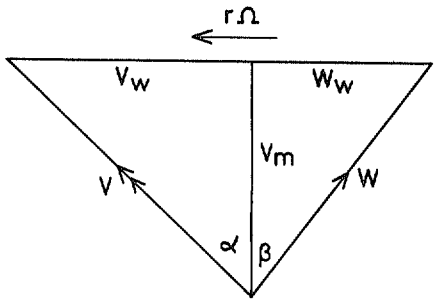

$$\text{Meridional momentum} = \frac{Q\,V_m}{g} + A_m\,P_s$$

which is the same in the relative and absolute frames

$$\text{Tangential momentum in absolute frame} = \frac{Q\,V\sin\alpha}{g}$$

$$\text{Tangential momentum in relative frame} = \frac{Q\,W\sin\beta}{g}$$

$$= \frac{Q}{g}(r\Omega - V\sin\alpha)$$

$$\therefore \quad \text{relative tangential momentum} = \frac{Q\,r\Omega}{g} - \text{absolute tangential momentum}$$

Hence if absolute momentum everywhere is conserved and there is no change of radius, then relative momentum everywhere is also conserved.

10. Mixing at rotor outlet

The mixing, assumed to be instantaneous at the blade trailing edges, changes the flow from a state where blockage exists due to blade thickness and to boundary layers having grown on the rotor passage walls, to a one-dimensional condition with circumferential uniformity. There is, of course, a loss of total pressure associated with that change. Given a certain value of the effective blockage, for example from some experimental measurement of average flow properties, there are two approaches.

First, to treat the mixing as a simple sudden enlargement in area (equal to the blockage) experienced by flow that is essentially one-dimensional both before and after the enlargement. That corresponds to setting equal the terms 1 - F and 1 - G in the mixing equations of Reference 8. The equations for continuity and conservation of tangential momentum give the relation

$$\frac{1 - G}{1 - F} W_4 \sin \beta_4 = W_5 \sin \beta_5$$

where F is a measure of blade trailing edge thickness and aggregated boundary layer displacement thickness δ^*, and G contains in addition the aggregated boundary layer momentum thickness θ. Consequently, if all blockage is treated like blade trailing edge thickness, effectively with $\delta^* = \theta = 0$, then

$$W_4 \sin \beta_4 = W_5 \sin \beta_5$$

and it follows that

(i) both relative and absolute tangential velocities are unchanged through the mixing

(ii) the relative flow angle increases ($\beta_5 > \beta_4$)

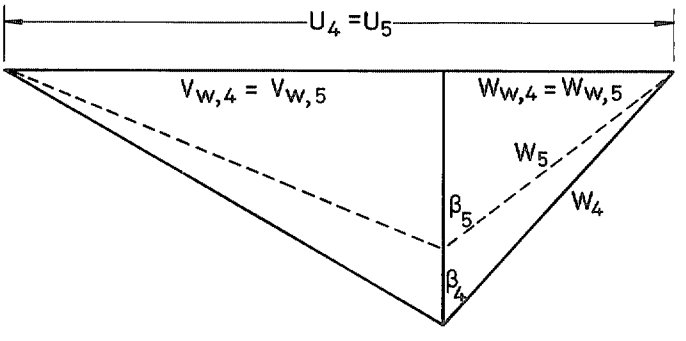

In the second approach, consistent with estimation of blockage from a boundary layer treatment, $\frac{1 - G}{1 - F} < 1$, and for typical solutions there may be only a small difference between β_4 and β_5, perhaps a few degrees either way, depending upon the mean value of H and upon blade trailing edge thickness. Drawing velocity triangles for the particular case of $\beta_4 = \beta_5$

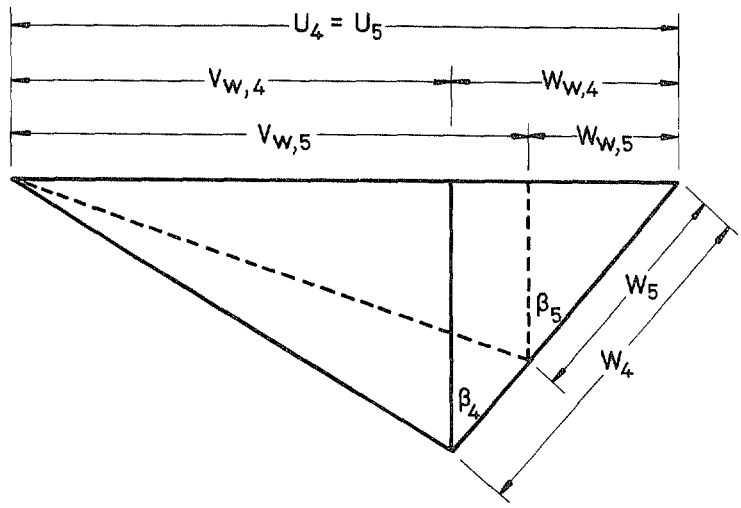

it is seen that

$V_{w,5} > V_{w,4}$ and

$W_{w,5} < W_{w,4}$

Now the work equation requires that

$$\left[\Sigma\, V_w\, dQ\right]_4 = Q \cdot V_{w,5}$$

Noting that, unlike the first approach in which the flow before the enlargement was already one-dimensional, in this second approach W_4 relates to an assumed isentropic "core" (both "core" and boundary layer having uniform angle β_4), the work equation becomes

$$\left(\frac{1 - \delta}{1 - \delta^*}\right) V_{w,4} + \left(\frac{\delta - \delta^*}{1 - \delta^*}\right) \overline{V_w}_{,BL} = V_{w,5}$$

where $\overline{V_w}_{,BL}$ is the mass mean absolute whirl velocity of the boundary layer flow. Since $\left\{\begin{array}{l} V_w = U - W_w \\ U = \text{constant} \end{array}\right\}$ throughout, it follows that

$$(1 - \delta)\, W_{w,4} + (\delta - \delta^*)\, \overline{W_w}_{,BL} = (1 - \delta^*)\, W_{w,5}$$

where $\overline{W_w}_{,BL}$ is the mass mean relative whirl velocity of the boundary layer flow. But as $W_{w,5} < W_{w,4}$

$$(1 - \delta)\, W_{w,4} + (\delta - \delta^*)\, \overline{W_w}_{,BL} < (1 - \delta^*)\, W_{w,4}$$

or

$$\overline{W_w}_{,BL} < W_{w,4}$$

This is clearly correct, since the boundary layer profile is such that at any point within the boundary layer $W < W_4$, and hence on the assumption of uniform flow angle β_4,

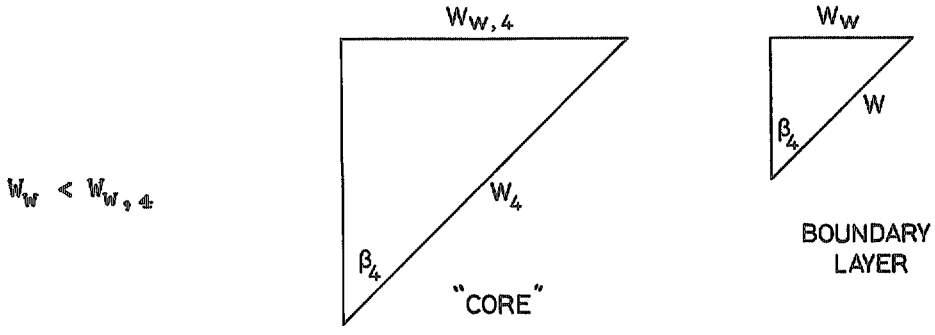

An interesting digression is to consider the case of blades with forward instead of backward sweep at outlet. Since the mixing calculation is concerned only with relative flow conditions (vide Appendix 3-9), the numerical solution is unchanged. Thus the velocity triangles (again for the case of $\beta_4 = \beta_5$) become

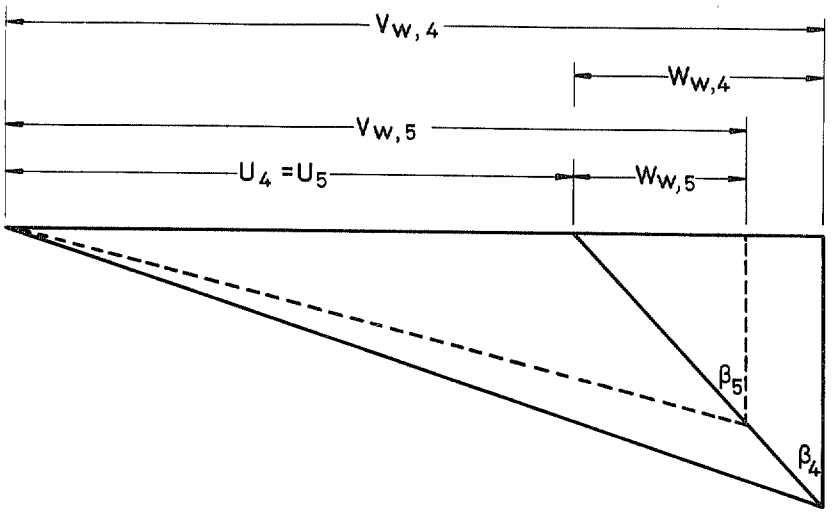

$W_{w,5} < W_{w,4}$ as before

But now $V_{w,5} < V_{w,4}$

In this case $\left\{ \begin{array}{l} V_w = U + W_w \\ U = \text{constant} \end{array} \right\}$ throughout, so that the work

equation leads as before to

$$\overline{W_{w,BL}} < W_{w,4}$$

In the special case of $\beta_4 = 0$, β_5 must also = 0 in both approaches and relative whirl velocities throughout are zero so that the work equation is satisfied.

11. Disc friction

This relates to the friction on two sides of an enclosed disc with zero throughflow. Leakage losses are additional when there is throughflow.

Two sources of data may be compared:

(i) Daily & Nece[17]: tests with liquids at values of rim speed up to 170 ft/sec, hence very low Mach number.

They define a dimensionless torque coefficient C_m such that

$$\text{Torque} = C_m \frac{1}{2g} \rho \Omega^2 r^5$$

C_m depends primarily on Reynolds number $\left(\frac{\rho \Omega r^2}{\mu}\right)$, and weakly on the ratio axial clearance/radius; four regimes of flow are distinguished. Where large changes of ρ and μ occur from inlet to outlet of a real machine, some mean value must be used in the expressions for torque and Re above.

For ranges of clearance/radius and Re typical of radial compressors, the recommended relation for C_m (regime IV*) gives approximately

$$C_m = 0.07 \left(\frac{\bar{\rho} \Omega r^2}{\bar{\mu}}\right)^{-0.2}$$

Then work loss is

$$Q \Delta(C_p T_t) = \frac{\text{torque} \times \Omega}{J}$$

$$= 0.07 \frac{\bar{\rho} \Omega^3 r^5}{2gJ} \left(\frac{\bar{\rho} \Omega r^2}{\bar{\mu}}\right)^{-0.2}$$

where all quantities are in ft-lb-sec-CHU units.

---

*In the paper[17] the coefficient in the empirical relation for Regime IV should read 0.102 not 0.0102.

(ii) Ribary[18]: tests with gases at subsonic rim speed; the author warns that when rim Mach number ≥ 1, some dependence on it ought to be included in the relation.

The formula is given[*]

$$\text{Power in Kilowatts} = 1.26 \times 10^{-4} \frac{\rho U^3 D^2}{g} \left(\frac{\rho U D}{\mu}\right)^{-0.2}$$

where ρ is in kg/m^3, U in m/sec, D in m, g in m/sec^2, and μ in kg/m sec.

After conversion to ft-lb-sec-CHU units the work loss becomes

$$Q\,\Delta(C_p T_t) = 0.0894 \frac{\bar{\rho}\, \Omega^3 r^5}{2gJ} \left(\frac{\bar{\rho}\, \Omega r^2}{\bar{\mu}}\right)^{-0.2}$$

These two sources give relations of identical form, with coefficients that agree quite well (0.07 in one case, $\approx$ 0.09 in the other) and a mean value of 0.08 may be taken.

---

[*] In the paper[18] there is confusion between symbols ξ and ξ', but the graph (Figure 1 of Reference 18) indicates that the experimental constant 1.26×10^{-4} is to be compared with the theoretical value 2.05×10^{-4}, and hence that this experimental constant evidently relates to equation (9), rather than (6) as stated.

12. Leakage losses

There are basically two sorts of loss associated with flow leakage.

First: leakage from outlet to inlet via shroud
under the action of pressure gradient;
this is called "recirculation".

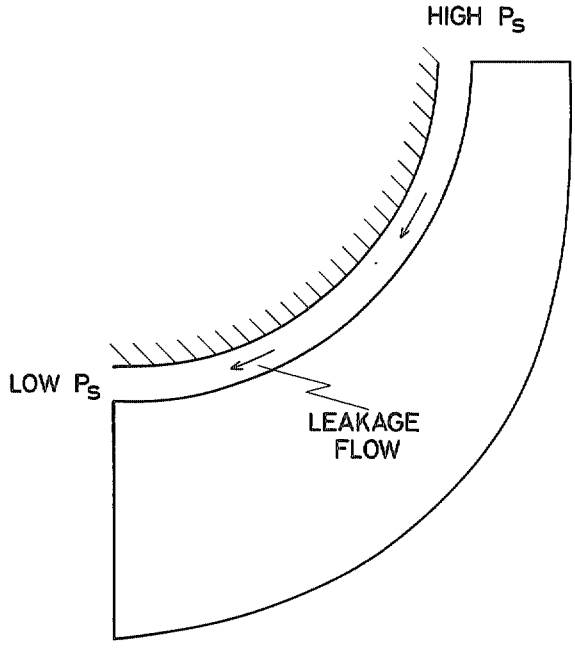

There is no satisfactory treatment for this. Three references mention it:

(i) Coppage, Dallenbach, et al[19] of Airesearch suggest tentatively

$$\Delta(C_p\, T_t) = 0.02\, (\tan \alpha_s) \cdot k\, \frac{U_s^2}{gJ}$$

where k is a "diffusion factor" (apparently having its origin in NASA axial cascade work) which is defined as

$$k = 1 - \frac{1}{W_{s,tip}} \left\{ W_s - \frac{1.5\, \pi \cdot gJ \left(C_p\, T_{t,s} - C_p\, T_{t,s} \right)}{\mathfrak{N} \left[n \left(D_s - D_{s,tip} \right) + 2\pi D_{s,tip} \right]} \right\}$$

This is entirely speculation and no evidence is cited to support either the form of relation or the constant used. There ought to be some dependence on gap size.

(ii) Rodgers[20] gives an expression for "scrubbing" and "recirculation" jointly, involving $\frac{1}{\Phi^2}$ where his Φ is the "inlet flow coefficient" $\frac{\overline{V_{m,3}}}{U_5}$, but says in the preceding text that the loss varies as the inverse of Φ, i.e. as $\frac{1}{\Phi}$ not $\frac{1}{\Phi^2}$. As by "scrubbing" he appears to mean disc friction, the $\frac{1}{\Phi^2}$ is presumably an error, since $\overline{V_{m,3}} = \frac{Q \cos \bar{\alpha}_3}{\bar{\rho}_3 A_3}$, so that his relation would read

$$\Delta(C_p T_t) = 0.0032 \frac{1}{\Phi} \cdot \frac{U_5^2}{gJ}$$

or

$$Q \Delta(C_p T_t) = 0.0032 \frac{\bar{\rho}_3 A_3 U_5^3}{gJ \cos \bar{\alpha}_3}$$

and noting that A_3 has dimensions similar to D_5^2, this expression matches that for disc friction (vide supra); it would not do so if $\frac{1}{\Phi^2}$ were used.

But one can get no further: the breakdown between disc friction and recirculation is not given, and without any supporting evidence it would be inadvisable to adopt an unproven relation for the two effects together.

(iii) Rodgers & Sapiro[21] of Solar again combine disc friction and recirculation, and give

$$Q \Delta(C_p T_t) = 0.5 \times 10^{-5} \left(\frac{\bar{\rho}_3 + \rho_5}{2} \right) \cdot \frac{U_5^3 D_5^2}{gJ} \cdot \frac{\cos \beta_{\infty_4}}{(\text{slip factor})}$$

The group $\frac{1}{2}\left(\bar{\rho}_3 + \rho_5\right) U_5^3 D_5^2$ is exactly that appearing in the normal relations for disc friction (vide supra), but with Reynolds number omitted; the group $\cos \beta_{\infty 4}$/(slip factor) is not understood. Supposing the latter be assumed ≈ 1, which is at least of the correct order, then a comparison may be made with disc friction alone, by extracting the common group $\bar{\rho}\ \Omega^3\ r_5^5/2gJ$ and leaving

Solar relation	Disc friction
4×10^{-5}	$0.08 \left(\frac{\bar{\rho}\ \Omega\ r_5^2}{\bar{\mu}}\right)^{-0.2}$

This Reynolds number is typically[/] in the range 0.2 to 1.5×10^7 so producing a value of 2.9 to 4.4×10^{-3} on the right-hand side (= C_m). By comparison the Solar relation is far too small, and appears to contain a major error.

There is one other relation of possible relevance. Rodgers & Sapiro (ibid) do not make clear what they mean by "recirculation" in the context of the last relation, and they give a further expression for the loss "due to axial clearance" said to be derived from tests of shrouded impellers. This is

$$\Delta\eta = \kappa \left(\frac{\text{gap}}{h_4}\right) \quad \text{where } \kappa = 0.15 \text{ to } 0.2$$

For no prewhirl one may write

$$\Delta\eta = \frac{\Delta\left(C_p\ T_t\right)}{V_{w,5}\ U_5/gJ}$$

Hence the last relation becomes, to sufficient accuracy

$$\Delta\left(C_p\ T_t\right) = 0.2 \left(\frac{\text{gap}}{h_4}\right) \frac{V_{w,5}\ U_5}{gJ}$$

[/] Evaluated for eight compressors covering pressure ratios 3 to 6½

Now the only leakage in a shrouded impeller should be that here called "recirculation", and it is therefore possible that the last relation is intended to apply to that loss. But the situation is too confused to be useful.

Thus none of the references provide an acceptable estimate for this type of leakage loss alone.

Second: leakage past unshrouded blade tips under the action of the pressure difference between pressure and suction surfaces.

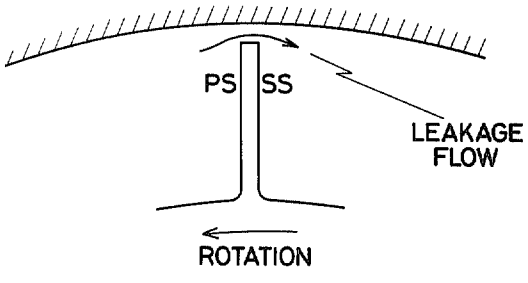

Jansen[22] gives the theoretical expression

$$\Delta\left(C_p\, T_t\right) = \frac{0.6}{gJ}\left(\frac{gap}{h_4}\right)\left[\frac{2\pi\, V_{w,5}^{3}\, \overline{V}_{m,3}\left(D_{3,tip}^{2} - D_{3,hub}^{2}\right)}{n\, h_4\left(1 + \rho_5/\bar{\rho}_3\right)\left(D_4 - D_{3,tip}\right)}\right]^{\frac{1}{2}}$$

which is said to agree satisfactorily with test data.

In any experiment it would be hard to separate the two types of leakage loss, since changes of clearance affect both, and so it seems likely that Jansen's relation should be regarded as fitting total loss from leakage, even though it is not derived on that basis. This supposition is supported by the fact that Jansen says his relation produces similar values to an empirical one obtained by Krylov & Spunde[23] from unshrouded radial inflow turbine tests, where both forms of leakage loss would be present.

Krylov & Spunde give

$$\Delta\eta = 2\left(\frac{gap}{h_4}\right)\left(\frac{D_{3,tip}}{D_4} - 0.275\right)$$

where "gap" is defined as the clearance normal to the surface of the casing - presumably an average figure through the whole passage.

But note that in a radial inflow turbine the meridional pressure difference acts from outer to inner diameter, this being in the direction of flow, whereas in a centrifugal compressor the pressure difference acts the same way while the flow direction is opposite. Thus the stimulus for flow to take the so-called recirculation leakage path is not the same in the two cases, and for the turbine that leakage flow is not in fact recirculated, so in general the penalty may be lower in the turbine case. Nevertheless, examination of test data for centrifugal compressors, from five different sources, indicates that the Krylov & Spunde relation much overestimates the rate of fall of efficiency with increase of clearance in the range $0.035 < \text{gap}/h_4 < 0.15$ (a normal value of gap/h_4 at design speed is between 0.025 and 0.04).

To sum up, the literature does not provide any satisfactory working relation for leakage loss.

Now axial compressor experience suggests that tip clearance loss follows a pattern as shown in the sketch, and it may be surmised that a similar form applies to centrifugals. The centrifugal compressor data surveyed support a slope at normal and greater clearances approximately given by

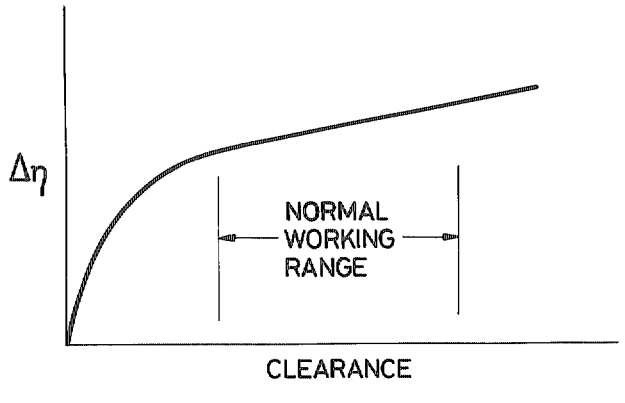

$$0.475 \frac{D_{s,tip}}{D_4}$$

On this somewhat slender basis the following arbitrary relations are proposed for working purposes:-

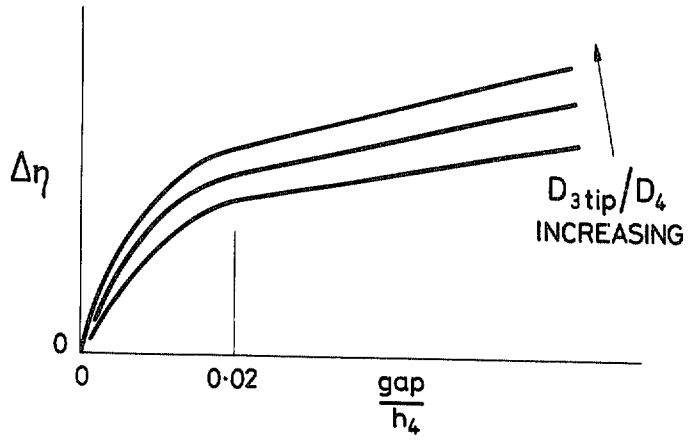

when $gap/h_4 \geq 0.02$*

$$\Delta\eta = \left[0.475\left(\frac{gap}{h_4}\right) + 0.02\right]\frac{D_{3,tip}}{D_4}$$

when $gap/h_4 < 0.02$

$$\Delta\eta = \left[2.475\left(\frac{gap}{h_4}\right) - 50\left(\frac{gap}{h_4}\right)^2\right]\frac{D_{3,tip}}{D_4}$$

---

*For a centrifugal compressor "gap" should be taken as the axial clearance between rotor and casing at rotor outlet. In practice this clearance varies with speed, but there is no evidence as to how leakage loss should be assessed at part speed, so the relation is used with design speed clearance at all conditions.

13. Parasitic losses in general

With a shrouded compressor rotor, it is easy to distribute losses realistically (even though quantitative estimation may be difficult). In that situation the rotor flow passages are fully enclosed by rotating walls, on which boundary layers can be deemed to develop according to the local surface relative velocity distribution. Between the rotating shroud and stationary casing there is a clearance gap, leading to two effects. First of these is the type of friction associated with zero throughflow, which is similar to that on the rear face of the rotor; the friction loss of a fully-enclosed two-sided disc is then representative. Second is the leakage loss referred to as "recirculation", which exists where there is throughflow, whereby a small proportion of the fluid returns from rotor outlet to inlet.

When there is no rotating shroud, cataloguing of losses becomes much more confusing. A similar recirculation path exists as mentioned above, and also similar "disc" friction on the rear face (only) of the rotor. But it is no longer obvious how to treat the remaining effects. Growth of a boundary layer on the outer side of the flow passage combines in some manner with the zero-throughflow friction on the casing, and additional loss takes place due to peripheral leakage around the blade tips. The latter is primarily associated with blade loading and hence with throughflow, so that, as noted earlier, tip leakage and recirculation losses could not readily be distinguished in any experiment.

For want of a better approach, the method adopted here is to assume that the losses from boundary layer growth and friction together are the same for an unshrouded rotor as for a shrouded one. Hence boundary layer growth on the passage outer side is treated in the same way as on the other sides, additional friction is included corresponding to a double-sided disc, and a clearance loss is added according to the best available correlation.

The question then arises how to treat the work represented by parasitic losses. In the case of a shrouded rotor, "recirculation loss" can be regarded as involving an unchanging mass of fluid, equal to a small proportion of the throughflow, which is continuously following a cycle of compression in the rotor (a → b), expansion along the leakage path with

some heat loss to the casing and rotor (b → c), and final cooling by giving up heat to the through-flowing air (c → a). "Disc friction" also heats the casing and rotor. Much of the heat passing to the rotor from these sources is then absorbed by the through-flowing air progressively throughout its passage within the rotor. This violates the normal adiabatic state during compression upon which conservation of rothalpy is based, and leads to an increase of stagnation temperature rise unmatched by any increase in Euler work. Additionally there is the quasi-instantaneous increase of rotor inlet enthalpy due to cooling the recirculating fluid. A qualitatively similar situation must exist in the case of an unshrouded rotor.

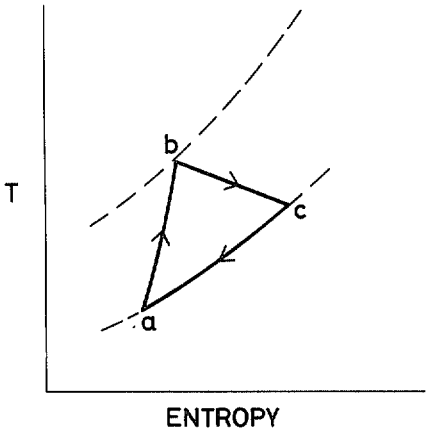

As a crude representation, some arbitrary proportions of the aggregate parasitic loss could be assumed to pass to the through-flowing air as discrete additions of heat at rotor inlet and at rotor outlet. Supposing that half of the lost work reaches the air, that would mean an increase of enthalpy rise of $1\frac{1}{2}$-$2\frac{1}{2}$ per cent, or typically 3-6° in outlet stagnation temperature; i.e. $\frac{2}{3}$-1 per cent increase in temperature. Since the major result of this would appear in the diffuser as an increase in level of Mach number via $\frac{Q\sqrt{T_t}}{A\,P_t}$, the net effect would be small, and in order to avoid further complication of the method it is for the present purpose ignored.

14. Flow and boundary layer growth in the vaneless diffuser

Treatment of the flow in this region follows the analysis by Stanitz[24], but correction is required. Stanitz says "The effective height of the diffuser at each point on the mean surface of revolution is equal to the geometric height of the diffuser minus the assumed displacement thickness of the boundary layer on the diffuser walls. Only the effective height of the diffuser is considered in this report; ..... boundary layer displacement thickness ..... can be assumed or estimated from boundary layer theory". Unfortunately that approach is not satisfactory; continuity and momentum relations require different areas, so that use of a single "effective height" is not permissible.

The main assumption in the treatment is that outside the boundary layer the flow is uniform across the passage at any radius. Static pressure and flow angle are assumed uniform across boundary layer and mainstream. For the present purpose simplifications are made to Stanitz's treatment, in that the vaneless diffuser is regarded as having its centreline radial, and heat transfer is neglected.

Boundary layer terms cannot readily be incorporated in an analysis using, as Stanitz did, the fluid particle acceleration method, and it has therefore been necessary to rewrite the analysis using the stream-tube momentum box method. Consequently the derivation of the working equations must be given in full.

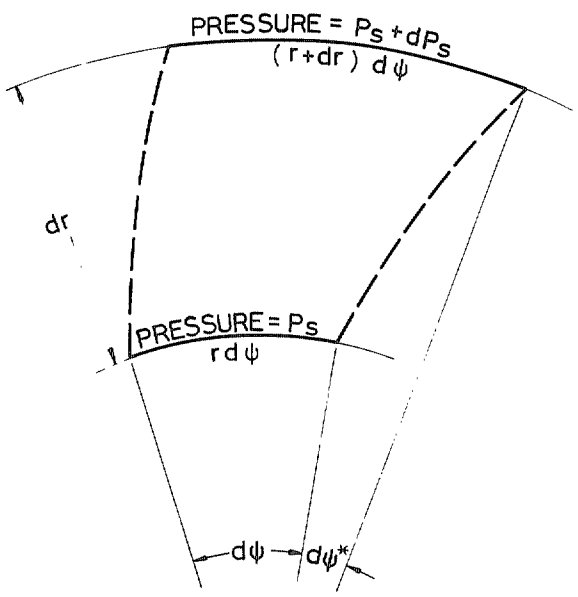

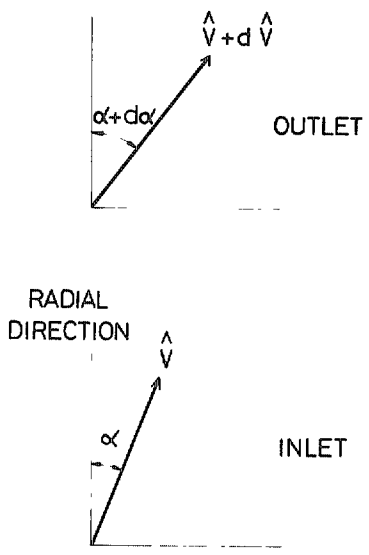

At inlet to momentum box: velocity = $\hat{V}$ inclined at α

pressure = P_s

flow area = $r\, d\psi \cdot h' \cos\alpha$

At outlet from momentum box: velocity = $\hat{V} + d\hat{V}$ inclined at $\alpha + d\alpha$

pressure = $P_s + dP_s$

flow area = $(r + dr)\, d\psi\, (h' + dh') \cos(\alpha + d\alpha)$

Define
- h = geometric width of passage
- $h' = h - 2\delta^*$
- $h'' = h - 2\delta^* - 2\theta$

Pressure forces

It may be shown that, neglecting third order small terms:-

Net radial pressure force = $h\, r\, dP_s \cdot d\psi$

(directed inwards)

Net tangential pressure force = 0

Mass flow

$$dQ = \hat{\rho} \cdot r\, d\psi\, h' \cos\alpha \cdot \hat{V}$$

Shear force

Force opposite to average direction of motion = $C_f \cdot \frac{\hat{\rho}\,\hat{V}^2}{2g}$ (wetted area)

Wetted area = $2\, r\, d\psi \sqrt{(dr)^2 + (\tfrac{1}{2}\, dh)^2}$

$\therefore$ Force = $C_f \cdot \frac{\hat{\rho}\,\hat{V}^2}{g} \cdot r\, d\psi\, dr \cdot \zeta$

where $\zeta = \sqrt{1 + \frac{1}{4}\left(\frac{dh}{dr}\right)^2}$

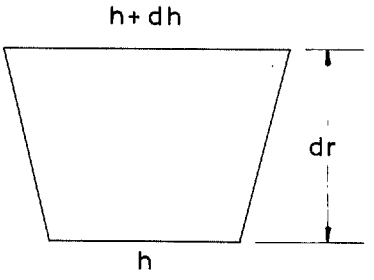

Momentum

In direction of local motion,

$$\text{inlet momentum} = \frac{\hat{\rho} \cdot r\, d\psi\, h'' \cos\alpha \cdot \hat{V}^2}{g}$$

$$= dQ \cdot \frac{h''}{h'} \frac{\hat{V}}{g}$$

$$\text{outlet momentum} = dQ \cdot \frac{(h'' + dh'')}{(h' + dh')} \cdot \frac{(\hat{V} + d\hat{V})}{g}$$

Tangential force balance

$$\frac{dQ\ (\hat{V} + d\hat{V})}{g} \left(\frac{h'' + dh''}{h' + dh'}\right) \sin(\alpha + d\alpha + d\psi^* + \tfrac{1}{2} d\psi)$$

$$+ C_f \zeta \frac{\hat{\rho}\ \hat{V}^2}{g} r\, d\psi\, dr \sin\alpha = \frac{dQ \cdot \hat{V}}{g} \frac{h''}{h'} \sin(\alpha + \tfrac{1}{2} d\psi)$$

On substituting for dQ and rearranging, this gives

$$\left(1 + \frac{d\hat{V}}{\hat{V}}\right)\left(1 + \frac{dh''}{h''}\right)\left(1 - \frac{dh'}{h'}\right)\left[1 + \cot\alpha\ (d\alpha + d\psi^* + \tfrac{1}{2} d\psi)\right]$$

$$- \left(1 + \cot\alpha \cdot \tfrac{1}{2} d\psi\right) + C_f \zeta \frac{dr}{h'' \cos\alpha} = 0$$

Retaining only first order small terms at this stage, we have

$$\frac{d\hat{V}}{\hat{V}} + \frac{dh''}{h''} - \frac{dh'}{h'} + \cot\alpha\ (d\alpha + d\psi^*) + C_f \zeta \frac{dr}{h'' \cos\alpha} = 0$$

Now $\frac{d\psi^*}{dt} = \frac{\hat{V} \sin\alpha}{r}$ and $\frac{dr}{dt} = \hat{V} \cos\alpha$, whence $d\psi^* = \tan\alpha \frac{dr}{r}$

$$\therefore \quad \frac{dh''}{h''} - \frac{dh'}{h'} + \frac{d\hat{V}}{\hat{V}} + \frac{d\alpha}{\tan\alpha} + dr\left(\frac{1}{r} + \frac{C_f \zeta}{h'' \cos\alpha}\right) = 0 \qquad \ldots.(1)$$

Radial force balance

$$\frac{dQ\ (\hat{V} + d\hat{V})}{g}\left(\frac{h'' + dh''}{h' + dh'}\right)\cos(\alpha + d\alpha + d\psi^* + \tfrac{1}{2}\,d\psi) + hr\,dP_s\,d\psi$$

$$+ C_f\,\zeta\,\frac{\hat{\rho}\,\hat{V}^2}{g}\,r\,d\psi\,dr\cos\alpha = \frac{dQ\cdot\hat{V}}{g}\,\frac{h''}{h'}\cos(\alpha + \tfrac{1}{2}\,d\psi)$$

Substituting for dQ as before leads to

$$\left(1 + \frac{d\hat{V}}{\hat{V}}\right)\left(1 + \frac{dh''}{h''}\right)\left(1 - \frac{dh'}{h'}\right)\left[1 - \tan\alpha\,(d\alpha + d\psi^* + \tfrac{1}{2}\,d\psi)\right] - \left(1 - \tan\alpha\cdot\tfrac{1}{2}\,d\psi\right)$$

$$+ \frac{h}{h''}\,\frac{g\,dP_s}{\hat{\rho}\,\hat{V}^2\cos^2\alpha} + C_f\,\zeta\,\frac{dr}{h''\cos\alpha} = 0$$

which becomes

$$\frac{dh''}{h''} - \frac{dh'}{h'} + \frac{d\hat{V}}{\hat{V}} - \tan\alpha\cdot d\alpha + \frac{h}{h''}\,\frac{g\,dP_s}{\hat{\rho}\,\hat{V}^2\cos^2\alpha} + dr\left(\frac{C_f\,\zeta}{h''\cos\alpha} - \frac{\tan^2\alpha}{r}\right) = 0 \qquad \ldots.(2)$$

Combined force equations

Multiplying equation (1) by $\tan^2\alpha$ and adding the result to equation (2) gives

$$\frac{dh''}{h''} - \frac{dh'}{h'} + \frac{d\hat{V}}{\hat{V}} + \frac{h}{h''}\,\frac{g\,dP_s}{\hat{\rho}\,\hat{V}^2} + \frac{C_f\,\zeta\,dr}{h''\cos\alpha} = 0 \qquad \ldots.(3)$$

Alternatively, subtracting equation (2) from (1) gives

$$\frac{d\alpha}{\tan \alpha} - \frac{h}{h''} \frac{g \, dP_s}{\hat{\rho} \, \hat{V}^2} + \frac{dr}{r} = 0 \qquad \ldots.(4)$$

Continuity

For the whole flow

$$\hat{\rho} \cdot 2\pi r \, h' \cos \alpha \cdot \hat{V} = \text{constant}$$

$$\therefore \quad \frac{d\hat{\rho}}{\hat{\rho}} + \frac{dr}{r} + \frac{dh'}{h'} - \tan \alpha \cdot d\alpha + \frac{d\hat{V}}{\hat{V}} = 0 \qquad \ldots.(5)$$

Equation of state

$$\hat{\rho} = \frac{P_s}{R \, \hat{T}_s}$$

$$\therefore \quad \frac{d\hat{\rho}}{\hat{\rho}} = \frac{dP_s}{P_s} - \frac{d\hat{T}_s}{\hat{T}_s} \qquad \ldots.(6)$$

Energy

$$T_t = \hat{T}_s + \frac{\hat{V}^2}{2gJ \, C_p} = \text{constant}$$

$$\therefore \quad d\hat{T}_s + \frac{\hat{V} \, d\hat{V}}{gJ \, C_p} = 0$$

$$\therefore \quad \frac{d\hat{T}_s}{\hat{T}_s} + \left(\frac{\gamma - 1}{\gamma} \right) \frac{\hat{\rho} \, \hat{V} \, d\hat{V}}{g \, P_s} = 0 \qquad \ldots.(7)$$

Total pressure

Since T_t and $\hat{P}_t$ are constant, the isentropic relation gives

$$\frac{d\hat{T}_s}{\hat{T}_s} = \left(\frac{\gamma - 1}{\gamma}\right) \frac{dP_s}{P_s} \qquad \ldots.(8)$$

Auxiliary equations

From equations (6) and (8)

$$\frac{d\hat{\rho}}{\hat{\rho}} = \frac{1}{\gamma} \frac{dP_s}{P_s} \qquad \ldots.(9)$$

From equations (7) and (8)

$$dP_s + \frac{\hat{\rho}\,\hat{V}\,d\hat{V}}{g} = 0 \qquad \ldots.(10)$$

Equations (9) and (10) are, of course, familiar ones for any flow situation in which total pressure and total temperature are constant.

From the definition of Mach number

$$\hat{M}^2 = \frac{\hat{V}^2}{g\,\gamma\,R\,\hat{T}_s}$$

$$\therefore \quad 2\frac{d\hat{M}}{\hat{M}} = 2\frac{d\hat{V}}{\hat{V}} - \frac{d\hat{T}_s}{\hat{T}_s} \qquad \ldots.(11)$$

From equations (7) and (11)

$$\frac{d\hat{V}}{\hat{V}} = \frac{d\hat{M}}{\hat{M}} \left(\frac{1}{1 + \frac{\gamma - 1}{2}\hat{M}^2}\right) \qquad \ldots.(12)$$

From equations (4) and (10)

$$\frac{d\alpha}{\tan \alpha} + \frac{h}{h''} \frac{d\hat{V}}{\hat{V}} + \frac{dr}{r} = 0 \qquad \ldots\ldots(13)$$

In the absence of friction ($h = h' = h''$ and $C_f = 0$) equations (1) and (13) would both reduce to the familiar free vortex relation $r V \sin \alpha = \text{constant}$.

From equations (3) and (10)

$$\frac{dh''}{h''} - \frac{dh'}{h'} + \frac{d\hat{V}}{\hat{V}} \left(1 - \frac{h}{h''}\right) + \frac{C_f \zeta \, dr}{h'' \cos \alpha} = 0 \qquad \ldots\ldots(14)$$

From equations (5), (9), (10) and (13),

eliminating $d\hat{\rho}$; $d\alpha$; dP_s

$$\frac{dh'}{h'} + \frac{d\hat{V}}{\hat{V}} \left(1 - \hat{M}^2 + \frac{h}{h''} \tan^2 \alpha\right) + \sec^2 \alpha \frac{dr}{r} = 0 \qquad \ldots\ldots(15)$$

<u>The momentum integral relation</u>

This is derived by combining equations (14) and (15) and noting that

$$dh'' = dh' - 2d\theta$$

Thus equation (14) can be rewritten

$$2\theta \frac{dh'}{h'} - 2d\theta - 2\theta (1 + H) \frac{d\hat{V}}{\hat{V}} + \frac{C_f \zeta \, dr}{\cos \alpha} = 0$$

Substituting for $\frac{dh'}{h'}$ from equation (15) then gives

$$\frac{d\theta}{dr} = \tfrac{1}{2} C_f \zeta \sec \alpha - \frac{\theta \sec^2 \alpha}{r} - \frac{\theta}{\hat{V}} \frac{d\hat{V}}{dr} \left(2 + H - \hat{M}^2 + \varepsilon \tan^2 \alpha\right) \qquad \ldots\ldots(16)$$

where $$\varepsilon = \frac{h}{h''} = \left[1 - \frac{2\theta}{h}(1 + H)\right]^{-1}$$

Equation (16) is in conventional form, and is the momentum integral equation for compressible spiral flow.

A more convenient form for the present purpose, using equation (12), is

$$d\theta = \left(\frac{C_f \zeta \sec \alpha}{2} - \frac{\theta \sec^2\alpha}{r}\right) dr - \frac{\theta\, d\hat{M}}{\hat{M}} \left(\frac{2 + H - \hat{M}^2 + \varepsilon \tan^2\alpha}{1 + \frac{\gamma - 1}{2}\hat{M}^2}\right) \quad ....(17)$$

Working equations

For greatest convenience the calculation procedure employs as variables $\frac{d\hat{M}}{dr}$; $\frac{d\alpha}{dr}$; $\frac{d\theta}{dr}$, for which three equations are required.

Now for a turbulent boundary layer with one-seventh-power velocity profile, Stratford & Beavers[6] give

$$\frac{\delta^*}{\theta} = H = 1.286\left(1 + 0.8\hat{M}^2\right)^{0.44}\left(1 + 0.1\hat{M}^2\right)^{0.7}$$

$$\therefore \quad \frac{d\delta^*}{\delta^*} - \frac{d\theta}{\theta} = \frac{d\hat{M}}{\hat{M}}\left(\frac{0.704\hat{M}^2}{1 + 0.8\hat{M}^2} + \frac{0.14\hat{M}^2}{1 + 0.1\hat{M}^2}\right)$$

$$\therefore \quad dh' = dh - 2d\delta^*$$

$$= dh - 2Hd\theta - 2H\theta \frac{d\hat{M}}{\hat{M}}\left(\frac{0.704\hat{M}^2}{1 + 0.8\hat{M}^2} + \frac{0.14\hat{M}^2}{1 + 0.1\hat{M}^2}\right) \quad ....(18)$$

Substituting equations (12), (17) and (18) into (15) leads after collection of terms to

$$dh + \left(\frac{h \sec^2\alpha}{r} - H C_f \zeta \sec \alpha\right) dr + \frac{d\hat{M}}{\hat{M}}\left[\frac{h\left(1 - \hat{M}^2 + \varepsilon \tan^2\alpha\right) + 2H(1 + H)\theta}{1 + \frac{\gamma - 1}{2}\hat{M}^2} - 2H\theta\left(\frac{0.704\hat{M}^2}{1 + 0.8\hat{M}^2} + \frac{0.14\hat{M}^2}{1 + 0.1\hat{M}^2}\right)\right] = 0 \quad ....(19)$$

Equation (19) allows $\frac{d\hat{M}}{dr}$ to be calculated.

From equations (12) and (13)

$$\frac{d\alpha}{\tan \alpha} + \frac{d\hat{M}}{\hat{M}} \left(\frac{\varepsilon}{1 + \frac{\gamma - 1}{2} \hat{M}^2} \right) + \frac{dr}{r} = 0 \qquad \ldots.(20)$$

Knowing $\frac{d\hat{M}}{dr}$, equations (17) and (20) give $\frac{d\theta}{dr}$ and $\frac{d\alpha}{dr}$ respectively.

15. Fully developed conditions in the vaneless diffuser

If the vaneless space is sufficiently large the boundary layers on the two side walls will join, and the mainstream or core of isentropic flow then disappears. A reasonable approximate treatment thereafter is to assume that a similar (one-seventh-power) velocity profile is maintained, with $\delta = \frac{1}{2} h$. Then $\frac{\delta^*}{h}$ and $\frac{\theta}{h}$ can be taken as functions of $\hat{M}$ alone (Stratford & Beavers[6]), $\hat{P}_t$ is no longer constant, and the superscript $\wedge$ refers throughout to centreline values only. Of the equations in the previous section (Appendix 3-14), numbers (1) to (7) also (11) and (12) continue to apply: (8) to (10) and (13) et seq do not. In this case the major variables are $\frac{d\hat{M}}{dr}$; $\frac{d\alpha}{dr}$; $\frac{d\hat{P}_t}{dr}$, for which fresh equations are required.

From equations (4), (5), (6) and (7), eliminating $d\hat{\rho}$; $d\alpha$; $d\hat{T}_s$

$$\frac{g\, dP_s}{\hat{\rho}\, \hat{V}^2}\left(\gamma \hat{M}^2 - \frac{h}{h''}\tan^2\alpha\right) + \frac{d\hat{V}}{\hat{V}}\left[1 + (\gamma - 1)\hat{M}^2\right] + \frac{dh'}{h'} + \sec^2\alpha\, \frac{dr}{r} = 0 \qquad \ldots.(21)$$

Substituting for $\frac{g\, dP_s}{\hat{\rho}\, \hat{V}^2}$ from equation (3) and for $\frac{d\hat{V}}{\hat{V}}$ from equation (12)

gives, after some re-arrangement

$$\frac{d\hat{M}}{\hat{M}}\left[\frac{\sec^2\alpha - \hat{M}^2 + \gamma \hat{M}^2\left(1 - \frac{h''}{h}\right)}{1 + \frac{\gamma - 1}{2}\hat{M}^2}\right] +$$

$$+ \frac{1}{h}\left(\frac{h}{h''}\tan^2\alpha - \gamma \hat{M}^2\right)\left(dh'' - \frac{h''}{h'}dh' + \frac{C_f\, \zeta\, dr}{\cos\alpha}\right) + \frac{dh'}{h'} + \frac{\sec^2\alpha\, dr}{r} = 0 \qquad \ldots.(22)$$

Now
$$\left.\begin{aligned} \frac{2\delta^*}{h} &\simeq 0.125\left(1 + 0.8\,\hat{M}^2\right)^{0.44} \\ \frac{2\theta}{h} &\simeq 0.097\left(1 + 0.1\,\hat{M}^2\right)^{-0.7} \end{aligned}\right\} \text{ from Stratford \& Beavers}^{6}$$

Hence
$$h' = h\left[1 - 0.125\left(1 + 0.8\,\hat{M}^2\right)^{0.44}\right] \qquad \ldots.(23)$$

$$h'' = h\left[1 - 0.125\left(1 + 0.8\,\hat{M}^2\right)^{0.44} - 0.097\left(1 + 0.1\,\hat{M}^2\right)^{-0.7}\right] \qquad \ldots.(24)$$

$$dh' = \frac{h'}{h}\,dh - h\left[0.088\,\hat{M}^2\left(1 + 0.8\,\hat{M}^2\right)^{-0.56}\right]\frac{d\hat{M}}{\hat{M}} \qquad \ldots.(25)$$

$$dh'' = \frac{h''}{h}\,dh - h\left[0.088\,\hat{M}^2\left(1 + 0.8\,\hat{M}^2\right)^{-0.56} - 0.0136\,\hat{M}^2\left(1 + 0.1\,\hat{M}^2\right)^{-1.7}\right]\frac{d\hat{M}}{\hat{M}} \qquad \ldots.(26)$$

Substitution of equations (25) and (26) into (22) produces, upon collection of terms, an equation of the form

$$K_a\frac{d\hat{M}}{\hat{M}} + \frac{dh}{h} + K_b\,dr = 0 \qquad \ldots.(27)$$

where

$$K_a = \frac{\sec^2\alpha - \hat{M}^2 + \gamma\hat{M}^2\left(1 - \frac{h''}{h}\right)}{1 + \frac{\gamma - 1}{2}\hat{M}^2} +$$

$$+ \left(\frac{h}{h''}\tan^2\alpha - \gamma\hat{M}^2\right)\left[0.0136\,\hat{M}^2\left(1 + 0.1\,\hat{M}^2\right)^{-1.7}\right] -$$

$$- \frac{h}{h'}\left[1 + \left(\frac{h'}{h} - \frac{h''}{h}\right)\left(\frac{h}{h''}\tan^2\alpha - \gamma\hat{M}^2\right)\right]\left[0.088\,\hat{M}^2\left(1 + 0.8\,\hat{M}^2\right)^{-0.56}\right]$$

$$K_b = \frac{\sec^2\alpha}{r} + \left(\frac{h}{h''}\tan^2\alpha - \gamma\hat{M}^2\right)\frac{C_f\,\zeta}{h\cos\alpha}$$

The ratios $\frac{h''}{h}$ and $\frac{h'}{h}$ are functions of $\hat{M}$ only, given by equations (23) and (24).

Thus $\frac{d\hat{M}}{dr}$ can be found.

Next, elimination of $\frac{g\,dP_s}{\hat{\rho}\,\hat{V}^2}$ between equations (4) and (21) gives

$$\frac{d\alpha}{\tan\alpha}\left(\frac{h''}{h}\gamma\hat{M}^2 - \tan^2\alpha\right) + \frac{d\hat{M}}{\hat{M}}\left[\frac{1 + (\gamma-1)\hat{M}^2}{1 + \frac{\gamma-1}{2}\hat{M}^2}\right] + \frac{dh'}{h'} + \left(1 + \frac{h''}{h}\gamma\hat{M}^2\right)\frac{dr}{r} = 0 \qquad \ldots.(28)$$

Substitution for dh' from equation (25) then produces

$$\frac{d\alpha}{\tan\alpha}\left(\frac{h''}{h}\gamma\hat{M}^2 - \tan^2\alpha\right) + \frac{d\hat{M}}{\hat{M}}\left\{\frac{1 + (\gamma-1)\hat{M}^2}{1 + \frac{\gamma-1}{2}\hat{M}^2} - \frac{h}{h'}\left[0.088\,\hat{M}^2\left(1 + 0.8\,\hat{M}^2\right)^{-0.56}\right]\right\} + \frac{dh}{h} + \left(1 + \frac{h''}{h}\gamma\hat{M}^2\right)\frac{dr}{r} = 0 \qquad \ldots.(29)$$

Knowing $\frac{d\hat{M}}{dr}$, equation (29) enables $\frac{d\alpha}{dr}$ to be calculated.

Now $$\frac{\hat{P}_t}{P_s} = \left(1 + \frac{\gamma-1}{2}\hat{M}^2\right)^{\frac{\gamma}{\gamma-1}}$$

$$\therefore \quad \frac{d\hat{P}_t}{\hat{P}_t} = \frac{dP_s}{P_s} + \frac{\gamma\hat{M}^2}{1 + \frac{\gamma-1}{2}\hat{M}^2}\cdot\frac{d\hat{M}}{\hat{M}} \qquad \ldots.(30)$$

Elimination of dP_s between equations (21) and (30) leads to

$$\frac{d\hat{P}_t}{\hat{P}_t}\left(1 - \frac{h}{h''}\frac{\tan^2\alpha}{\gamma\hat{M}^2}\right) + \frac{d\hat{M}}{\hat{M}}\left[\frac{1 - \hat{M}^2 + \frac{h}{h''}\tan^2\alpha}{1 + \frac{\gamma - 1}{2}\hat{M}^2}\right] + \frac{dh'}{h'} + \sec^2\alpha\,\frac{dr}{r} = 0 \qquad \ldots.(31)$$

As before substitution for dh' from equation (25) then gives

$$\frac{d\hat{P}_t}{\hat{P}_t}\left(1 - \frac{h}{h''}\frac{\tan^2\alpha}{\gamma\hat{M}^2}\right) + \frac{d\hat{M}}{\hat{M}}\left\{\frac{1 - \hat{M}^2 + \frac{h}{h''}\tan^2\alpha}{1 + \frac{\gamma - 1}{2}\hat{M}^2} - \frac{h}{h'}\left[0.088\,\hat{M}^2\left(1 + 0.8\,\hat{M}^2\right)^{-0.5\bar{6}}\right]\right\} + \frac{dh}{h} + \sec^2\alpha\,\frac{dr}{r} = 0 \qquad \ldots.(32)$$

Knowing $\frac{d\hat{M}}{dr}$, equation (32) enables $\frac{d\hat{P}_t}{dr}$ to be calculated.

16. Mean total pressure of flow with boundary layer

For the core flow

$$\hat{P}_t = P_s + \hat{\tau}\left(\frac{\hat{\rho}\,\hat{V}^2}{2g}\right)$$

For any station in boundary layer

$$P_t = P_s + \tau\left(\frac{\rho\,V^2}{2g}\right)$$

where $$\tau = 1 + \tfrac{1}{4}M^2 + \frac{2-\gamma}{24}M^4 + \ldots\ldots$$

(i) Mass mean total pressure

Define $$\left[\overline{P_t}\right]_{mm} = \frac{\int_0^\infty P_t\,\rho\,V\,dy}{\int_0^\infty \rho\,V\,dy}$$

$$= P_s + \frac{\frac{\hat{\rho}\,\hat{V}^2}{2g}\int_0^\infty \tau\left(\frac{\rho}{\hat{\rho}}\right)^2\left(\frac{V}{\hat{V}}\right)^3 dy}{\int_0^\infty \frac{\rho}{\hat{\rho}}\cdot\frac{V}{\hat{V}}\,dy}$$

$$= P_s + \frac{\left(\hat{P}_t - P_s\right)\int_0^\infty \left(\frac{\tau}{\hat{\tau}}\right)\left(\frac{\rho}{\hat{\rho}}\right)^2\left(\frac{V}{\hat{V}}\right)^3 dy}{\int_0^\infty dy - \delta^*}$$

Noting that $$\delta^{**} = \int_0^\infty \frac{\rho\, V}{\hat{\rho}\, \hat{V}} \left[1 - \left(\frac{V}{\hat{V}}\right)^{m}\right] dy$$

the foregoing expression for $\overline{P_t}$, <u>for incompressible flow only</u>, reduces to

$$\left[\frac{\overline{P_t} - P_s}{\hat{P}_t - P_s}\right]_{mm} = 1 - \frac{\delta^{**}}{\int_0^\infty dy - \delta^*}$$

[Note: even if variation of τ can be neglected, this relation does not apply for varying ρ.]

Then, for fully-developed incompressible flow

$$\left[\frac{\overline{P_t} - P_s}{\hat{P}_t - P_s}\right]_{mm} = 1 - \frac{\delta_{ic}^{**}}{\delta - \delta_{ic}^{*}}$$

$$= 1 - \frac{H_{ic}'}{\frac{\delta}{\theta_{ic}} - H_{ic}}$$

$$= 0.802$$ using the values for a one-seventh-power boundary layer, viz:

$$\frac{\delta}{\theta_{ic}} = 10.3 \; ; \quad H_{ic} = 1.286$$

and Fernholz's relation[25]

$$H_{ic}' = \frac{1.272\, H_{ic}}{H_{ic} - 0.37} + 5.4 \left(\frac{H_{ic}}{10}\right)^4$$

(ii) Area mean total pressure

$$\text{Define} \qquad \left[\overline{P_t}\right]_{am} = \frac{\int_0^\infty P_t \, dy}{\int_0^\infty dy}$$

$$= P_s + \frac{\frac{\hat{\rho}\,\hat{V}^2}{2g} \int_0^\infty \tau \left(\frac{\rho}{\hat{\rho}}\right)\left(\frac{V}{\hat{V}}\right)^2 dy}{\int_0^\infty dy}$$

$$= P_s + \frac{\left(\hat{P}_t - P_s\right) \int_0^\infty \left(\frac{\tau}{\hat{\tau}}\right)\left(\frac{\rho}{\hat{\rho}}\right)\left(\frac{V}{\hat{V}}\right)^2 dy}{\int_0^\infty dy}$$

If variation of τ can be neglected, i.e. low Mach number,

$$\left[\frac{\overline{P_t} - P_s}{\hat{P}_t - P_s}\right]_{am} = 1 - \frac{\delta^* + \theta}{\int_0^\infty dy}$$

[Note: this relation holds for varying ρ.]

Then, for fully-developed incompressible flow

$$\left[\frac{\overline{P_t} - P_s}{\hat{P}_t - P_s}\right]_{am} = 1 - \frac{\delta^*_{ic} + \theta_{ic}}{\delta}$$

$$= 1 - \frac{H_{ic} + 1}{\frac{\delta}{\theta_i}}$$

$$= 0.778 \qquad \text{using the previous values}$$

Or, for fully-developed quasi-compressible flow (τ constant)

$$\left[\frac{\overline{P_t} - P_s}{\hat{P}_t - P_s}\right]_{am} = 1 - 0.097\left(1 + 0.1\,\hat{M}^2\right)^{-0.7} - 0.125\left(1 + 0.8\,\hat{M}^2\right)^{0.44}$$

(from Stratford & Beavers[6])

which has the following values

$\hat{M}$	$\left[\frac{\overline{P_t} - P_s}{\hat{P}_t - P_s}\right]_{am}$	$\frac{\text{incompressible}}{\text{quasi-compressible}}$
0	0.7780	1.0
0.2	0.7766	1.002
0.4	0.7723	1.007
0.6	0.7657	1.016
0.8	0.7572	1.027
1.0	0.7474	1.041

Now it may be reasonable to assume that, for fully-developed flow, values of $\left(\overline{P_t} - P_s\right)/\left(\hat{P}_t - P_s\right)$ are connected thus:

$$\frac{\text{mass mean incomp.}}{\text{mass mean comp.}} - 1 \simeq 2\left[\frac{\text{area mean incomp.}}{\text{area mean quasi-comp.}} - 1\right]$$

Consequently the incompressible area mean (0.778) is likely to be a fairly close approximation to the compressible mass mean for Mach numbers not exceeding about 0.6.

If this correspondence is assumed to apply also to flow which is not fully-developed but has relatively thick boundary layers, then

$$\left[\frac{\overline{P_t} - P_s}{\hat{P}_t - P_s}\right]_{mm} = 1 - \frac{H_{ic} + 1}{\frac{1}{2}\frac{h}{\theta_{ic}}} \qquad \text{where} \qquad h = 2\int_0^\infty dy$$

$$= 1 - 4.572\,\frac{\theta_{ic}}{h}$$

For convenience θ_{ic} can be taken as $\simeq \theta$, since the dependence of θ on M is weak.

17. The vaned diffuser

This component can be divided into two distinct regions: that from leading edge to throat, and the fully-enclosed channel following the throat. The vital link between these regions is throat blockage; upon this the channel pressure recovery depends, and that blockage is determined primarily by the flow behaviour between leading edge and throat.

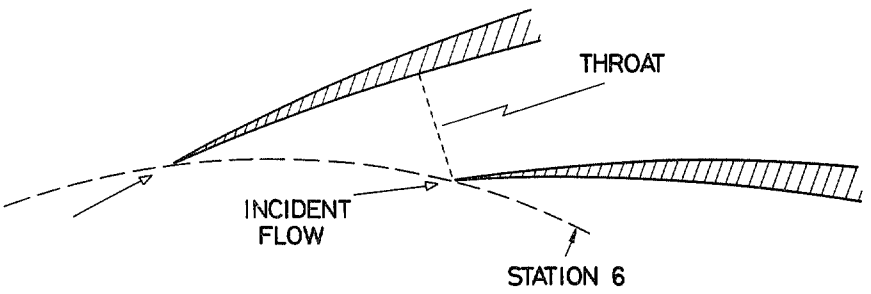

At the leading edge pitch circle, bulk flow conditions are known: $\hat{M}_6$; α_6; $\hat{P}_{t,6}$; B_6. B_6 is usually sufficiently near unity not to be significant. $\hat{M}_6$ and α_6 vary with operating condition, although the change of α_6 is fairly small (typically $\nmid \pm 5^\circ$). $\hat{M}_6$ may be either >1 or <1. Leading edge incidence ($\alpha_6 \neq \omega$) will alter the value of $\hat{M}$ entering the initial part of the vaned diffuser. Thus a variety of situations in terms of Mach number and incidence have to be catered for. But because the treatment is to be general, no precise vane shapes are specified. Consequently the pressure distributions between leading edge and throat (that on the vane surface and that on the sidewalls) upon which B_{th} will depend must be arbitrary. It is therefore not reasonable to assume the presence of any shocks or supersonic expansion except at the leading edge (due to incidence) when $\hat{M}_6 > 1$. In some particular designs of diffuser, significant vane surface expansion and/or shocks may exist between leading edge and throat, but such can usually be avoided by suitable design and so are omitted from a general treatment. For the usual range of compressors $\hat{M}_6 \nmid 1.2$, so the form of shock assumed to exist at leading edge is not important and loss of $\hat{P}_t$ through that shock is trivial and can be neglected. The effect of a leading edge shock on sidewall boundary layers, although possibly important in practice, is unquantifiable and hence of necessity ignored.

Shocks will only form downstream of the throat (i.e. inside the channel) in choked operation, when pressure recovery is of no interest.

In the choking case $\hat{M}$ either increases or only slightly decreases between leading edge and throat, according to whether $\hat{M}_e < 1$ or >1. Thus there is little change of B from leading edge to throat, and the pressure distributions assumed are not important in determining choking flow.

At lower flow, significant diffusion occurs between leading edge and throat, and considerable blockage develops. The primary factor is the overall change of Mach number, and the path followed between given end values has only a minor effect. Linear distributions of $\hat{M}$ are therefore assumed between the pitch circle of leading edges and the channel throat. Because the sidewall boundary layers grow from finite thickness at the leading edge pitch circle (corresponding to B_e), the two sidewalls together usually contribute most of the throat blockage.

Having regard to the large degree of simplification in the nature of the flow which has to be assumed for general purposes and easy calculation, no model can be constructed for the growth of boundary layers on vane surface and sidewalls, and hence throat blockage, which is strictly defensible. In the first place, variation of $\hat{M}$ across the throat (in the radial plane) would, if allowed, be wholly arbitrary, and it seems preferable to assume that flow diffuses to the same terminal (i.e. throat) Mach number along both the vane surface and sidewall mean paths. Boundary layer growth along those paths is calculated, for the sake of convenience in a general treatment, as for attached flow with one-seventh-power velocity profiles, throat blockage following from the resulting displacement thicknesses. With reduction of flow towards surge, however, such calculations can lead to a situation where the physical thickness of boundary layers exceeds the passage dimension, so that a "core" region of undiminished total pressure can no longer be deemed to exist. Additionally, as flow is reduced and the amount of diffusion to the throat condition becomes large (a pressure rise coefficient between leading edge and throat in excess of 0.4 often being achieved), the assumption of attached flow with a shape factor (H) in the region of 1.6 loses its credibility. In these circumstances, to be realistic a model requires some means of catering for reduction in mainstream total pressure, for which purpose a schedule of total pressure loss with throat blockage factor is employed. The relation used has been chosen on empirical grounds; it applies smoothly throughout the whole range of throat blockage factor, so as to

avoid any abrupt discontinuity in form of a compressor characteristic curve, although the total pressure loss which it introduces at diffuser choking condition is negligible. That the treatment in this region of the machine contains some inconsistency cannot be denied; the difficulty is to find a better.

There is some likelihood that surge with a vaned diffuser is promoted by reaching a limiting diffusion between leading edge and throat - see Appendix 5. The phenomenon of surge may perhaps also be influenced by interaction between diffuser vanes and rotor, but there are wholly insufficient test data available to disentangle the many possible factors of significance. Examination of limited data (Appendix 5) suggests that simple two-parameter correlations relating to the region between leading edge and throat (for example a diffusion factor and some geometric parameter) will not apply universally for predicting surge.

Beyond the throat, channel pressure recovery is evaluated from data for straight-centreline single channels in terms of geometric parameters and the calculated value of B_{th} (Appendix 3-19 and Appendix 4).

18. Diffuser throat choking

For a particular flow Q it is required to find whether

$$\frac{Q\sqrt{T_{t,th}}}{B_{th}\ A_g\ \hat{P}_{t,th}} \gtrless \text{critical value.}$$

But B_{th} is unknown and can only be found by the iterative procedure (together with $\hat{M}_{th}$) if the diffuser throat is not choking, i.e. if $\hat{M}_{th} < 1$. So an alternative criterion is required. This may be constructed as follows.

The iterative procedure (see main text) compares two values of B_{th}, one obtained from the continuity relation = $B_{th}(\text{cont.})$, and the other obtained from boundary layer relations = $B_{th}(\text{b.l.})$. For a solution

$$B_{th}(\text{cont.}) = B_{th}(\text{b.l.})$$

Now suppose diffuser throat is not choking, there is a solution

$$\begin{cases} \hat{M}_{th} < 1 \\ B_{th}(\text{cont.})_{SOL} - B_{th}(\text{b.l.})_{SOL} = (\Delta B_{th})_{SOL} = 0 \end{cases}$$

For the same flow Q consider the assumption that $\hat{M}_{th} = 1$: then

$$\begin{cases} B_{th}(\text{cont.})_{M=1} - B_{th}(\text{b.l.})_{M=1} = (\Delta B_{th})_{M=1} \neq 0 \\ B_{th}(\text{cont.})_{M=1} < B_{th}(\text{cont.})_{SOL} \\ B_{th}(\text{b.l.})_{M=1} \gtrless B_{th}(\text{b.l.})_{SOL} \end{cases}$$

Hence

$$(\Delta B_{th})_{M=1} = B_{th}(\text{cont.})_{M=1} - B_{th}(\text{cont.})_{SOL} - B_{th}(\text{b.l.})_{M=1} + B_{th}(\text{b.l.})_{SOL}$$

which is negative

Thus the condition for diffuser throat choking is

$$(\Delta B_{th})_{M=1} \gtrless 0$$

19. Channel pressure recovery data

Two-dimensional straight-channel diffusers have been extensively investigated by Runstadler[11], who gives experimental pressure recovery data varying with inlet centreline flow conditions $\left(\hat{P}_t;\ \hat{M}\right)$, inlet blockage, inlet passage aspect ratio (AS), length/inlet width ratio (LWR), and outlet/inlet area ratio (AR). Those data are presented as a series of "maps" in which contours of C_{pr} are plotted on scales of LWR and AR. Each map is drawn for a particular combination of $\hat{M}_{th}$, B_{th}, and AS. Lines of included divergence angle (2θ) are unique, since

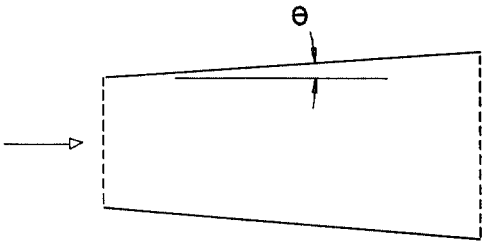

$$2\theta = 2 \tan^{-1} \frac{AR - 1}{2 \cdot LWR}$$

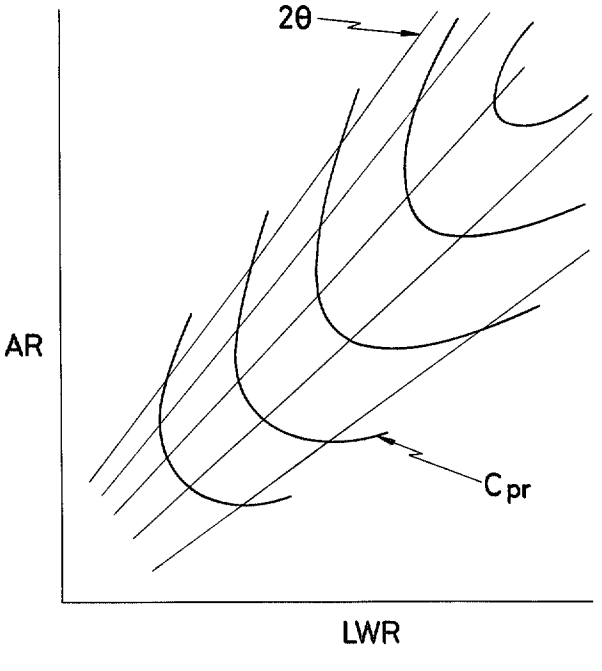

The effect of $\hat{P}_{t,th}$ is included in the definition of

$$C_{pr}\left[= \frac{P_{s,out} - P_{s,th}}{\hat{P}_{t,th} - P_{s,th}} \right].$$

Various points arise in applying these data, due to the multiplicity of variables and the necessarily limited range of conditions covered by Runstadler's tests.

(1) $\hat{M}_{th}$: test range 0.2 to 1.0. Of all the variables considered this is the least important; for any particular geometry of channel B_{th} is the dominant inlet flow parameter. In the usual compressor operating range $\left(0.6 < \hat{M}_{th} < 1.0\right)$ it is reasonable to take an average C_{pr} independent of $\hat{M}_{th}$ - the error is unlikely to exceed 2 per cent, and

about 5 per cent in C_{pr} corresponds to 1 per cent in overall efficiency. Other uncertain factors in the application of Runstadler's data to a compressor could easily be of greater significance, such as centreline curvature and non-uniformity of inlet flow direction and velocity.

(2) B_{th}: test range 0.98 to 0.88 in intervals of 0.02. Where values are encountered <0.88, the most practicable course is to extrapolate from the test range by means of a linear relation for C_{pr}, derived for the same geometry from the 6 standard values of B_{th}, using a least-squares fit.

(3) AS: test values 5, 1, $\frac{1}{4}$ only. Large effects are evident from the data, but correspond to a range of AS greater than is met in compressor diffusers - seldom >1, unlikely to be >2, usually between $\frac{1}{2}$ and 1. The nature of the data does not permit reliable interpolation, so uncertainty is inevitable at AS appreciably <1. A simple and approximate basis for that case is suggested by certain observations from the data:-

(i) For AS = 1, the optimum 2Θ at a particular LWR shifts from ≈9° at high B_{th} to ≈$7\frac{1}{2}$° at low B_{th}.

(ii) For AS = $\frac{1}{4}$, the optimum 2Θ at a particular LWR does not shift with B_{th} and is ≈13°.

(iii) Allowing for the difference in optimum 2Θ, the peak C_{pr} at a particular LWR and B_{th} is about the same for AS = $\frac{1}{4}$ as for AS = 1.

(iv) Between AS = 1 and AS = 5, there is little difference in optimum 2Θ at a particular LWR, but the peak C_{pr} is lower for AS = 5.

(v) All these features are effectively independent of the value of LWR over the narrow range of LWR where comparison can be made.

These observations lead to a possible procedure:-

When AS < 1, apply a change in 2Θ $\left[= \Delta(2\Theta)\right]$ at the given LWR so as to produce an effective 2Θ (and hence an effective AR) at that LWR, for use with data at AS = 1; that is to say, assume

$$C_{pr}\left[\text{LWR};\ 2\Theta;\ \text{AS} < 1\right] = C_{pr}\left[\text{LWR};\ 2\Theta - \Delta(2\Theta);\ \text{AS} = 1\right]$$

where $$\Delta(2\Theta) = f\left(\text{AS};\ B_{th}\right)$$

The data at AS = $\frac{1}{4}$ and 1 support a value of $\Delta(2\Theta) \simeq 5^{\circ}$ within the range $B_{th} \leq 0.94$ of usual interest for compressor diffusers. Assume an arbitrary variation of $\Delta(2\Theta)$ with AS

$$\Delta(2\Theta) = \left(\frac{1}{6\ AS} + 1\right)\left(\frac{1}{AS} - 1\right)$$

the form being taken to agree with a trend derived later.

When AS > 1, within the usual range of interest only small error is likely by treating as if AS = 1. The error will give C_{pr} too high.

(4) LWR and AR (at AS = 1): test range confined to $10 < LWR < 20$ and $6^{\circ} < 2\Theta < 12^{\circ}$. Many compressor diffusers have $3 < LWR < 10$, and some means of extrapolating Runstadler's data to low LWR must be derived, even though the values will be of uncertain reliability. Now Runstadler's data for a particular B_{th} appear as shown on a plot of C_{pr} vs. LWR; the lines of constant 2Θ merge together towards optimum 2Θ, and those for higher-than-optimum 2Θ lie among the lower-than-optimum. The 2Θ lines tend to straighten out at LWR ≃ 10.

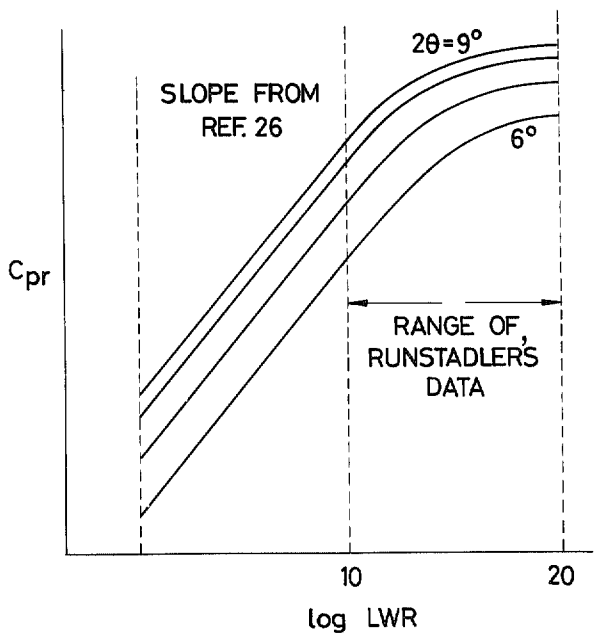

Reference 26 gives the result of applying to two-dimensional straight channels a theoretical boundary layer method for assessing C_{pr}, in the range $3 < LWR < 10$. The values of C_{pr} so obtained are not themselves believable, as there is no merging of 2Θ lines towards an optimum - there is in fact no optimum 2Θ; this is due to failure of the calculation method used in Reference 26 to account for stalling. But it is noteworthy that all the 2Θ lines derived from Reference 26 (plotted as shown) are straight and have similar slopes, which slopes

match quite well those of the Runstadler data lines where the latter straighten around LWR ≈ 10. Extrapolating the Runstadler data according to such "master slope" (which varies slightly with B_{th}) therefore seems an acceptable procedure in default of anything better.

Given LWR and 2Θ, AR follows from

$$AR = 1 + 2 \cdot LWR \tan\left[\tfrac{1}{2}(2\Theta)\right]$$

so that "maps" of the original Runstadler form can be constructed at low LWR.

- - - - - - -

All the foregoing notes relate to two-dimensional channels, i.e. with parallel sidewalls. For diverging sidewalls no comparably extensive test data and no sure method of treatment are available. A tentative procedure arises from consideration of the observed effects of throat aspect ratio with parallel sidewalls (section 3 supra).

Four cases are drawn for AR = 2, by way of example:

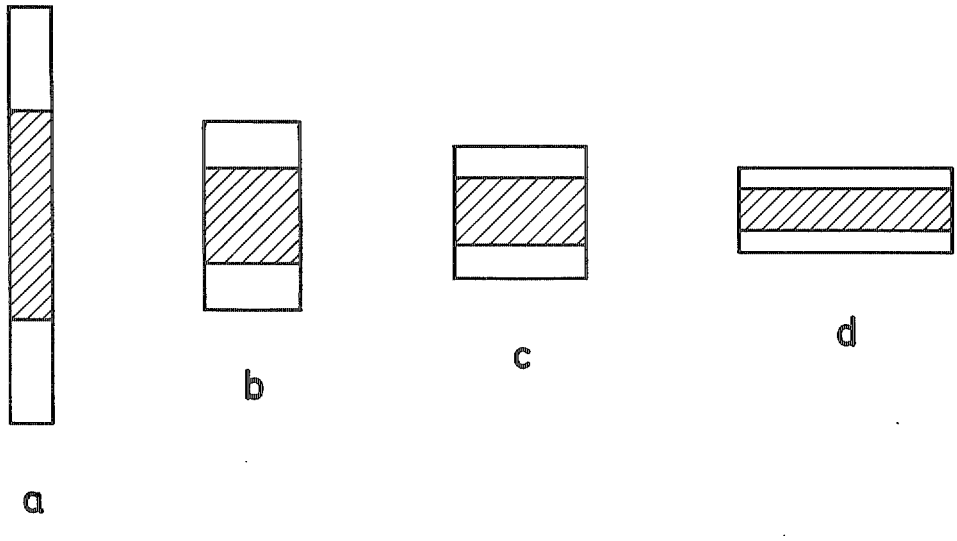

Suppose these all to have the same ℓ/w_{th}

case a:	AS = $\frac{1}{5}$	length $\propto$ 11.2 units
case b:	AS = 1 minimum inlet perimeter	length $\propto$ 5 units
case c:	AS = 2 = AR minimum outlet perimeter	length $\propto$ 3.5 units
case d:	AS = 5	length $\propto$ 2.4 units

The increase of optimum 2Θ (at constant ℓ/w_{th}) from case 'b' (AS = 1) to case 'a' (AS << 1) is attributable to the increasing predominance of sidewall boundary layers as the outlet aspect ratio (h/w_{out}) falls. The higher outlet blockage in case 'a' means that the effective area ratio for 'a' is less than for 'b', and to arrive at the same effective area ratio the value of 2Θ in case 'a' must be greater than in case 'b'. This can be seen more precisely as follows:

In general the effective area ratio is given by

$$AR_{eff} = \frac{AR}{B_{th}} \left[1 - \frac{2\left(w_{out} + h_{out}\right) \bar{\delta}^*_{out}}{w_{out}\, h_{out}} \right]$$

where the term in square brackets is simply B_{out}.

Now consider two channels, both with parallel sidewalls, both channels having the same ℓ/w_{th}, the same AR_{eff} and the same B_{th}, but different AS: both should then have the same pressure recovery. In this situation, for the simplest case of zero inlet blockage $\left(B_{th} = 1,\ \bar{\delta}^*_{th} = 0\right)$

$$\bar{\delta}^*_{out} \propto \ell \text{ approximately, } \left(\text{say } \bar{\delta}^*_{out} = K \cdot \ell\right)$$

so that

$$AR_{eff} = AR - 2K \frac{\ell}{w_{th}} \left(\frac{AR}{AS} + 1\right) = \text{constant}$$

since $AR = w_{out}/w_{th}$ and $h_{out} = h_{th}$.

This relation shows that AR must increase as AS falls, the effect being small when AS > 1 but large when AS << 1. For example, taking arbitrary values of K = 0.004, ℓ/w_{th} = 10 and AR_{eff} = 2:

when	AS =	∞	5	1	0.25	0.1
then	AR =	2.08	2.11	2.26	3.06	10.4
	2Θ =	6.18	6.35	7.21	11.76	50.35

While these numbers are not themselves meaningful, the trend is clearly evident and explains the observed effect of AS on optimum 2Θ for two-dimensional channels. The relation previously given (3 supra) connecting Δ2Θ and AS is chosen to reflect this trend.

Coming on to channels with sidewall divergence, the requirement is to define parameters for a "two-dimensional equivalent", so that pressure recovery can be estimated by the means set out for parallel sidewalls. The foregoing argument regarding effect of AS has shown the significance of outlet blockage. In the present case effective area ratio will be closely preserved if the following quantities are maintained in the "equivalent" system:-

$$AR;\ B_{th};\ \ell;\ w_{out};\ h_{out} \qquad \text{(and hence } A_g\text{)}$$

the situation then appearing as in the sketch

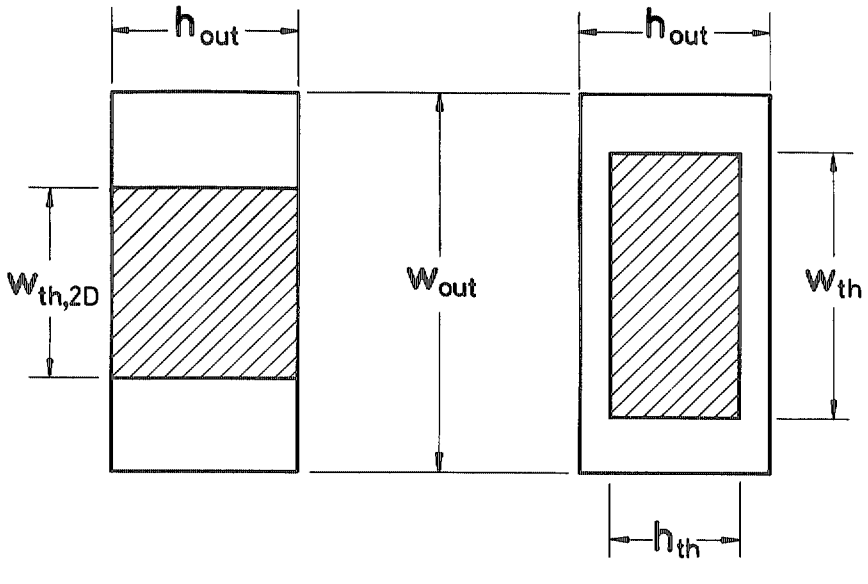

where $$w_{th,2D} = w_{th} \cdot \frac{h_{th}}{h_{out}}$$

Thus the parameters defining the "two-dimensional equivalent" channel are assumed to be

$$AR\ ; \quad LWR_{2D} = \frac{\ell}{w_{th,2D}}\ ; \quad AS_{2D} = \frac{h_{out}}{w_{th,2D}}\ ; \quad B_{th}$$

Note: this method may not be very satisfactory for large values of h_{out}/h_{th}, because the requirement of constant $\bar{\delta}^*_{out}$ depends upon maintaining not only the same ℓ but also the same $\bar{\delta}^*_{th}$, and for constant B_{th} (<1) the value of $\bar{\delta}^*_{th}$ varies with the throat perimeter

$$\left[\text{from } \left(w_{th} + h_{th}\right) \text{ to } \left(w_{th} \cdot \frac{h_{th}}{h_{out}} + h_{th} \cdot \frac{h_{out}}{h_{th}}\right)\right].$$

APPENDIX 4

EVALUATION OF C_{pr}

Data are assumed to be available in the form presented by Runstadler[11], namely "maps" giving contours of C_{pr} on scales of LWR and AR, one map for each of 6 values of B_{th} (from 0.98 to 0.88 in intervals of 0.02). Map regions outside the range of Runstadler's tests have been constructed by the means described in Appendix 3-19. There are thus 3 input parameters, namely

B_{th}; LWR; AR.

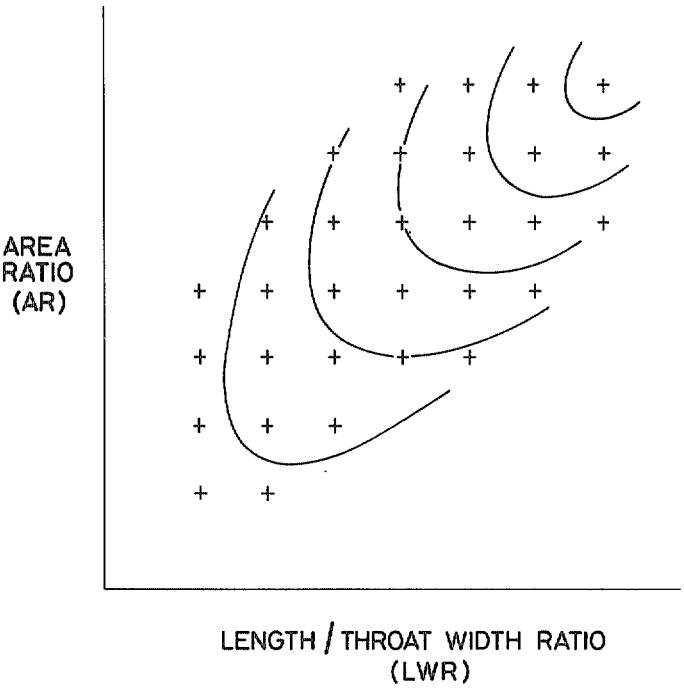

On each map real values of C_{pr} are known at each point +
For each of 6 values of B_{th} feed in 3 input arrays

X(I) I = 1,MX where X corresponds to LWR (MX = number of LWR values)

Y(J) J = 1,MY where Y corresponds to AR (MY = number of AR values)

N(I,J) I = 1,MX J = 1,MY
where N corresponds to C_{pr}

Where real values of C_{pr} are not known put dummy values, say >1.

All 6 plots have same points +, only C_{pr} values differ.

Check if required geometry is within overall limits of data (see table following)

$$1.3 \leqslant AR \leqslant 4.0$$

$$2.4 \leqslant LWR \leqslant 20$$

Compare required LWR with X(1) etc. until a value of X > LWR is reached

i.e. LWR > X(1) ..... X(I), LWR < X(I+1)

Compare required AR with Y(1) etc. until a value of Y > AR is reached

i.e. AR > Y(1) ..... Y(J), AR < Y(J+1)

Thus values of X and Y, I and J are known at 4 corners of enclosing rectangle.

If the required B_{th} > 0.98, use 0.98; if <0.88, see later.

Otherwise take 2 values of B_{th} that lie either side of required value.

For each B_{th}, C_{pr} is known at 4 corners of rectangle.

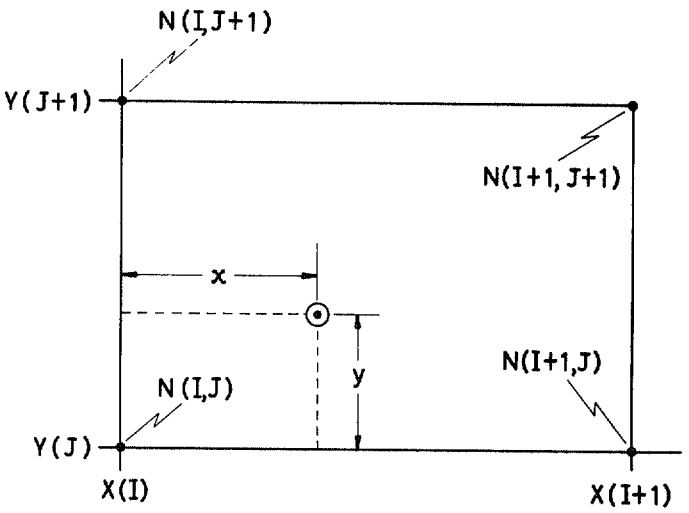

Check that none of the 4 values N(I,J) etc is a dummy; if a dummy, see later.

Required value C_{pr} =

$$N(I,J)\left\{\left[1-\frac{x}{X(I+1)-X(I)}\right]\left[1-\frac{y}{Y(J+1)-Y(J)}\right]\right\}$$

$$+N(I,J+1)\left\{\left[1-\frac{x}{X(I+1)-X(I)}\right]\left[\frac{y}{Y(J+1)-Y(J)}\right]\right\}$$

$$+N(I+1,J)\left\{\left[\frac{x}{X(I+1)-X(I)}\right]\left[1-\frac{y}{Y(J+1)-Y(J)}\right]\right\}$$

$$+N(I+1,J+1)\left\{\left[\frac{x}{X(I+1)-X(I)}\right]\left[\frac{y}{Y(J+1)-Y(J)}\right]\right\}$$

where x = required LWR - X(I)

y = required AR - Y(J)

If two or more corner values are dummies, then stop.

If one of corner values is a dummy, then check whether required point lies within "real half" of rectangle or "dummy half".

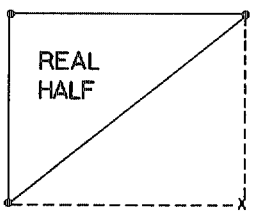

CASE 1

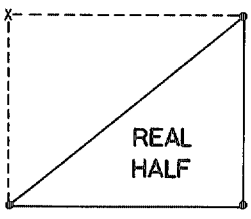

CASE 2

If in "dummy half" then stop. If in "real half" then proceed as below:

required value C_{pr} =

$$N(I,J)\left[1 - \frac{y}{Y(J+1) - Y(J)}\right]$$

$$+ N(I,J+1)\left[\frac{y}{Y(J+1) - Y(J)} - \frac{x}{X(I+1) - X(I)}\right]$$

$$+ N(I+1,J+1)\left[\frac{x}{X(I+1) - X(I)}\right] \qquad \text{in CASE 1}$$

or

$$N(I,J)\left[1 - \frac{x}{X(I+1) - X(I)}\right]$$

$$+ N(I+1,J)\left[\frac{x}{X(I+1) - X(I)} - \frac{y}{Y(J+1) - Y(J)}\right]$$

$$+ N(I+1,J+1)\left[\frac{y}{Y(J+1) - Y(J)}\right] \qquad \text{in CASE 2}$$

Having obtained C_{pr} values for each of two values of B_{th} either side of required B_{th}, interpolate linearly to find C_{pr} at required B_{th}.

If the required $B_{th} < 0.88$, obtain C_{pr} at each of the 6 datum values of B_{th}, 0.98 to 0.88, in the manner previously described (unless prevented by dummies), then fit a straight line through the 6 points (e.g. by method of least squares) and extrapolate to the required B_{th}.

		C_{pr}					
LWR	AR	B_{th} = .98	B_{th} = .96	B_{th} = .94	B_{th} = .92	B_{th} = .90	B_{th} = .88
2.4	1.3	.398	.371	.343	.318	.303	.273
2.4	1.4	.434	.408	.375	.343	.327	.294
2.4	1.5	.436	.411	.375	.343	.327	.294
3.2	1.3	.384	.360	.328	.322	.305	.274
3.2	1.4	.465	.436	.405	.377	.362	.331
3.2	1.5	.496	.467	.433	.402	.384	.350
3.2	1.6	.502	.475	.436	.404	.386	.350
4.0	1.4	.464	.431	.400	.386	.368	.336
4.0	1.5	.517	.486	.453	.426	.408	.375
4.0	1.6	.545	.513	.478	.446	.426	.393
4.0	1.7	.555	.525	.485	.451	.431	.393
4.0	1.8	.555	.525	.485	.451	.431	.393
4.8	1.5	.518	.480	.450	.431	.413	.380
4.8	1.6	.561	.527	.493	.464	.445	.412
4.8	1.7	.584	.552	.515	.483	.463	.427
4.8	1.8	.596	.563	.524	.490	.470	.435
4.8	1.9	.598	.566	.524	.490	.470	.435
4.8	2.0	.598	.566	.524	.490	.470	.435
5.6	1.6	.565	.525	.491	.472	.451	.416
5.6	1.7	.596	.563	.526	.497	.477	.444
5.6	1.8	.619	.586	.545	.515	.493	.458
5.6	1.9	.631	.597	.557	.522	.501	.465
5.6	2.0	.634	.602	.557	.522	.501	.465
5.6	2.1	.634	.602	.557	.522	.501	.465
6.4	1.6	.541	.514	.476	.469	.451	.414
6.4	1.7	.600	.558	.526	.503	.484	.447
6.4	1.8	.628	.595	.556	.526	.506	.471
6.4	1.9	.648	.615	.572	.540	.519	.484
6.4	2.0	.660	.625	.585	.550	.529	.492
6.4	2.1	.665	.630	.585	.550	.530	.492
6.4	2.2	.665	.631	.585	.550	.530	.492
6.4	2.3	.665	.631	.585	.550	.530	.492

		C_{pr}					
LWR	AR	B_{th} = .98	B_{th} = .96	B_{th} = .94	B_{th} = .92	B_{th} = .90	B_{th} = .88
7.2	1.7	.586	.555	.515	.502	.483	.444
7.2	1.8	.629	.588	.553	.530	.508	.472
7.2	1.9	.656	.618	.581	.550	.530	.495
7.2	2.0	.672	.639	.595	.564	.541	.505
7.2	2.1	.683	.648	.606	.573	.551	.514
7.2	2.2	.690	.655	.611	.575	.554	.516
7.2	2.3	.691	.659	.611	.575	.554	.516
7.2	2.4	.691	.659	.611	.575	.554	.516
7.2	2.5	.691	.655	.611	.575	.554	.516
8.0	1.8	.625	.588	.550	.533	.513	.475
8.0	1.9	.658	.618	.581	.555	.534	.498
8.0	2.0	.681	.642	.604	.572	.552	.516
8.0	2.1	.695	.658	.616	.583	.562	.526
8.0	2.2	.707	.671	.628	.593	.571	.533
8.0	2.3	.714	.677	.635	.598	.575	.537
8.0	2.4	.716	.681	.635	.598	.575	.537
8.0	2.5	.716	.680	.635	.598	.573	.535
8.0	2.6	.716	.677	.635	.597	.571	.531
8.0	2.7	.716	.670	.635	.595	.569	.528
8.8	1.9	.653	.614	.575	.557	.536	.499
8.8	2.0	.683	.640	.603	.577	.556	.520
8.8	2.1	.705	.665	.625	.593	.572	.536
8.8	2.2	.718	.680	.636	.603	.580	.546
8.8	2.3	.728	.690	.648	.613	.588	.552
8.8	2.4	.736	.696	.655	.618	.591	.555
8.8	2.5	.739	.700	.655	.618	.590	.552
8.8	2.6	.739	.699	.655	.617	.588	.550
8.8	2.7	.739	.697	.655	.615	.586	.547
8.8	2.8	.739	.693	.654	.613	.584	.542
9.6	2.0	.680	.639	.600	.579	.556	.520
9.6	2.1	.702	.662	.625	.596	.576	.538
9.6	2.2	.723	.684	.643	.611	.587	.553
9.6	2.3	.735	.694	.655	.622	.594	.562
9.6	2.4	.746	.705	.665	.630	.600	.568
9.6	2.5	.754	.711	.672	.635	.603	.570
9.6	2.6	.757	.714	.672	.635	.602	.569
9.6	2.7	.760	.715	.672	.634	.601	.566
9.6	2.8	.760	.713	.671	.632	.599	.562
9.6	2.9	.757	.709	.670	.628	.596	.557
9.6	3.0	.754	.703	.668	.625	.592	.551

		C_{pr}					
LWR	AR	B_{th} = .98	B_{th} = .96	B_{th} = .94	B_{th} = .92	B_{th} = .90	B_{th} = .88
10.4	2.0	.670	.635	.593	.580	.560	.520
10.4	2.1	.706	.661	.625	.603	.580	.542
10.4	2.2	.720	.680	.645	.618	.590	.557
10.4	2.3	.740	.700	.660	.630	.602	.570
10.4	2.4	.750	.710	.670	.636	.606	.576
10.4	2.5	.763	.719	.679	.644	.611	.580
10.4	2.6	.767	.723	.684	.645	.612	.581
10.4	2.7	.771	.726	.686	.647	.611	.581
10.4	2.8	.773	.727	.688	.647	.610	.580
10.4	2.9	.773	.725	.686	.645	.609	.575
10.4	3.0	.773	.722	.682	.640	.607	.568
10.4	3.1	.771	.716	.678	.637	.604	.562
10.4	3.2	.770	.710	.666	.618	.597	.550
12.0	2.2	.716	.672	.640	.620	.595	.550
12.0	2.4	.752	.710	.673	.642	.613	.581
12.0	2.6	.773	.732	.693	.657	.623	.590
12.0	2.8	.788	.743	.703	.663	.626	.594
12.0	3.0	.794	.749	.705	.664	.626	.593
12.0	3.2	.794	.748	.702	.661	.621	.589
12.0	3.4	.790	.740	.690	.650	.613	.576
13.6	2.4	.743	.702	.669	.642	.617	.575
13.6	2.6	.770	.730	.694	.660	.627	.593
13.6	2.8	.792	.748	.707	.669	.634	.602
13.6	3.0	.803	.759	.716	.673	.638	.605
13.6	3.2	.807	.765	.721	.675	.637	.604
13.6	3.4	.808	.768	.720	.673	.633	.599
13.6	3.6	.807	.764	.711	.668	.627	.591
13.6	3.8	.804	.753	.690	.650	.619	.578
15.2	2.4	.725	.690	.655	.634	.620	.558
15.2	2.6	.760	.721	.690	.659	.629	.592
15.2	2.8	.782	.745	.707	.670	.638	.600
15.2	3.0	.802	.760	.720	.677	.644	.612
15.2	3.2	.809	.769	.727	.683	.648	.615
15.2	3.4	.814	.782	.731	.685	.649	.616
15.2	3.6	.817	.786	.731	.685	.645	.615
15.2	3.8	.819	.782	.727	.682	.639	.608
15.2	4.0	.816	.773	.713	.673	.626	.590
16.8	2.6	.735	.708	.680	.650	.630	.580
16.8	2.8	.767	.740	.704	.667	.639	.605
16.8	3.0	.792	.754	.717	.678	.647	.613
16.8	3.2	.805	.765	.727	.686	.653	.620
16.8	3.4	.812	.777	.736	.693	.656	.625
16.8	3.6	.817	.790	.741	.696	.656	.627
16.8	3.8	.824	.790	.741	.695	.654	.626
16.8	4.0	.830	.790	.737	.690	.650	.622

		C_{pr}					
LWR	AR	B_{th} = .98	B_{th} = .96	B_{th} = .94	B_{th} = .92	B_{th} = .90	B_{th} = .88
18.4	2.8	.751	.732	.699	.660	.638	.600
18.4	3.0	.775	.745	.712	.673	.646	.612
18.4	3.2	.796	.757	.723	.685	.653	.620
18.4	3.4	.806	.768	.732	.694	.658	.627
18.4	3.6	.811	.776	.742	.702	.663	.633
18.4	3.8	.817	.783	.746	.704	.663	.635
18.4	4.0	.824	.790	.748	.699	.661	.632
20.0	2.8	.730	.705	.685	.644	.634	.580
20.0	3.0	.757	.740	.704	.663	.643	.607
20.0	3.2	.780	.747	.716	.677	.650	.617
20.0	3.4	.799	.760	.726	.687	.656	.625
20.0	3.6	.805	.767	.735	.694	.662	.630
20.0	3.8	.810	.774	.743	.698	.669	.640
20.0	4.0	.816	.779	.750	.710	.670	.640

The foregoing range of LWR and AR is shown graphically in Figure 1.

APPENDIX 5

Notes on surge

Test data show that, for a given rotor at a given speed, surge usually occurs at a higher flow when the rotor is followed by a vaned diffuser than when it is followed only by a vaneless space. This implies that in a particular compressor arrangement a variety of potential surge-producing mechanisms exist, and one which is associated in some manner with the presence of a vaned diffuser is usually the first to come into play. Since compressors with vaned diffusers are the case of greatest practical importance for aircraft gas turbines, it is that for which a means of surge prediction is chiefly required, and to which these notes relate.

A further general point to be observed from test data is that a reduction in diffuser channel throat area (e.g. by a change of axial dimension, other features remaining the same) can, in some instances at least, lower the surge flow — and by a greater proportion than that by which the choking flow is simultaneously lowered, so that flow range is extended. In such cases, quite a small change to throat area has an appreciable effect upon surge. Since this small reduction of throat area usually does not significantly alter the value of parameters which govern performance of the subsonic channel following the throat (the behaviour of which is now fairly well understood from the work of Runstadler[11]), this evidence suggests that the important region as regards surge-promoting mechanism lies ahead of the vaned diffuser channel throat, i.e. in the so-called 'semi-vaneless space' between vane leading edge and throat. Except at flows near to diffuser choking the semi-vaneless region also acts as a diffuser, mean throat Mach number being less than the incident at vane leading edge, so reduction of throat area at given operating condition serves to raise throat Mach number and reduce the amount of diffusion in the semi-vaneless space. The literature already contains suggestions relating surge in centrifugal compressors to some measure of the diffusion ahead of the vaned diffuser channel throat (e.g. References 21, 27, 28, 29).

Examination of data from fourteen builds of compressor (comprising nine different rotors, in several cases with changes of vaned diffuser) reveals a fact of much apparent significance. The pressure rise coefficient of the semi-vaneless space (PRC), defined as $\left(P_{s,th} - P_{s,e}\right) \div \left(\hat{P}_{t,e} - P_{s,e}\right)$

and calculated by the present method of analysis for the experimentally determined surge flows, shows a notable degree of consistency in value over the speed range for a given compressor: there is, however, a very wide variation of the surge value of PRC among the different compressors. In seven cases out of the fourteen (involving five different rotors, four with and one without sweepback of blades at rotor outlet) the value of calculated PRC at surge for all speeds lies above 0.4 – in one case close to 0.6; among the other compressors (all with rotor sweepback) values as low as 0.15 to 0.2 appear. This consistency between speeds for a given compressor affords strong support for the theory that surge is somehow related to a limiting value of semi-vaneless space diffusion. But evidently that limit depends upon individual features of a particular compressor arrangement.

A further fact which may or may not be coincidence is that among the same fourteen compressors, six out of the seven giving data which exhibit high calculated values of PRC at surge (in the range 0.4 to 0.6) had vaned diffusers discharging into annular "dump" collectors of snail-shell form, the "tongue" of the off-take pipe from the collector being reasonably remote from the trailing edges of the diffuser vanes. (It is well known that a snail-shell collector in too close proximity to diffuser vane trailing edges can promote a considerable circumferential non-uniformity of static pressure and cause premature surge.) And all those compressors with calculated values of PRC at surge below 0.4 discharged into radial-to-axial bends followed by one or more rows of axial cascade vanes, the latter serving to provide further diffusion and subsequent flow straightening. Whether this difference in the type of delivery system really has a governing influence on surge of compressor stages remains at present in doubt; the available data are insufficient to afford any approach to certainty.

Despite the fact that almost constant PRC at surge coincides with almost constant α_6, diffuser vane leading edge incidence is discounted as a surge-controlling parameter. This is because, among the fourteen compressor builds examined, wide variation of calculated leading edge incidence at surge is encountered (amounting to some $\pm 5^{\circ}$), and that variation corresponds to no order of merit in terms of operating range.

In view of the evidence relating to PRC cited herein, much attention has been devoted to seeking some analogy between diffusion in the semi-vaneless space and that in a simple divergent channel such as was tested by Runstadler[11]. Parameters for the semi-vaneless space analogous to those

which characterise the performance of simple channels vary with compressor operating condition, because of change in α_e and B_e, but for a given compressor are approximately constant at surge, due to the approximate constancy of α_e which has already been noted. Some possible forms of these parameters include the throat blockage factor B_{th}, a calculated quantity which could be open to doubt, but the failure of any universally consistent pattern to emerge from the data surveyed does not seem attributable to that cause.

The data for one rotor tested with four different vaned diffusers (in all cases followed by a bend-plus-axial-vane type of delivery system) show some correlation between calculated PRC at surge and the geometric property "wetted surface area of the semi-vaneless space/geometric throat area" $\left[A_w/A_g\right]$, where A_w can be approximated by the expression

$$n_d \left\{ \left[w_{th} + \frac{h_e + h_{th}}{2} \right] \sqrt{\left(D_e \sin \frac{\pi}{n_d} \right)^2 - w_{th}^2} - \frac{D_e^2}{4} \left(\frac{2\pi}{n_d} - \sin \frac{2\pi}{n_d} \right) \right\}$$

The range of A_w/A_g in this case is from 5.16 to 7.60. The parameter A_w/A_g may be regarded as simply a form of passage 'L/D'; since wetted area = length × perimeter and A_g = cross-sectional area, it follows that A_w/A_g is proportional to length/hydraulic mean depth. Supposing there to be a diffusion pressure gradient for the semi-vaneless space at which some critical degree of stall exists, then the longer the passage (i.e. the larger is 'L/D') the greater the overall pressure rise attainable at that gradient, and so the further flow can be reduced before reaching the critical situation. Thus a large value of A_w/A_g might be expected to give wide operating range and vice versa. Such a correlation would serve to explain the reason for two effects which have been found to lower surge flow and thus improve compressor stage operating range, namely:-

(1) reduction of vane number at constant A_g and h_{th}; this increases w_{th} and hence A_w

(2) reduction of A_g by change of h_{th} at constant n_d; A_g is reduced in proportion to h_{th}, but A_w is reduced less than pro rata with h_{th}, so that A_w/A_g increases.

The degree of correlation obtained for those four builds of compressor (with the same rotor) encouraged hope that the same trend would

apply quantitatively as well as qualitatively to other compressors, and so provide some general means of surge prediction for compressors with vaned diffusers and similar delivery systems. But data for others of the compressors examined fail to conform at all adequately.

One is thus left with no firm ground upon which to base a simple method of predicting surge. The only positive indications emerging from present evidence are:

(a) It seems notably easier to obtain wide operating range from compressor stages which discharge into snail-shell collectors than those with bend-plus-axial-vane delivery systems.

(b) Approximately the same value of (calculated) PRC at surge applies at all speeds of a given compressor stage.

(c) Mean values of PRC at surge greater than about 0.55 have not been found.

(d) For some compressors improved operating range may be obtainable by arranging the semi-vaneless space so as to give a high value of the quantity A_w/A_g.

ACKNOWLEDGEMENT

The author cannot pay too high a tribute to the part taken by Mr P. M. Came during the formulation of this analytical treatment. To numerous discussions over a long period is due such merits as it may possess.

REFERENCES

No.	Author(s)	Title, etc
1	D. Eckardt	Instantaneous measurements in the jet-wake discharge flow of a centrifugal compressor impeller ASME paper 74-GT-90, 1974
2	D. G. Ainley G. C. R. Mathieson	A method of performance estimation for axial-flow turbines ARC R & M 2974, 1957
3	M. V. Herbert	A discussion on the prediction of profile loss for axial-flow turbine blades ARC paper 34757 (Turbo 276), 1973
4	J. Dunham	A review of cascade data on secondary losses in turbines J. Mech. Eng. Sci. Vol 12 no. 1, p.48,1970
5	J. Dunham P. M. Came	Improvements to the Ainley-Mathieson method of turbine performance prediction ASME paper 70-GT-2, 1970
6	B. S. Stratford G. S. Beavers	The calculation of the compressible turbulent boundary layer in an arbitrary pressure gradient - a correlation of certain previous methods ARC R & M 3207, 1961
7	R. C. Dean Y. Senoo	Rotating wakes in vaneless diffusers J. Basic Engineering, Sept. 1960, p.563
8	M. V. Herbert	Some notes on loss coefficients relating to turbine blades with finite trailing edge thickness ARC paper 34755 (Turbo 274), 1972
9	F. J. Wiesner	A review of slip factors for centrifugal impellers J. Engineering for Power, Oct. 1967, p.559
10	J. E. Green D. J. Weeks J. W. F. Brooman	Prediction of turbulent boundary layers and wakes in compressible flow by a lag-entrainment method ARC R & M 3791, 1977
11	P. W. Runstadler	Pressure recovery performance of straight-channel single-plane divergence diffusers at high Mach numbers USAAVLABS Technical Report 69-56, 1969

REFERENCES (cont'd)

No.	Author(s)	Title, etc
12	N. A. Dimmock	A compressor routine test code ARC R & M 3337, 1963
13	J. D. Stanitz G. O. Ellis	Two-dimensional compressible flow in centrifugal compressors with straight blades NACA TN 1932, 1949 and NACA Report 954, 1950
14	J. D. Stanitz V. D. Prian	A rapid approximate method for determining velocity distribution on impeller blades of centrifugal compressors NACA TN 2421, 1951
15	R. C. Davis J. L. Dussourd	A unified procedure for the calculation of off-design performance of radial turbomachinery ASME paper 70-GT-64, 1970
16	J. Moore	A wake and an eddy in a rotating, radial-flow passage. Part I - experimental observations ASME paper 73-GT-57, 1973
17	J. W. Daily R. E. Nece	Chamber dimension effects on induced flow and frictional resistance of enclosed rotating discs J. Basic Engineering, Mar. 1960, p.217
18	F. Ribary	The friction losses of steam turbine discs Brown Boveri Review, Jul. 1934, p.120
19	J. E. Coppage F. Dallenbach et al	Study of supersonic radial compressors for refrigeration and pressurization systems WADC Technical Report 55-257 ASTIA Document AD 110467 1956
20	C. Rodgers	Influence of impeller and diffuser characteristics and matching on radial compressor performance "Centrifugal compressors": SAE Technical Progress Series, Vol 3, p.31, 1961
21	C. Rodgers L. Sapiro	Design considerations for high-pressure-ratio centrifugal compressors ASME paper 72-GT-91, 1972

REFERENCES (cont'd)

No.	Author(s)	Title, etc
22	W. Jansen	A method for calculating the flow in a centrifugal impeller when entropy gradients are present Paper 12, Inst. Mech. Eng. Conference on internal aerodynamics (turbomachinery) 1970
23	E. P. Krylov Y. A. Spunde	Concerning the effect of clearance between the working blades and the casing of a radial turbine upon its characteristics (In Russian) "Energetika" no. 7, p.66, 1965
24	J. D. Stanitz	One-dimensional compressible flow in vaneless diffusers of radial- and mixed-flow centrifugal compressors, including effects of friction, heat transfer and area change NACA TN 2610, 1952
25	H. Fernholz	A new empirical relationship between the form-parameters H_{32} and H_{12} in boundary layer theory J. R.Ae.Soc. Vol. 66, p.588, Sept. 1962
26	P. Pinot	Diffuser performance at low area ratio and length/width ratio Rolls-Royce Technical Note LTN 72395 January 1977
27	D. P. Kenny	Supersonic radial diffusers AGARD Lecture Series No. 39 on Advanced Compressors, 1970
28	S. Baghdadi A. T. Macdonald	Performance of three vaned radial diffusers with swirling transonic flow J. Fluids Eng. June 1975, p.155
29	K. Toyama P. W. Runstadler R. C. Dean	An experimental study of surge in centrifugal compressors J. Fluids Eng. March 1977, p.115

Fig.1

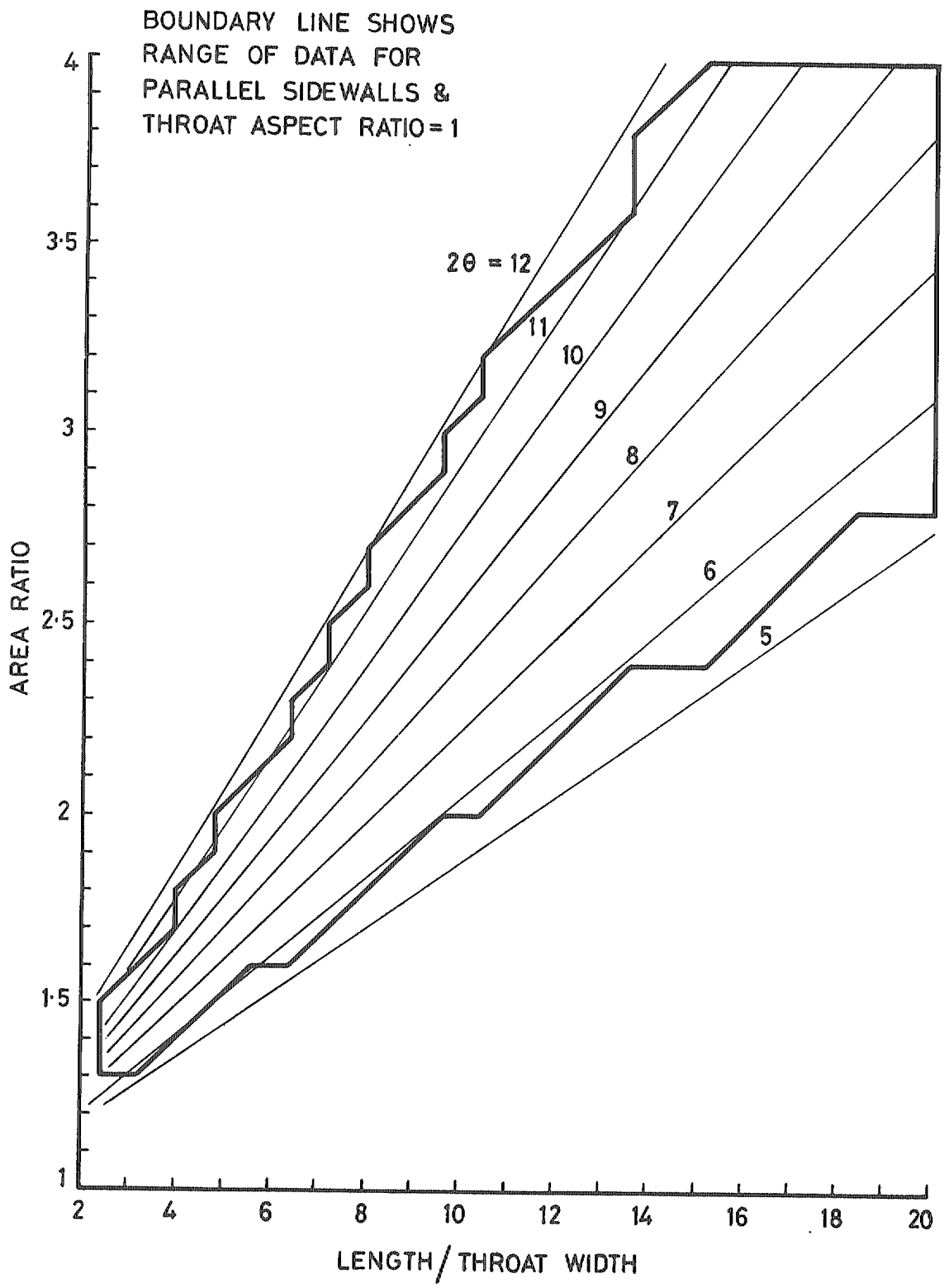

FIG. 1 CHANNEL DIFFUSER MAP

Fig.2

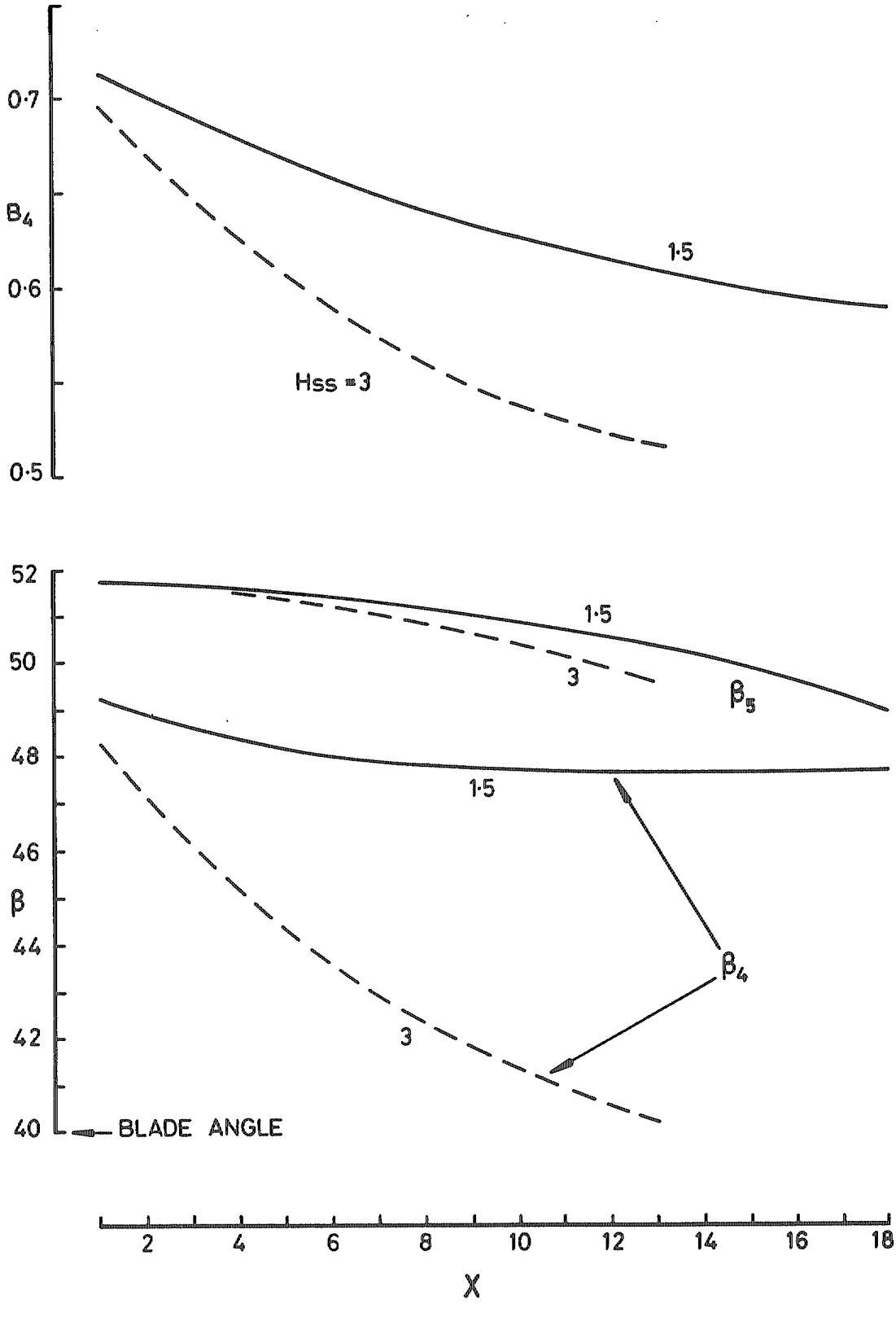
0·7
B4
0·6
0·5
1·5
Hss = 3
52
50
48
46
β
44
42
40
1·5
3
β5
1·5
β4
3
BLADE ANGLE
2
4
6
8
10
12
14
16
18
X

Fig.3

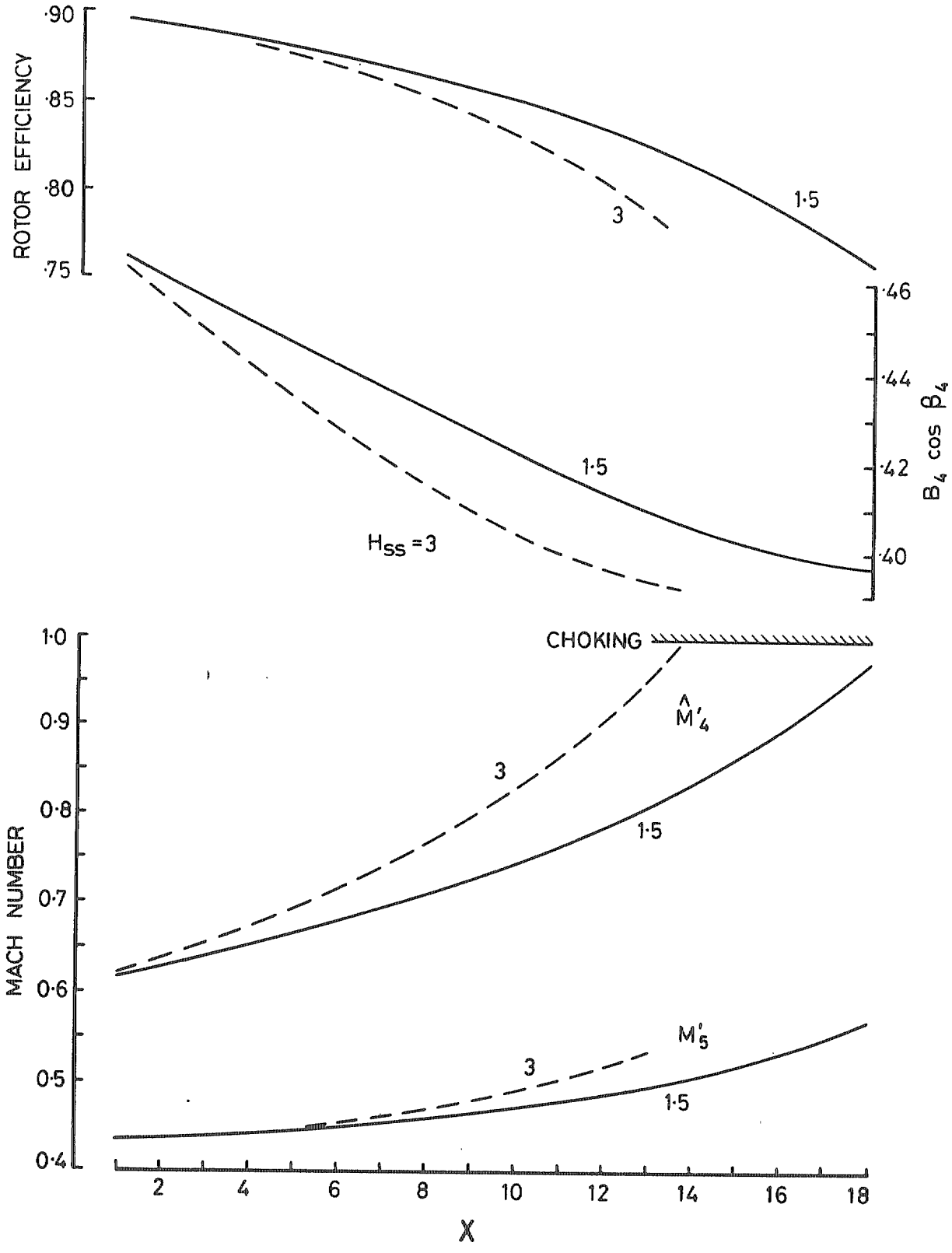
ROTOR EFFICIENCY
·90
·85
·80
·75
3
1·5
1·5
H_{SS} = 3
·46
·44
·42
·40
$B_4 \cos \beta_4$
MACH NUMBER
1·0
0·9
0·8
0·7
0·6
0·5
0·4
CHOKING
$\hat{M}'_4$
3
1·5
M'_5
3
1·5
2
4
6
8
10
12
14
16
18
X

PART II - COMPARISON WITH EXPERIMENT

1. Introduction

Part I of this work gives a full statement of the assumptions and modelling procedures which form the analytical treatment. That treatment is applied by means of a computer program. Predictions by this method are now presented for a selection of compressors for which test data are available. They embrace cases of a rotor alone, rotor plus vaneless space, and a full stage including vaned diffuser.

As explained at the start of Part I, a general prediction method is by definition required to ignore details of, for instance, rotor blade passage shape, so it cannot discriminate between compressors built with the same overall geometric properties but having different levels of performance, and hence cannot give an "absolute" answer. Some empirical datum or standard of performance must be set, and the predictions "tuned" to agree with it. For this reason, when comparing predictions for a number of compressors with test results, some latitude in agreement of efficiency level must be accepted. Those compressors taken for the comparisons shown herein all correspond to a fairly similar standard of design quality, and the prediction method has been "tuned" to give the best average agreement with those test cases.

2. The predictions

Compressor performance maps are presented in Figures 1 to 7 for the machines listed in Table 1. Compressor number 1 is that described in Reference 1, the compressors numbered 2 to 6 are described in Reference 2, and compressor number 7 in Reference 3. In the case of Figures 2 to 7 three performance quantities are shown, for each of which a good match to test values is required. Since pressure ratio is derived from work input ($\Delta H/U^2$) and efficiency, it follows that if both the latter are accurate then so should be the pressure ratio, but accurate pressure ratio can also be obtained as a result of opposing errors in work input and efficiency - an example of this is to be observed in Figure 5. In general no consistent pattern of errors appears: sometimes one of the three quantities is predicted the most accurately and sometimes another.

For these comparisons the rotor blockage growth factor called Z in Part I has been scheduled as 0.7 x rotor design-point pressure ratio, this relation being adopted to assist in matching the test results.

At the choking condition it will be seen that in some cases $\Delta H/U^2$ falls vertically, similarly to efficiency and pressure ratio, while in others $\Delta H/U^2$ remains at a constant value. This difference in behaviour goes according to whether or not choking takes place in the throat of a vaned diffuser. If it is the diffuser which chokes first then rotor outlet conditions remain constant as the diffuser goes into supercritical operation (with supersonic flow and a high-loss shock system within the diverging channel); if it is the rotor inducer which chokes first, then the velocity triangle at rotor outlet changes shape as pressure ratio falls, leading to a fall in $\Delta H/U^2$. The annotation "inducer choking" or "diffuser choking" on the Figures relates to the predicted situation.

Some doubt attaches to the test values of $\Delta H/U^2$ at the lowest speed shown in Figure 5; no other vaned diffuser case exhibits such a difference of level at low speed and the prediction method clearly does not support it.

A matter of some interest is how the locus of peak efficiency with changing speed behaves. The mean slope of this locus over the range of speed 50 to 90 per cent of design appears as follows:

	Vaned diffuser			Vaneless diffuser
Compressor	4	5	6	7
Test results	steep positive	steep positive	positive	negative
Prediction	slightly positive	slightly positive	almost flat	flat

Thus in general the prediction tends more nearly towards flatness of the locus, resulting in quite considerable errors in predicted efficiency at lowest speed. From this comparison it might be inferred that the sense of the error changes according as to whether the compressor has or has not a vaned diffuser, but other evidence refutes such a conclusion. At least one compressor is known for which the mean slope of locus is negative for builds both with and without vaned diffuser; predictions for the vaned case show a locus with slightly negative slope, so matching the direction of the experimental slope but again flatter. Hence, as regards this locus, the test data shown here are not fully representative. On the sparse evidence at present available, not too much importance is attached to partial failure of prediction to match the experimental slope of locus.

3. Comment

In order to satisfy the primary objective, that of giving a designer a "preview" of stage performance, it is necessary to predict with fair accuracy (i) choking flow, (ii) surge flow, (iii) the shape of mass-flow/pressure-ratio characteristic between choking and surge, (iv) work input, and (v) efficiency level. Let us look at these in turn.

Choking of the inducer throat depends in the treatment of Part I upon an empirical relation for throat blockage; the relation selected gives satisfactory answers for most of the available test cases (see for example Figures 2 and 7). It should be noted here that the compressors numbered 2 to 7 all had rotor blade angle distributions up to the throat similar to one another and to the model used in the treatment of Part I, also that all had 17 or more inducer blades. In the case of machines with markedly different blade angle distributions in that region, or much wider inducer blade pitching at casing diameter (due either to fewer blades or relatively larger casing diameter), then some adjustment to the theoretical model would be required in order to obtain a correct prediction of inducer choking flow.

Vaned diffuser throat blockage depends to some extent upon an empirical schedule of mainstream total pressure loss between the pitch circle of vane leading edges and the channel throat, but the assumed loss is effectively zero at the diffuser choking condition. Diffuser choking is satisfactorily evaluated in almost all cases (see for example Figures 3, 4, 5 and 6). Were shocks of significant strength to be present ahead of the diffuser throat, the agreement might not hold.

Generally then, choking flow is well predicted. But there is one possible defect to note. In both Figures 5 and 6 at 110 per cent speed the diffuser does not choke and choking flow is not as well predicted as usual, the error being the same (2 per cent over-prediction) in both cases. These two compressors both have prewhirl, and in the absence of any test data for a prewhirl compressor without vaned diffuser the possibility remains that prediction of inducer choking flow as treated is somewhat in error for any prewhirl machine. Only further test results can tell.

As regards surge, the situation is decidedly unsatisfactory. Experimental data show that when a given rotor is followed by a vaned diffuser surge usually occurs at a higher flow than when the same rotor is followed by only a vaneless space. The vaned diffuser case is that of greatest

practical importance for aircraft gas turbines, and it is that to which attention has been primarily directed in seeking a prediction treatment. Appendix 5 of Part I contains a summary of the evidence obtained from analysing, by the present method, the performance of 14 such compressor builds at their experimental surge flows. The most significant parameter appears to be the pressure rise coefficient of the so-called "semi-vaneless space" (between diffuser vane leading edge and channel throat), which to a quite close approximation has the same value at surge for all speeds of any given compressor. But the mean surge value of that pressure rise coefficient (PRC) can differ considerably between compressors, and can change with the build of vaned diffuser which follows a given rotor. Further complexity is introduced by observing that it is generally easier to obtain a wide operating range (i.e. lower surge flow as a proportion of choking flow, and hence higher PRC at surge) when the vaned diffuser discharges into a "dump" collector of snail-shell form than when it is followed by a radial-to-axial bend and one or more rows of axial cascade vanes. No simple empirical correlations have emerged from this study which can be regarded as universally applicable, and on present knowledge the onset of surge cannot reliably be included in this performance prediction method. That is of course a serious defect.

It is worth noting that even were surge flow predictable, the predicted flow is not the only factor in matching an experimental surge line, since the predicted line would be that connecting certain values of flow lying on the predicted pressure ratio characteristics. Thus errors in level of the characteristics can either magnify or reduce the effect on surge line matching of errors in surge flow prediction.

In general the predicted shape of mass-flow/pressure-ratio characteristic is substantially correct at all speeds. But some errors of level in either sense are to be found.

Work input is fairly well predicted in normal circumstances. In the case of compressor number 6 an oblique contraction occurs in axial passage width immediately after rotor outlet; the effective dimension for the mixed-out flow is then open to some doubt, and has been adjusted in order to give the correct work input.

Efficiency level is only approximately right. Here the chief difficulty is to distinguish errors in rotor loss from errors in diffuser loss, as reliable test results for hardly any machines are available both

with and without vaned diffuser. This makes it difficult to decide upon a value for the factor Z which determines the predicted level of rotor efficiency. Loss of efficiency in the vaneless space is both small and able to be estimated quite accurately so that one may regard Figures 1, 2 and 7 as forming one class: to judge from that evidence the prediction of rotor efficiency is correct within 2 per cent at design speed, although sometimes more at low speed.

Hence the value of Z used appears fairly satisfactory for "normal" amounts of diffusion. Where the relative velocity ratio of a rotor is extreme, i.e. the diffusion much greater or much less than is conventional, then it is possible that the value of Z would require alteration.

Having set the rotor efficiency, stage efficiency then depends mainly on diffuser channel pressure recovery. The major problem here is catering for a range of geometric variables far wider than is covered by single-channel test data[4]. By employing a procedure of extensive extrapolation, on somewhat doubtful basis (but one nevertheless believed to be justified by the results), a treatment was developed in Part I for most two-dimensional cases likely to be encountered. Channels with diverging sidewalls, as in most of the compressors providing available test data (including all those shown here), are dealt with by defining an "equivalent two-dimensional" channel. The resulting values of channel pressure recovery coefficient may well not be very accurate, but because 1 per cent of channel pressure recovery coefficient reflects as only about $\frac{1}{4}$ to $\frac{1}{6}$ per cent of stage efficiency the treatment is thought to be acceptable.

For the examples shown (Figures 3 to 6), the error in predicted stage efficiency is consistent neither in sense nor in relation to change of speed. That error lies within ±1 to 2 per cent at the design condition, but is often considerably greater at low speed. The difference between measured and predicted trends of maximum efficiency locus with changing speed has already been commented upon. So far as design-point conditions are concerned, the error in stage efficiency looks to be no worse than the error in rotor efficiency. That conclusion lends some confidence to the treatment of diffuser channel pressure recovery.

It is possible that some loss of stage efficiency should be ascribed to the quality of the flow entering the diffuser system. The treatment of Part I assumes that flow conditions both at vane leading edge and at channel throat are uniform except for the presence of wall boundary layers, and the

single-channel test data on which estimation of pressure recovery is based relate to inlet flow in that well-regulated state. The considerable variation, both axially and circumferentially, of time-average flow properties existing in a compressor at vane leading edge could conceivably affect not only the growth of blockage to the throat but, if non-uniformity persists that far, also the subsequent channel pressure recovery. There is no way of quantifying such effects, the extent of which may in any case differ between individual compressors, and one can do no more at present than note the situation as possibly contributory to an error in predicted stage efficiency. Should it transpire that effects of this nature are significant, there might be need to revise the selection of the quantity Z determining rotor efficiency, since, as already observed, the division of losses between rotor and diffuser is somewhat uncertain.

To conclude, it should perhaps be noted that some margin of error in efficiency does not prevent a prediction method of this sort being used to assess (for instance) diffuser vane leading edge incidence and channel throat conditions, so affording information at the design stage of use in matching a diffuser system to a rotor, or for diagnosis of test performance.

4. Conspectus

In a predominantly analytical treatment such as the present method, endless scope for refinement exists. But given the basic requirement for a "rapid" calculation of overall performance properties, it is felt that approximately the right balance has been struck in modelling the flow between the grossly over-simple and the unprofitably sophisticated.

The chief defect in this prediction method is the failure to discover any satisfactory general treatment for the onset of surge. In other respects the predictions here presented are considered good enough for the method to appear useful, bearing in mind the cardinal point that only overall geometric properties of a compressor are specified.

TABLE 1

Compressor details

Compressor	Nominal design-point pressure ratio	Prewhirl	Sweep-back angle	Rotor tip diameter	Diffuser outlet diameter	Diffuser system*
1	3	no	0	0.4	0.6760	VS (long)
2	4	no	40	0.2509	-	RO
3	3½	no	40	0.2534	0.3279	VD
4	5	no	30	0.2925	0.5080	VD
5	5	yes	30	0.2925	0.5080	VD
6	7	yes	44	0.2463	0.3683	VD
7	7½	no	30	0.2748	0.2921	VS (short)

*Key: RO = Rotor only

VS = Vaneless space

VD = Vaned diffuser

Dimensions in metres

Note: All compressors with vaned diffusers discharged into radial-to-axial bends followed by rows of axial cascade vanes.

REFERENCES

No.	Author(s)	Title, etc
1	D. Eckardt	Instantaneous measurements in the jet-wake discharge flow of a centrifugal compressor impeller ASME paper 74-GT-90, 1974
2	M. G. Beard C. M. Pratt P. H. Timmis	Recent experience on centrifugal compressors for small gas turbines ASME paper 78-GT-193, 1978
3	P. M. Came	The development, application and experimental evaluation of a design procedure for centrifugal compressors Proc.I.Mech.E. Vol 192, no. 5, 1978
4	P. W. Runstadler	Pressure recovery performance of straight-channel single-plane divergent diffusers at high Mach numbers USAAVLABS Technical Report 69-56, 1969

FIG. 1

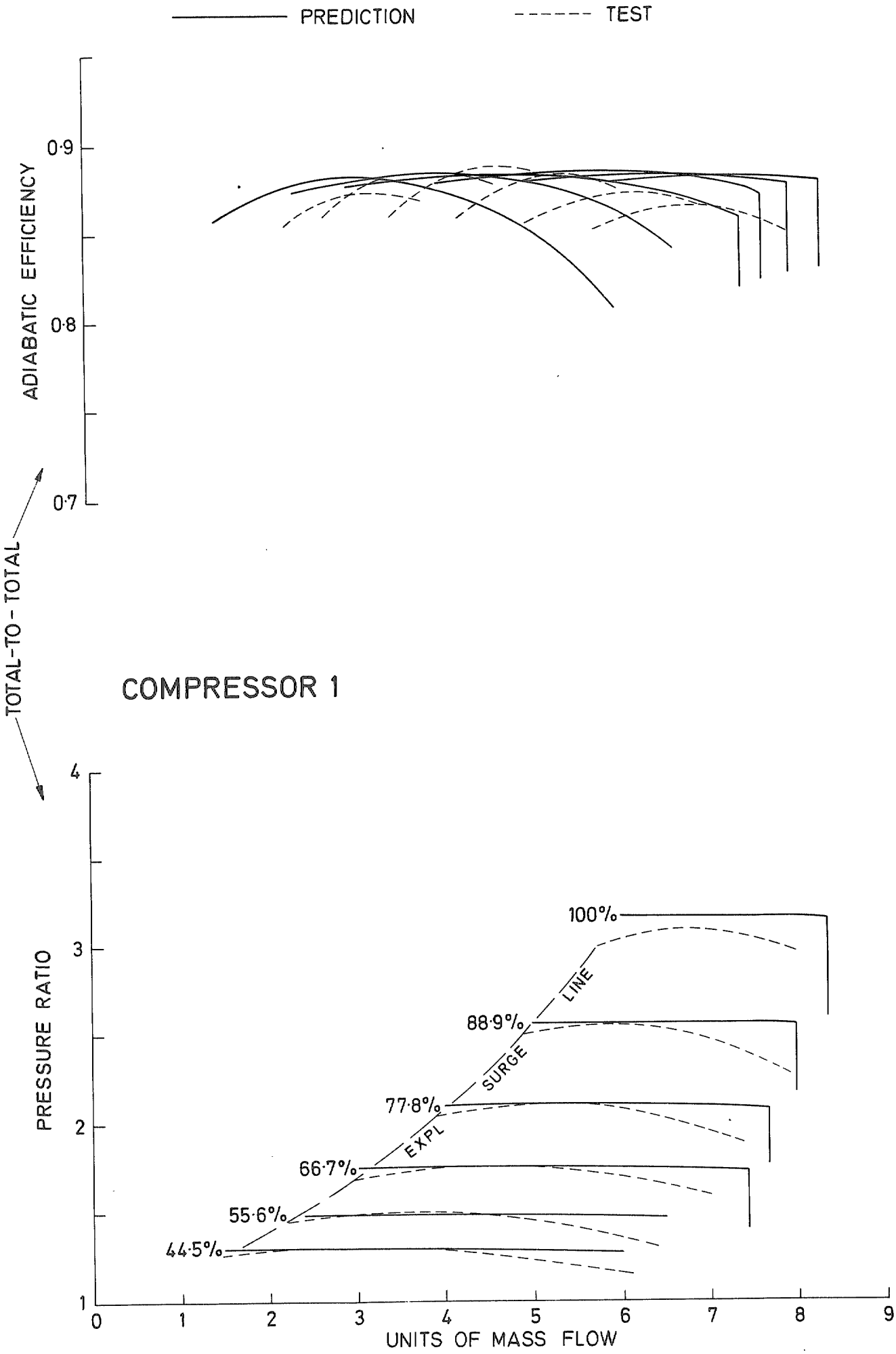
PREDICTION
TEST
ADIABATIC EFFICIENCY
0·9
0·8
0·7
TOTAL-TO-TOTAL
COMPRESSOR 1
PRESSURE RATIO
4
3
2
1
100%
88·9%
77·8%
66·7%
55·6%
44·5%
LINE
SURGE
EXPL
0
1
2
3
4
5
6
7
8
9
UNITS OF MASS FLOW

FIG. 2

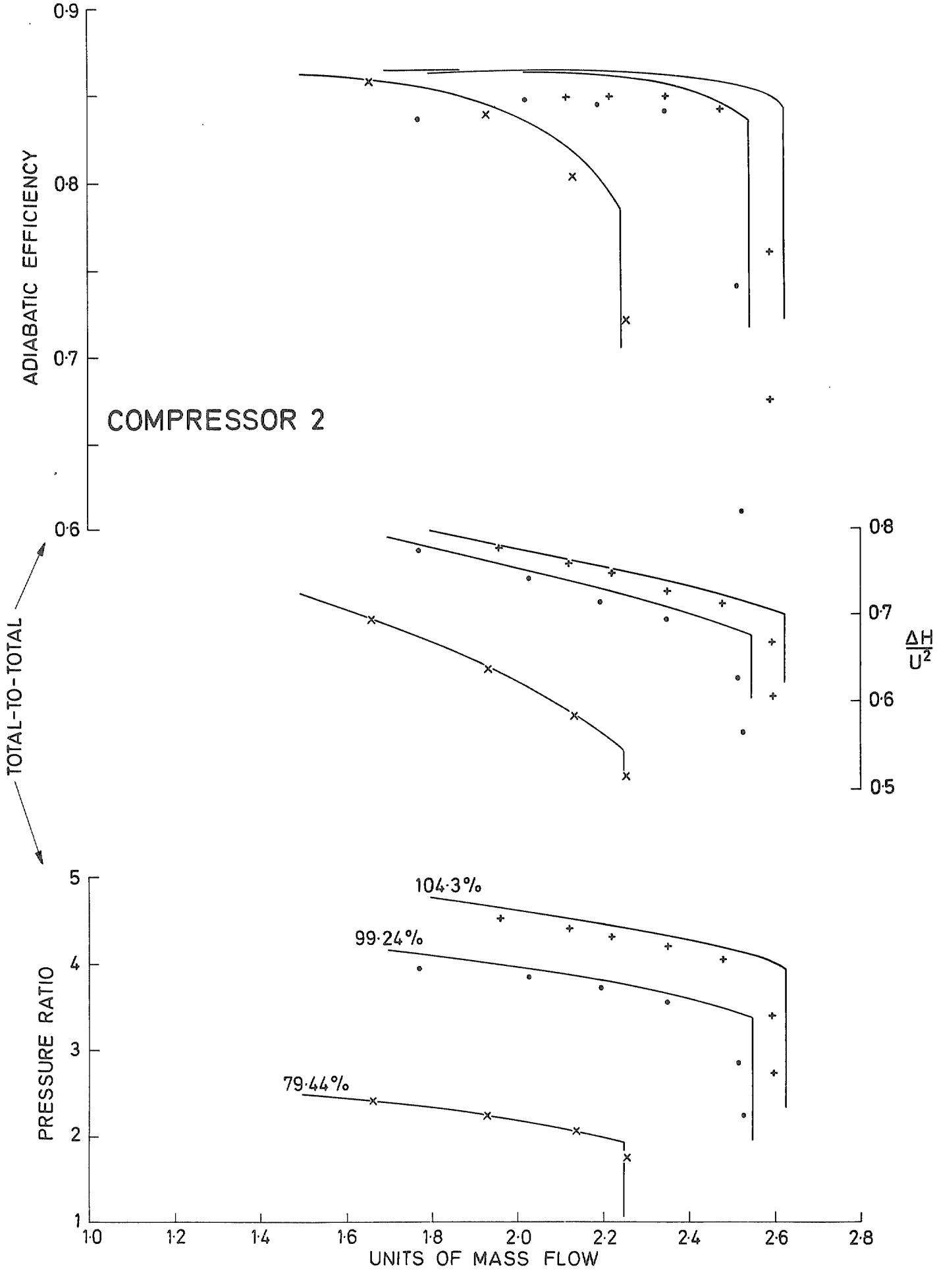
PREDICTION
SYMBOLS = TEST POINTS
ADIABATIC EFFICIENCY
0·9
0·8
0·7
0·6
COMPRESSOR 2
TOTAL-TO-TOTAL
0·8
0·7
0·6
0·5
ΔH/U²
104·3%
99·24%
79·44%
PRESSURE RATIO
5
4
3
2
1
1·0
1·2
1·4
1·6
1·8
2·0
2·2
2·4
2·6
2·8
UNITS OF MASS FLOW

FIG. 3

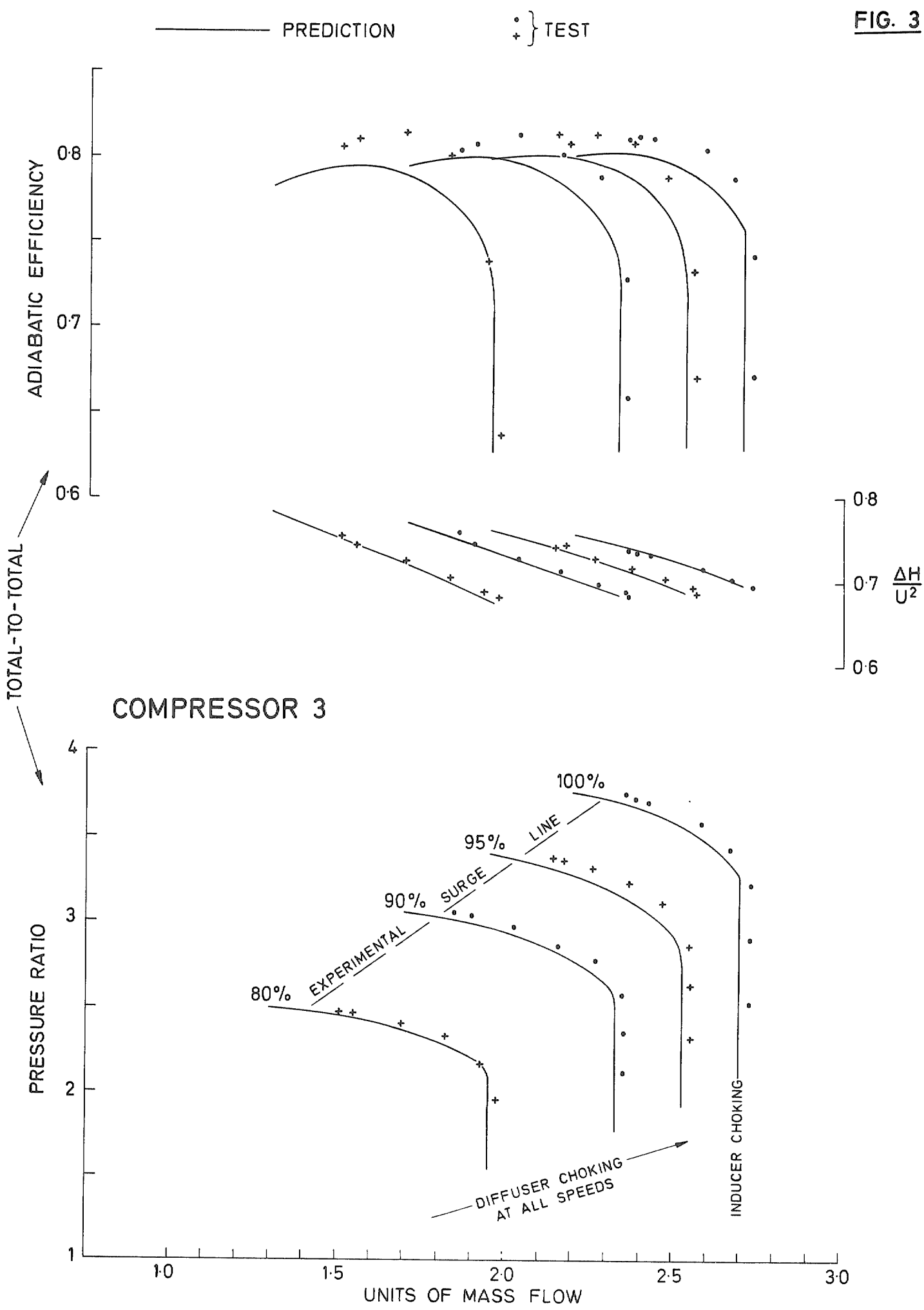
PREDICTION
TEST
ADIABATIC EFFICIENCY
0·8
0·7
0·6
TOTAL-TO-TOTAL
0·8
0·7
ΔH/U²
0·6
COMPRESSOR 3
PRESSURE RATIO
4
3
2
1
100%
95%
90%
80%
LINE
SURGE
EXPERIMENTAL
DIFFUSER CHOKING AT ALL SPEEDS
INDUCER CHOKING
1·0
1·5
2·0
2·5
3·0
UNITS OF MASS FLOW

FIG. 4

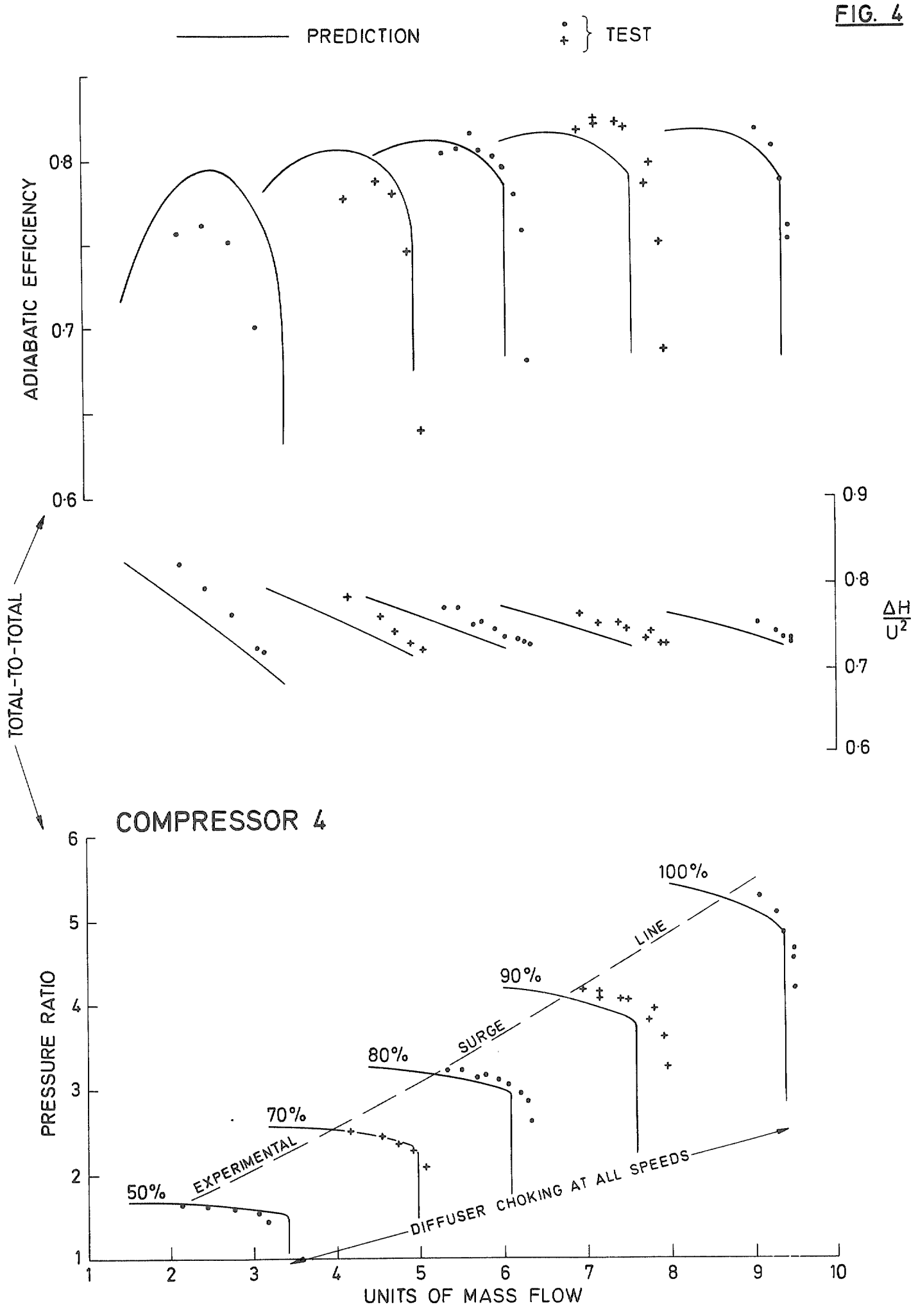
PREDICTION
TEST
ADIABATIC EFFICIENCY
0·8
0·7
0·6
TOTAL-TO-TOTAL
0·9
0·8
0·7
0·6
ΔH/U²
COMPRESSOR 4
PRESSURE RATIO
6
5
4
3
2
1
100%
90%
80%
70%
50%
SURGE LINE
EXPERIMENTAL
DIFFUSER CHOKING AT ALL SPEEDS
1
2
3
4
5
6
7
8
9
10
UNITS OF MASS FLOW

FIG. 5

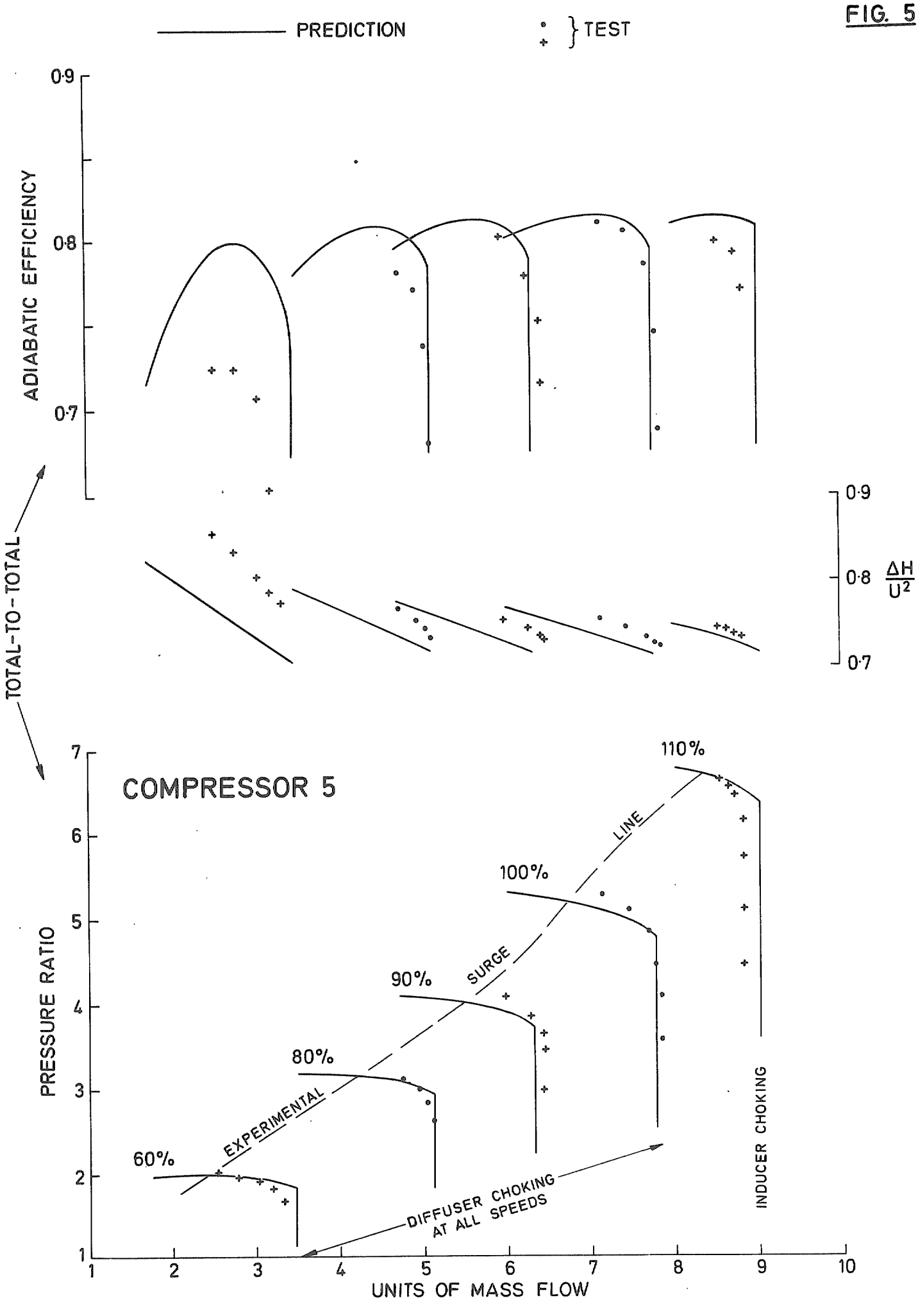
PREDICTION
TEST
ADIABATIC EFFICIENCY
0·9
0·8
0·7
TOTAL-TO-TOTAL
0·9
0·8
0·7
ΔH/U²
COMPRESSOR 5
110%
100%
90%
80%
60%
LINE
SURGE
EXPERIMENTAL
DIFFUSER CHOKING AT ALL SPEEDS
INDUCER CHOKING
PRESSURE RATIO
UNITS OF MASS FLOW
1
2
3
4
5
6
7
8
9
10

FIG. 6

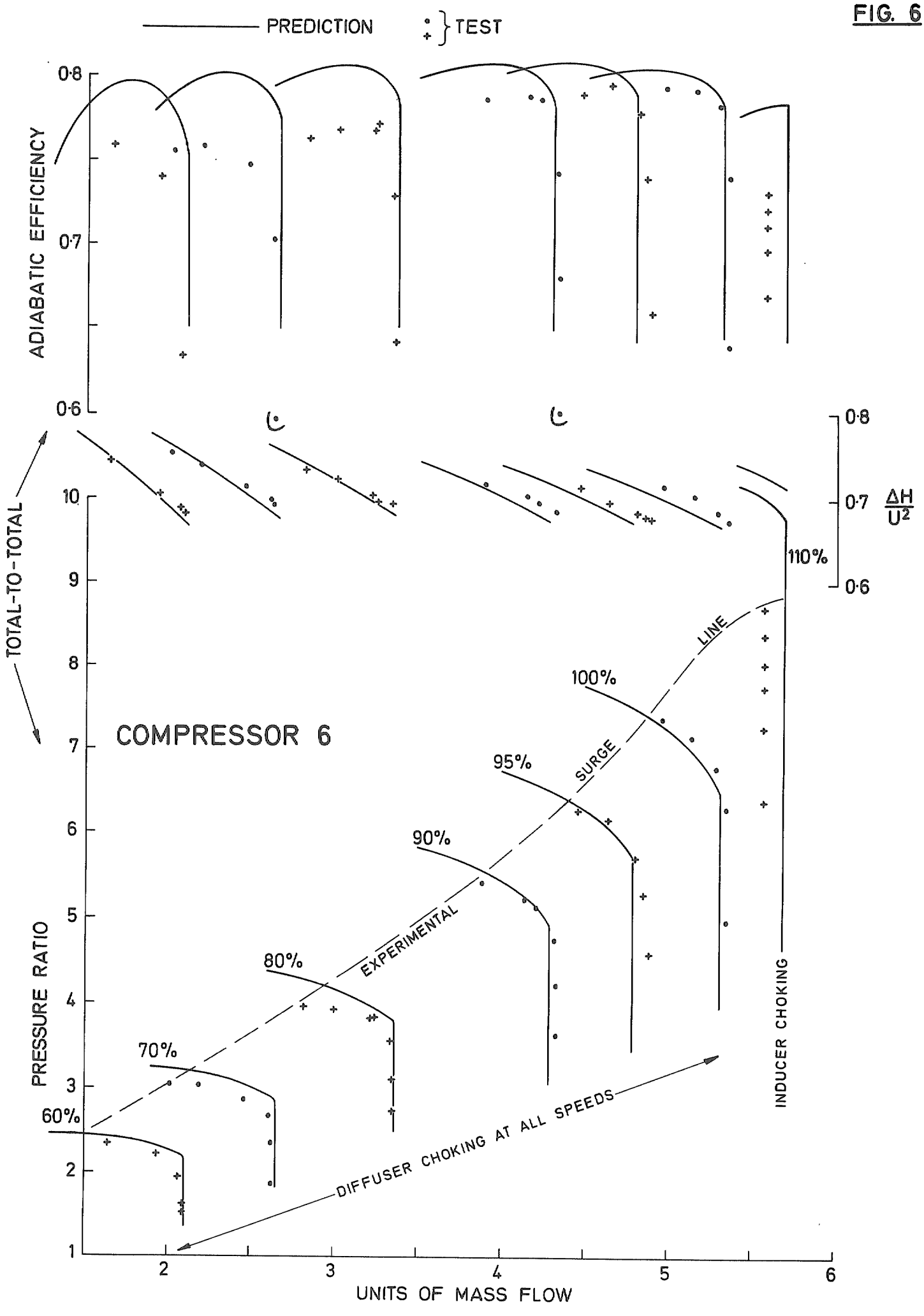
PREDICTION
TEST
ADIABATIC EFFICIENCY
0·8
0·7
0·6
TOTAL-TO-TOTAL
PRESSURE RATIO
10
9
8
7
6
5
4
3
2
1
ΔH/U²
0·8
0·7
0·6
110%
100%
95%
90%
80%
70%
60%
LINE
SURGE
EXPERIMENTAL
COMPRESSOR 6
INDUCER CHOKING
DIFFUSER CHOKING AT ALL SPEEDS
2
3
4
5
6
UNITS OF MASS FLOW

FIG. 7

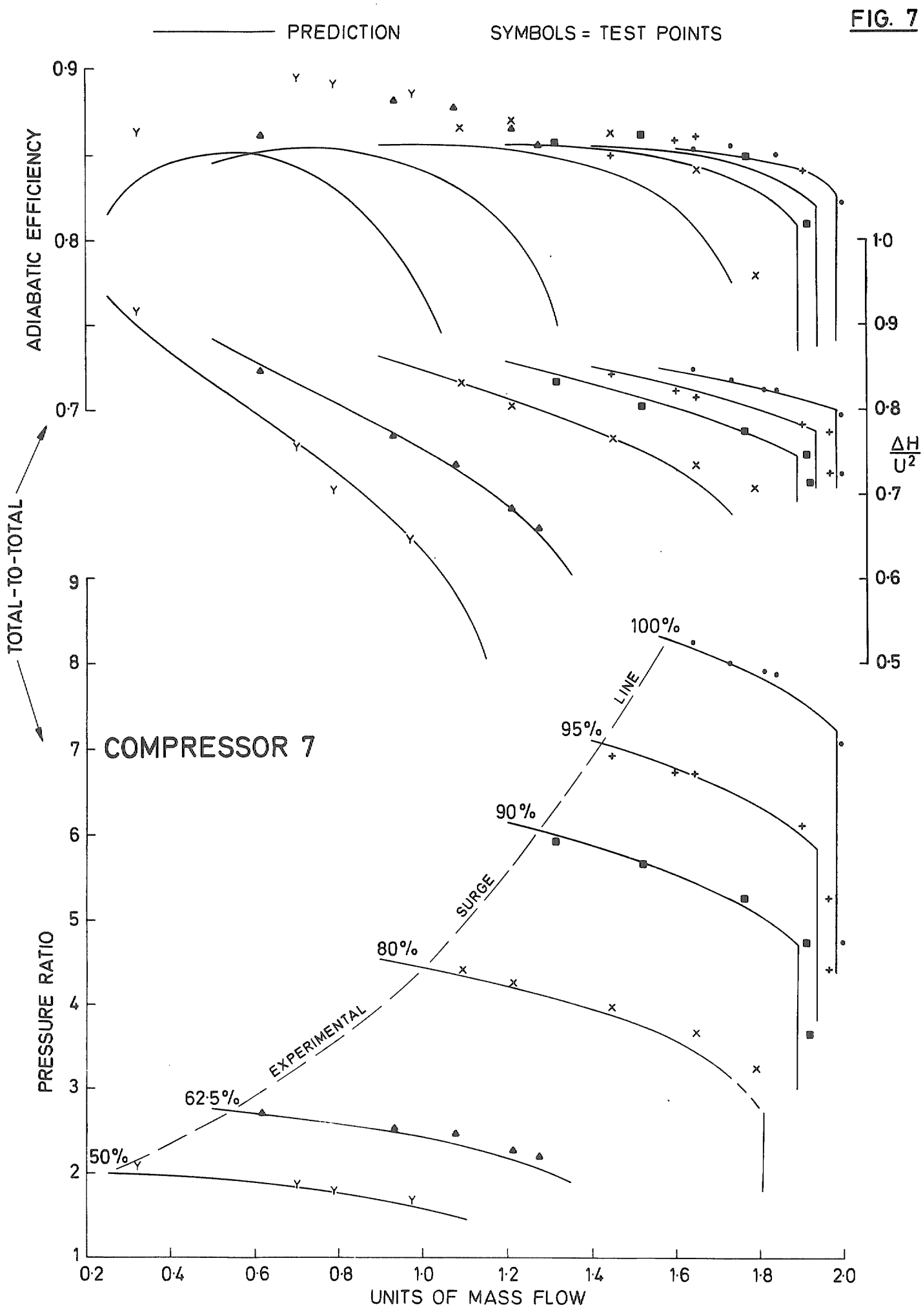

Printed in England for Her Majesty's Stationery Office by the Royal Aircraft Establishment, Farnborough. Dd.596060 K4 2/80.

First published 1980

HER MAJESTY'S STATIONERY OFFICE

Government Bookshops
49 High Holborn, London WC1V 6HB
13a Castle Street, Edinburgh EH2 3AR
41 The Hayes, Cardiff CF1 1JW
Brazennose Street, Manchester M60 8AS
Southey House, Wine Street, Bristol BS1 2BQ
258 Broad Street, Birmingham B1 2HE
80 Chichester Street, Belfast BT1 4JY

Government Publications are also available through booksellers

R &M No. 3843
ISBN 0114711763